Neuroeconomics of Charitable Giving and Learning

Dissertation
submitted to the Faculty of Economics,
Business Administration and Information Technology
of the University of Zurich

to obtain the degree of
Doctor of Neuroeconomics, Dr. sc.

presented by

Chaohui Guo
from China

Approved in April 2014 at the request of
Prof. Dr. Ernst Fehr
Prof. Dr. Todd Hare

The Faculty of Economics, Business Administration and Information Technology of the University of Zurich hereby authorizes the printing of this dissertation, without indicating an opinion of the views expressed in the work.

Zurich, 02.04.2014
Chairman of the Doctoral Board: Prof. Dr. Todd Hare

To hardworking, optimism and persistence.

Acknowledgements

During the past years of my PhD studies, I received a lot of support and kind help from my supervisors, advisors, colleagues and friends. Here I would like to express my sincerest gratitude to the following people and institutions:

First of all, to my supervisor Ernst Fehr. His scientific research inspired me and was one important reason why I started this endeavor. This thesis and my research projects would not have been possible without his constant support and the inspiring discussions I had with him.

Second, to my co-supervisor Todd Hare for his valuable feedback and suggestions for my research projects and this thesis.

Third, to all of my collaborators: Kerstin Preuschoff, Yosuke Morishma, Christian Ruff, Sunhae Sul and Nora Heinzelmann. Particularly, Kerstin Preuschoff was my co-advisor during the first year of PhD studies and kindly provided me with much guidance and led me into the projects on learning behavior under uncertainty. Yosuke was my officemate and I learned many practical skills in data analysis from him.

Fourth, to my colleagues: Friederike Meyer, Tony Williams, Justin Chumbley, Thomas Epper, Aidan Makwana, Susanna Weber, Rafael Polania and others from whom I have learned a lot through our valuable discussions. Also I greatly appreciate their comments and suggestions for my thesis.

Fifth, to Sally Gschwend and Helen Bernhard for their great support with the administrative stuff during my PhD studies.

Sixth, I gratefully acknowledge financial support of the System X and National Centres of Competence in Research (NCCR).

Last but not least, my deepest gratitude goes to my parents for their unconditional love and long-lasting support.

TABLE OF CONTENT

1. Introduction

Neuroeconomics (NE) is an interdisciplinary subject that spans over multiple domains such as neuroscience, economics, and psychology. Despite the common goal of understanding how humans make decisions, the research of these disciplines was isolated from one another. NE has been developed to combine the methodologies and evidence from these disciplines and ultimately to produce computational and neurobiological accounts of decision-making (Fehr and Rangel 2011; Glimcher 2011; Glimcher and Rustichini 2004; Camerer 2013; Camerer, Loewenstein, and Prelec 2005; Camerer, Bhatt, and Hsu 2007; Camerer 2007; Camerer, Loewenstein, and Prelec 2004). The development of NE has greatly relied on the technology of measuring brain activity and is closely related to the research in other domains such as neuroscience, economics and psychiatry. In the following, I will briefly introduce the methodology in NE research and how research in NE can deepen our understanding of human behavior and improve research in other domains such as neuroscience, economics and psychiatry.

1.1 Methodology

Functional magnetic resonance imaging (fMRI) is a widely used technique to study neural mechanisms underpinning human behavior. It measures brain activity through oxygenated blood flow in the brain. Due to its good spatial resolution (millimeters) and fine temporal resolution (seconds), fMRI has been the most commonly used technique in NE research to identify the brain regions whose activity are associated with a decision-making process. Notably, it is often difficult to conclude on the functional necessity of regions for a specific task solely based on fMRI results. Several other approaches can aid fMRI on this issue and provide more insights. Such approaches include transcranial magnetic stimulation (TMS), transcranial direct-current stimulation (tDCS), pharmacological interventions (e.g. Oxytocin), and studying patients with lesions. Another branch of techniques focuses on the anatomical architectures of the brain. One such technique is Voxel-based morphometry (VBM), a neuroimaging analysis method that can be used to study

differences in brain anatomy across individuals or between groups. Such inter-individual anatomical differences can then be associated with individual characteristics, dispositions and stable preferences. Due to the view that the brain is a dynamic network, there has been an increased interest to investigate the connectivity between different brain regions. Approaches to study brain connectivity include resting state functional connectivity, dynamic causal modelling, diffusion tensor imaging etc. Due to the limitations of each method, recently more researchers have attempted to combine multiple approaches in a study. For example, studies combining fMRI and VBM allow us to link the functional and anatomical evidence to better understand the functions of brain regions (Morishima et al. 2012), and the combination of genetics with fMRI to identify the genetic determinants of brain functions (Fang et al. 2013).

1.2 Neuroeconomics improves research in neuroscience

NE shares many research questions of neuroscience, namely to establish knowledge to promote the understanding and explanation of human behavior, but with a focus on decision-making in economic environments. NE integrates the traditional neuroscience research with behavioral economics and opens up new inquiries that are closely linked to real-life decision-making. For example, paradigms in behavioral economics such as the Dictator game, the Ultimatum game, and the Trust game have been widely used in NE studies to identify the neural substrates for various components of social preferences (Fehr and Camerer 2007). Similarly, the measurements of economic preferences in the financial domain (e.g. risk, ambiguity, and inter-temporal preferences) have been adopted in neuroscience studies to identify the neural networks involved in financial decision-making such as saving and investment behavior (Knutson and Bossaerts 2007; Kable and Glimcher 2010; Kable and Glimcher 2007; Tymula et al. 2012; Brevers et al. 2012; Camerer, Bhatt, and Hsu 2007). These experimental paradigms improve the traditional measurement of human behavior in neuroscience, as these tasks provide clear incentives and similar social contexts as in real life.

NE also brings new inquiries and opens up new research regimes for neuroscience research. For example, one set of inquiries focus on the link between neural signals in

the brain and the constructs proposed in behavioral economics, such as the preference for immediate reward, ambiguity aversion, preference for fairness and altruism (Kable and Glimcher 2010; Morishima et al. 2012; Brevers et al. 2012; Baumgartner et al. 2011; Moll et al. 2006). Such understanding of the neural substrates for these variables permits predictions of human behavior (Tanaka et al. 2004; Salas et al. 2010; Camerer 2007; Wang, Spezio, and Camerer 2010) and allows for tests on the causal role of brain areas through non-invasive stimulation techniques such as TMS and tDCS (Young et al. 2010; Camus et al. 2009; Santiesteban et al. 2012).

1.3 Neuroeconomics improves research in economics

There has been much debate and controversial opinions over the potential contributions that NE can bring to research in economics (Camerer, Loewenstein, and Prelec 2005; Fehr and Rangel 2011; Glimcher 2011; Gul and Pesendorfer 2008; Bernheim 2008). For example, Camerer et.al (2005) demonstrated the potential value of NE to economics by making an analogy to the development of organizational economics. However, some economists are not fully convinced by such conceptualized reasoning and request more concrete examples. Below I focus on several aspects to discuss how NE can improve the research in economics.

First, NE can aid economics in providing mechanistic explanations for human behavior. Economists often aim to not just describe but also explain people's decisions. NE describes logical operations that not only predict behavior but also closely approximate the underlying physical and mental processes that lead to these behaviors (Glimcher 2011). For example, altruistic punishment is a well-documented phenomenon in behavioral economic studies. There have been competing theories about the sources of such behaviors (Fehr and Fischbacher 2003; de Quervain 2004; Fehr and Schmidt 1999), and it is difficult to differentiate and pin down the most probable explanation solely based on behavioral observations. NE findings show that altruistic punishment behavior activates a region of reward processing (the dorsal striatum) and participants with stronger activations in this region were willing to incur greater costs for altruistic punishment (Quervain et al, 2004). These findings support the explanation that the satisfaction derived from punishing norm violations is one of the factors that drive the altruistic behavior (analogue to why humans seek out primary rewards such as food and sex).

Second, NE provides a new perspective to verify and select among economic models. NE can guide the search for appropriate empirical models, leading to more rapid and effective identification. A combination of neural measurement and experimental design allows for direct tests of the extent to which the computations made by the brain at the time of decision-making are consistent with the mechanisms posted by different theories (Frydman et al. 2011). The study by Hsu et al (2009) provides a good example showing how NE can guide the selection of the functional form of economic models (Hsu et al. 2009). Here they find that brain activity during valuation of monetary gambles is nonlinear in probabilities, suggesting that the probability distortions may be a ubiquitous feature of human perception and cognition (Zhang and Maloney 2012). This study, together with the neurobiology finding that the valuation systems are not reference-point independent (Glimcher 2011), provide economists with additional reasons besides predictive considerations to favour prospect theory over traditional EUT models.

Another example is a study that aims to test competing theories of the disposition effect (i.e. the tendency of investors to sell assets whose price has increased, while keeping assets that have dropped in value) (Frydman et al. 2011). They find that activity in an area of the brain known to encode the value of decisions (i.e. ventral medial prefrontal cortex) correlates with the outcomes of trades, and that the size of these neural signals correlates across subjects with the strength of the behavioral disposition effects. Furthermore, they find that activity in an area of the brain known to encode experienced utility (e.g. ventral striatum) exhibits a sharp upward spike in activity at precisely the moment at which a subject issues a command to sell a stock at a gain. These results strongly support realization utility theory that assumes that in addition to deriving utility from consumption, investors also derive utility directly from realizing gains and losses on the sale of risky assets that they own (Barberis and Xiong 2012; Caplin and Leahy 2001). By contrast, they find no significant association between the functional activity of these regions and the predictions from other theories (e.g. the mean-reversion model).

Third, NE can help to develop new models with neurophysiological variables. Recent studies have started to develop this branch of research. For example, based on the premise that cognitive mechanisms (e.g. attention) affect behavior independently of preferences, an economic theory of addiction is developed by including psychological

variables (e.g. internal visceral states) in the model (Bernheim and Rangel 2004). Another example is that the experienced feelings related to our uncertainty about the future are incorporated to extend the expected utility theory, which can better explain behaviors inconsistent with standard rational economic models (Caplin and Leahy 2001).

Fourth, NE can help to make out of sample predictions. Prediction is one of the most important goals of positive economics. Economists wish to predict behavior under completely novel conditions (e.g. a new public policy). Models that do not take into account the mechanistic explanations often fail to provide reliable and robust out of sample predictions. In contrast, a good structural model, based on a deeper understanding of behavior, may permit reasonable predictions even when fundamental environmental changes occur (Camerer 2013). Due to the fact that the variance in behavior is ultimately mediated through the brain, the neurobiological signals contain important information to directly predict behavior. Mental states (e.g. conscious attention, fatigue, pain, and hunger, anxiety) have been shown to be very helpful in predicting choices (Loewenstein 2000; Loewenstein 1996; Caplin and Leahy 2001). NE provides some approaches to measure mental states, such as skin conductance, eye tracking, Electromyography (EMG), and facial action coding analysis. Moreover, it has been shown that financial choices can be predicted by antecedent neural activity (Knutson and Bossaerts 2007). A recent study demonstrates that non-choice neural data can be used for out of sample prediction (Smith et al. 2012). They find that non-choice neural responses from the whole brain measured by fMRI can be used to predict real choices made by a particular individual, or average decisions made by a group of individuals in new choice situations with modest prediction power.

1.4 Neuroeconomics improves research in psychiatry

Psychiatric disorders are among the most prevalent and costly ailments worldwide, which have caused devastating personal and family consequences, and high social and health care service costs (Kessler et al. 2005). Current treatments for psychiatric disorders include medications, cognitive-behavioral psychotherapy, electroconvulsive therapy etc. (Association 2006). However, there are still a large proportion of patients who do not respond adequately to available treatments and even for the patients who

respond well to treatment, relapse is quite common (Simpson et al. 2008). Therefore, there is great need for new techniques and perspectives to improve existing treatments.

Current psychiatric diagnoses are mostly based on clusters of symptoms and are inherently atheoretical. NE concepts may offer a potential integrated computationally based framework for understanding psychiatric problems and even improve the existing diagnosis and treatments. In the perspective of NE, people with mental disorders are considered as active agents, who attempts to make plans and obtain desired outcomes based on their judgments of the current and future states of environments. This perspective straightforwardly leads to the speculation that psychiatric disorders may be due to alternations or disruptions in the valuation process, such as reward perception, probability perception, and value assignment (Barke & Fairchild, 2012). It is proposed that a disrupted reward perception system would lead to the decreased ability to experience pleasure, one of the main symptoms of major depression. This speculation is supported by the study that deep brain stimulation (DBS) modulation of the NAcc had positive effects on anhedonia, which effectively led to an antidepressant treatment response (Schlaepfer et al, 2008). Notably, such improvement is shown in only a proportion of patients, and some adverse effects are observed in some patients after DBS treatments, suggesting the existence of more complicated causes for depression.

Moreover, many other domains of NE research can also shed light on the mechanisms and diagnoses of a variety of psychiatric disorders. For example, the understandings of social cognition may help us to better recognize the causes for autism and psychopathy. Studies on decision-making under risk, ambiguity, and over time may improve our understanding in disorders including anxiety disorders, addiction, ADHD, OCD, and conduct disorder.

2. Contents of this Thesis

In this thesis, my research aims to deepen our understanding of the neurobiological basis of charitable giving and learning behavior under uncertainty. I present three papers that offer novel insights on the neural mechanisms supporting human altruistic and learning behaviors. The key insights are summarized as follows.

My first paper finds that human altruistic behaviors can be modulated through disrupting the functional activity of one brain area that has been proposed to be important for altruism, the right Temporoparietal Junction (rTPJ). Our study provides the first evidence that human altruism causally depends on the functional integrity of the rTPJ, beyond the previous correlational evidence.

The second paper shows that the functional activity of locus coeruleus (LC) in the midbrain is associated with the learning rate in a changing environment. The learning rate is a fundamental parameter in reinforcement learning models that reflects the weight given to new information. Here I provide the first direct evidence for the direct link between the functional involvement of LC and the adaptive learning rate.

The third paper demonstrates that the individual learning ability in a changing environment is associated with both the grey matter (GM) volume and the functional involvement of some key regions in the sensorimotor learning system (e.g. the cerebellum). My findings suggest that the information-updating mechanism of the sensory-motor system also subserves the belief updating process in higher-level decision-making under uncertainty.

The remainder of this paper is structured as follows. A summary of each chapter in this thesis is provided in 2.1 to 2.3, respectively. Section 3 provides the discussion of my findings and a short outlook of the future research agenda.

2.1 The Causal Dependence of Human Altruism on the Functional Integrity of the Right TPJ

Human altruism has been an important evolutionary force and shapes contemporary social and economic interactions. Converging evidence documents correlations between the functional activity and neuroanotomical structures of the right Temporoparietal Junction (rTPJ) and human altruistic behavior. However, correlation does not imply causation as it is not known whether rTPJ activity causes people to be altruistic or whether altruistic choice induces rTPJ activity. The aim of this study is to provide causal evidence for the involvement of rTPJ in altruistic behavior by disrupting neural activity in rTPJ using transcranial magnetic stimulation (TMS). A total of 61 healthy subjects participated in this experiment and were randomly assigned to either the treatment (rTPJ) or control group (vertex). They were asked to complete a set of tasks. I measured subjects' judgments about 70 charities by asking them to rate the charities on deservingness, closeness, familiarity and charity age on a 5-point-scale before TMS was applied. Immediately after the application of TMS subjects started a donation task, in which they were endowed with 100 points (50 CHF) and asked to decide the amounts they would like to donate to each charity. One trial was randomly chosen at the end of the experiment. The amount donated in the chosen trial was transferred to the charity anonymously and the rest was given to the subject as payment. Following this, subjects re-evaluated a random half of the 70 charities on the four dimensions while the effects of TMS were still lasting. I included this step to test the hypothesis whether the perceived deservingness of the charities was changed by TMS. In this study I show that the disruption of rTPJ by theta-burst repetitive transcranial magnetic stimulation (TMS) substantially reduces subjects' donations to charities. Specifically, I find that the decreased charitable donations are probably driven by a decrease of willingness to donate but not by the change of perceived deservingness of charities. Moreover, I find that such effects of disrupting rTPJ activity are more pronounced for charities with concrete and vivid social contexts. These findings suggest a strong causal dependence of human altruism on the functional integrity of the rTPJ that seems to be causally involved in the encoding of the willingness to help rather than the perceptions of deservingness.

2.2 Neural Correlates of Learning Rate in a Changing Environment

Our interactions with the environment always involve imperfect observations. Updating beliefs correctly based on new observations is central to learning behaviors. The learning rate (LR) is a fundamental parameter in reinforcement learning models that reflects the weight given to new information. However, the neural substrates that encode the LR still remain unclear. Locus coeruleus (LC) has been proposed as the core component of the neural network of learning under uncertainty, which signals unexpected uncertainty and has other sophisticated regulation function in learning under uncertainty. There has also been indirect evidence that associates the functional activity of LC with the LR, while the direct empirical functional evidence is still missing.

To answer this question, I conduct an fMRI study in which subjects complete a number-guessing task. In this task, subjects are asked to guess the mean of the underlying distribution based on a series of samples while the mean and the noise level of the underlying distribution can both change unexpectedly for multiple times over a session. I estimate the learning rates based on a reinforcement learning model. The learning rates are then used as parametric modulators to trace the corresponding neural correlates. I find that participants' LRs vary according to local statistical features: (i) The LR is lower in contexts with a higher noise level, and (ii) The LR is higher in contexts with a changing mean and a stable noise level (a relevant change) compared to contexts with a stable mean and a changing noise level (an irrelevant change. Furthermore, I find that the adaptive LR is positively correlated with the functional activity of a region in pons, consistent with the position of locus coeruleus (LC), at the individual level, providing the first direct empirical evidence for the link between functional activity of LC and the adaptive LR.

2.3 Structural and Functional Neural Correlates of Individual Learning Ability

Individuals differ in their ability to learn the state of the world and hidden reward contingencies, particularly when the situation involves a high degree of uncertainty.

However, it still remains unclear what the neuroanatomical determinants underlying such heterogeneity are. Here I measure individual learning ability by comparing the learning performance of each individual with that of a Bayesian updating model. I find that there is a large variety in learning performance across subjects and such individual differences are associated with both the grey matter (GM) volume and functional involvement of cerebellum and a brain area covering the right postcentral gyrus, Inferior Parietal cortex and Supramarginal gyrus (I label this cluster as right postcentral parietal cortex). These results provide congruent evidence for the importance of the cerebellum, postcentral and parietal cortex in information integration and suggest a link between the lower-order sensory-motor information processing and the foresight process in higher-order learning under uncertainty.

3. Conclusion and discussion

The studies in my thesis provide empirical evidence and new insights for the existing theories on the neurobiology of altruism and learning behavior, and open up a branch of new research. Below I discuss these findings and provide some principle directions worth pursuing in future research.

In the first chapter, I find that disruption of the neural activity in rTPJ reduces charitable donations. Specifically, I find that the decreased charitable donations are probably driven by the decreased willingness to donate but not the perceived deservingness of charities. Moreover, I find that these effects of disrupting rTPJ activity are more evident for charities with more concrete and vivid social contexts. These findings suggest a strong causal dependence of human altruism on the functional integrity of the rTPJ that seems to be causally involved in the encoding of the willingness to help rather than the perceptions of deservingness. My TMS study provides empirical evidence of and new insights into the neurobiology of altruism. A model motivated by neuroimaging data is that altruistic decisions are constructed via the online computations in VMPFC, the general valuation region, by weighting information from multiple sources, such as the deservingness of the recipients and self-interest (*4*, *15*). Our findings suggest that rTPJ is not involved in the social perception per se, but rather in linking social knowledge to the construction of value signals. Further elucidation of the generalization of this causal role of rTPJ in other forms of altruism will be an important aspect of future research. In addition, my findings may shed light on the neural basis of inconsistent donation behavior in different contexts. For example, contexts directing one's attention to others can increase altruistic behaviors, such as having an imagined conversation or receiving a direct eye gaze before making decisions (Lin et al. 2012; Batson et al. 1988; Andreoni and Rao 2011). I speculate that these approaches successfully up-regulate the activity in rTPJ, which induces an increased willingness to conduct altruistic behaviors, just as a smell of freshly baked bread increases the purchase of bread. This may provide some insight into ways to pre-test the effectiveness of fundraising strategies, e.g. testing whether one strategy can induce higher activity in TPJ, which might be of great interest to non-profit organizations and charities as donations are their major

funding sources. Moreover, my results may expand economic models of charitable giving by incorporating the neural activity of rTPJ as a component in the models. Furthermore, my results fit in well with recent work on neuro-developmental disorders. Autism spectrum disorders (ASDs) typically have impairments in social abilities and are found to have deficiencies in the development of TPJ such as decreased grey matter volume (Steyer et al.; Greimel et al. 2012). Based on my results, I speculated that compared to normal controls, ASDs would have reduced donations and a decreased dependency of donations on judgments of charities. These are exactly the findings reported in a recent study on ASDs (Lin et al. 2012). This study expands previous neuroimaging findings and lends empirical evidence for the causal role of rTPJ in charitable giving. Still, I are not able to conclude the degree to which the observed effects are specific to the targeted region or instead reflect the combined result of the target and other regions to which it is connected, due to the limitation of TMS that the effects might spread over time to regions connected to the target rTPJ.

In the second chapter, I find that subjects adopt adaptive LR according to the local volatility and noise level, and such adaptive learning rate is associated with the functional activity of a region in pons, a position consistent with LC. These findings provide the first direct empirical evidence for the link between the functional involvement of LC and the adaptive LR, supporting the crucial role of LC in the regulation of optimal learning under uncertainty (Yu and Dayan 2003; Aston-Jones and Cohen 2005). Additionally, I find that a transient component of the learning rate is positively correlated with the functional activity of a different set of regions, ACC and RIFG, two core regions in the monitoring system, which have been documented to engage in swift cognitive control and working memory (e.g. Aron, Robbins, and Poldrack 2004; Chikazoe et al. 2007; Krawczyk 2002; Botvinick, Cohen, and Carter 2004; Holroyd et al. 2004; Achtziger et al. 2012). Moreover, the co-activation of ACC and RIFG was associated with the performance after a change of the reward contingency in reversal learning (Ghahremani et al. 2010). The encoding of LR can be a complex cognitive function that encompasses a diverse range of processes involved in linking multiple sources of information and selective retrieval of information from memory, which may be supported by anatomically distributed brain networks that share information in a dynamic manner. My findings here suggest that there may be two parallel systems supporting the adaptive adjustment of LR. The first system,

including LC, is mainly involved in tracking the average features of a recent history and adapt LR accordingly; whereas the second system, including ACC and RIFG, compensate the first system by providing more precise and swift adjustment based on spontaneous information at each time point. Some existing evidence supports this speculation. For example, it has been found that ACC and LC closely interact with each other in learning under uncertainty (e.g. Yu & Dayan, 2005). However, the dissociation and specific role of each network requires further research.

In the third chapter, I find that there is great heterogeneity in individual learning performances in a changing environment and that such individual differences are associated with the GM volume of regions in the cerebellum and right postcentral parietal cortex and with the functional involvement of these two regions during learning. These findings provide congruent structural and functional evidence for the importance of the cerebellum and right postcentral parietal cortex in successful learning and information integration. Our finding that the GM volume and functional involvement of cerebellum and postcentral parietal cortex are associated with individual learning performance suggest a link between the lower-order sensory-motor information processing and the belief updating process in higher-order learning under uncertainty. During evolution of human beings, higher cognitive functions evolved from the basic sensory-motor functions. Therefore, it is possible that the information updating mechanism of the sensory-motor system also serves the higher-level learning under uncertainty. Consistently, it has been reported that a relationship exists between the cerebellar brain volume and cognitive function (Hogan et al. 2011), between abnormal exploration in autism and cerebellum abnormality and between cerebellum brain volume with children with attention deficit hyperactivity (ADHD) (Pierce and Courchesne 2001).Furthermore, my findings may shed new light on developing treatments for clinical psychological patients. Negative emotions (e.g. frustration, anxiety and helplessness) and even psychological disorder symptoms (e.g. depression and anxiety disorders) can be induced if individuals lack the ability to correctly learn the state of the world. On the one hand, individuals can deviate from optimal updating by overweighting the history, which leads to insensitivity to the fundamental changes of environments and failure to adapt to new situations. On the other hand, individuals may overweight new information, which causes over alertness and response to stochastic fluctuations. The cerebellum has been proposed to be a

highly plastic and good target for clinical interventions (Mackie et al. 2007), providing new approaches for improving individual's learning ability and consequently alleviating negative emotions. Finally, I would like to point out that the relatively small sample size employed in my study allowed for the detection of moderate-sized effects, while brain structures whose GM volume correlate with learning performance of a smaller magnitude were not able to detect. Future research is required to test the generalizability of my findings, with larger and more diverse samples of participants.

Bibliography

Achtziger, Anja, Carlos Alos-Ferrer, Sabine Hugelschafer, and Marco Steinhauser. 2012. "The Neural Basis of Belief Updating and Rational Decision Making." *Social Cognitive and Affective Neuroscience* (September).

Andreoni, James, and Justin M Rao. 2011. "The Power of Asking: How Communication Affects Selfishness, Empathy, and Altruism." *Journal of Public Economics* 95 (7-8) (August 1): 513–520.

Aron, A R, T W Robbins, and R A Poldrack. 2004. "Inhibition and the Right Inferior Frontal Cortex." *Trends in Cognitive Sciences*.

Association, American Psychiatric. 2006. "American Psychiatric Association Practice Guidelines for the Treatment of Psychiatric Disorders: Compendium 2006."

Aston-Jones, Gary, and Jonathan D Cohen. 2005. "An Integrative Theory of Locus Coeruleus-Norepinephrine Function: Adaptive Gain and Optimal Performance.." *Annual Review of Neuroscience* 28: 403–450.

Barberis, Nicholas, and Wei Xiong. 2012. "Realization Utility." *Journal of Financial Economics* 104 (2): 251–271.

Batson, C D, J L Dyck, J R Brandt, J G Batson, A L Powell, M R McMaster, and C Griffitt. 1988. "Five Studies Testing Two New Egoistic Alternatives to the Empathy-Altruism Hypothesis.." *Journal of Personality and Social Psychology* 55 (1): 52.

Baumgartner, Thomas, Daria Knoch, Philine Hotz, Christoph Eisenegger, and Ernst Fehr. 2011. "Dorsolateral and Ventromedial Prefrontal Cortex Orchestrate Normative Choice." *Nature Neuroscience* 14 (11) (October 2): 1468–1474.

Bernheim, B Douglas. 2008. "On the Potential of Neuroeconomics: a Critical (but Hopeful) Appraisal."

Bernheim, B Douglas, and Antonio Rangel. 2004. "Addiction and Cue-Triggered Decision Processes." *The American Economic Review*: 1558–1590.

Botvinick, M M, J D Cohen, and C S Carter. 2004. "Conflict Monitoring and Anterior Cingulate Cortex: an Update." *Trends in Cognitive Sciences*.

Brevers, Damien, Axel Cleeremans, Anna E Goudriaan, Antoine Bechara, Charles Kornreich, Paul Verbanck, and Xavier Noël. 2012. "Decision Making Under Ambiguity but Not Under Risk Is Related to Problem Gambling Severity." *Psychiatry Research* 200 (2): 568–574.

Camerer, Colin F. 2007. "Neuroeconomics: Using Neuroscience to Make Economic

Predictions" 117 (519): C26–C42.

Camerer, Colin F. 2013. "Goals, Methods, and Progress in Neuroeconomics." *Annual Review of Economics* (0).

Camerer, Colin F, George Loewenstein, and Drazen Prelec. 2004. "Neuroeconomics: Why Economics Needs Brains." *The Scandinavian Journal of Economics* 106 (3): 555–579.

Camerer, Colin F, Meghana Bhatt, and Ming Hsu. 2007. "Neuroeconomics: Illustrated by the Study of Ambiguity Aversion." *Economics and Psychology: a Promising New Cross-Disciplinary Field, Bruno S. Frey and Alois Stutzer, Eds. Cambridge, MA: MIT Press*.

Camerer, Colin, George Loewenstein, and Drazen Prelec. 2005. "Neuroeconomics: How Neuroscience Can Inform Economics." *Journal of Economic Literature*: 9–64.

Camus, Mickael, Neil Halelamien, Hilke Plassmann, Shinsuke Shimojo, John O Doherty, Colin Camerer, and Antonio Rangel. 2009. "Repetitive Transcranial Magnetic Stimulation Over the Right Dorsolateral Prefrontal Cortex Decreases Valuations During Food Choices." *European Journal of Neuroscience* 30 (10) (November): 1980–1988.

Caplin, Andrew, and John Leahy. 2001. "Psychological Expected Utility Theory and Anticipatory Feelings." *The Quarterly Journal of Economics* 116 (1): 55–79.

Chikazoe, J, S Konishi, T Asari, and K Jimura. 2007. "Activation of Right Inferior Frontal Gyrus During Response Inhibition Across Response Modalities." *Journal of Cognitive Neuroscience*.

de Quervain, D J F. 2004. "The Neural Basis of Altruistic Punishment." *Science* 305 (5688) (August 27): 1254–1258.

Fang, Zhuo, Senhua Zhu, Seth J Gillihan, Marc Korczykowski, John A Detre, and Hengyi Rao. 2013. "Serotonin Transporter Genotype Modulates Functional Connectivity Between Amygdala and PCC/PCu During Mood Recovery." *Frontiers in Human Neuroscience* 7: 704.

Fehr, Ernst, and Antonio Rangel. 2011. "Neuroeconomic Foundations of Economic Choice Recent Advances." *The Journal of Economic Perspectives* 25 (4): 3–30.

Fehr, Ernst, and Colin F Camerer. 2007. "Social Neuroeconomics: the Neural Circuitry of Social Preferences." *Trends in Cognitive Sciences* 11 (10) (October): 419–427.

Fehr, Ernst, and Klaus M Schmidt. 1999. "A Theory of Fairness, Competition, and Cooperation." *The Quarterly Journal of Economics* 114 (3): 817–868.

Fehr, Ernst, and Urs Fischbacher. 2003. "The Nature of Human Altruism." *Nature* 425 (6960) (October 23): 785–791.

Frydman, Cary, Nicholas Barberis, Colin Camerer, Peter Bossaerts, and Antonio Rangel. 2011. "Testing Theories of Investor Behavior Using Neural Data." *Available at SSRN*.

Ghahremani, D G, J Monterosso, J D Jentsch, R M Bilder, and R A Poldrack. 2010. "Neural Components Underlying Behavioral Flexibility in Human Reversal Learning." *Cerebral Cortex* 20 (8) (July 9): 1843–1852.

Glimcher, Paul W. 2011. "Foundations of Neuroeconomic Analysis."

Glimcher, Paul W, and Aldo Rustichini. 2004. "Neuroeconomics: the Consilience of Brain and Decision." *Science* 306 (5695): 447–452.

Greimel, Ellen, Barbara Nehrkorn, Martin Schulte-Rüther, Gereon R Fink, Thomas Nickl-Jockschat, Beate Herpertz-Dahlmann, Kerstin Konrad, and Simon B Eickhoff. 2012. "Changes in Grey Matter Development in Autism Spectrum Disorder." *Brain Structure and Function* 218 (4) (July 10): 929–942.

Gul, Faruk, and Wolfgang Pesendorfer. 2008. "The Case for Mindless Economics." *The Foundations of Positive and Normative Economics*: 3–39.

Hare, Todd A, Colin F Camerer, Daniel T Knoepfle, and Antonio Rangel. 2010. "Value Computations in Ventral Medial Prefrontal Cortex During Charitable Decision Making Incorporate Input From Regions Involved in Social Cognition.." *The Journal of Neuroscience* 30 (2) (January 13): 583–590.

Hogan, Michael J, Roger T Staff, Brendan P Bunting, Alison D Murray, Trevor S Ahearn, Ian J Deary, and Lawrence J Whalley. 2011. "Cerebellar Brain Volume Accounts for Variance in Cognitive Performance in Older Adults." *Cortex; a Journal Devoted to the Study of the Nervous System and Behavior* 47 (4) (April): 441–450.

Holroyd, Clay B, Sander Nieuwenhuis, Nick Yeung, Leigh Nystrom, Rogier B Mars, Michael G H Coles, and Jonathan D Cohen. 2004. "Dorsal Anterior Cingulate Cortex Shows fMRI Response to Internal and External Error Signals." *Nature Neuroscience* 7 (5) (May): 497–498.

Hsu, Ming, Ian Krajbich, Chen Zhao, and Colin F Camerer. 2009. "Neural Response to Reward Anticipation Under Risk Is Nonlinear in Probabilities." *The Journal of Neuroscience* 29 (7) (February): 2231–2237.

Kable, Joseph W, and Paul W Glimcher. 2007. "The Neural Correlates of Subjective Value During Intertemporal Choice." *Nature Neuroscience* 10 (12) (December): 1625–1633.

Kable, Joseph W, and Paul W Glimcher. 2010. "An 'as Soon as Possible' Effect in Human Intertemporal Decision Making: Behavioral Evidence and Neural Mechanisms." *Journal of Neurophysiology* 103 (5) (May): 2513–2531.

Kessler, Ronald C, Patricia Berglund, Olga Demler, Robert Jin, Kathleen R Merikangas, and Ellen E Walters. 2005. "Lifetime Prevalence and Age-of-Onset Distributions of DSM-IV Disorders in the National Comorbidity Survey Replication." *Archives of General Psychiatry* 62 (6) (June): 593–602.

Knutson, Brian, and Peter Bossaerts. 2007. "Neural Antecedents of Financial Decisions." *The Journal of Neuroscience* 27 (31): 8174–8177.

Krawczyk, Daniel C. 2002. "Contributions of the Prefrontal Cortex to the Neural Basis of Human Decision Making." *Neuroscience & Biobehavioral Reviews* 26 (6) (October): 631–664.

Lin, A, K Tsai, A Rangel, and R Adolphs. 2012. "Reduced Social Preferences in Autism: Evidence From Charitable Donations." *Journal of Neurodevelopmental Disorders* 4 (1): 8.

Loewenstein, G. 1996. "Out of Control: Visceral Influences on Behavior." *Organizational Behavior and Human Decision Processes* 65 (3): 272–292.

Loewenstein, G. 2000. "Emotions in Economic Theory and Economic Behavior." *The American Economic Review* 90 (2): 426–432.

Mackie, Susan, Philip Shaw, Rhoshel Lenroot, Ron Pierson, Deanna K Greenstein, Tom F 3rd Nugent, Wendy S Sharp, Jay N Giedd, and Judith L Rapoport. 2007. "Cerebellar Development and Clinical Outcome in Attention Deficit Hyperactivity Disorder.." *American Journal of Psychiatry* 164 (4) (April): 647–655.

Moll, J, F Krueger, R Zahn, M Pardini, R de Oliveira-Souza, and J Grafman. 2006. "Human Fronto–Mesolimbic Networks Guide Decisions About Charitable Donation." *Proceedings of the National Academy of Sciences* 103 (42): 15623–15628.

Morishima, Yosuke, Daniel Schunk, Adrian Bruhin, Christian C Ruff, and Ernst Fehr. 2012. "Linking Brain Structure and Activation in Temporoparietal Junction to Explain the Neurobiology of Human Altruism." *Neuron* 75 (1) (July): 73–79.

Pierce, K, and E Courchesne. 2001. "Evidence for a Cerebellar Role in Reduced Exploration and Stereotyped Behavior in Autism." *Biological Psychiatry* 49 (8) (April): 655–664.

Salas, Ramiro, Philip Baldwin, Mariella de Biasi, and P Read Montague. 2010. "BOLD Responses to Negative Reward Prediction Errors in Human Habenula." *Frontiers in Human Neuroscience* 4: 36.

Santiesteban, Idalmis, Michael J Banissy, Caroline Catmur, and Geoffrey Bird. 2012. "Enhancing Social Ability by Stimulating Right Temporoparietal Junction." *Current Biology: CB* 22 (23) (December 4): 2274–2277.

Smith, Alec, B Douglas Bernheim, Colin Camerer, Antonio Rangel, and Caltech HSS.

2012. “Neural Activity Reveals Preferences Without Choices.” *Work. Pap., Calif. Inst. Technol., Pasadena*.

Steyer, R, P Schwenkmezger, P Notz, and M Eid. “Befindlichkeitsfragebogen (MDBF) [Multidimensional Mood Questionnaire] (Hogrefe, Go¨ttingen, 1997).”

Tanaka, Saori C, Kenji Doya, Go Okada, Kazutaka Ueda, Yasumasa Okamoto, and Shigeto Yamawaki. 2004. “Prediction of Immediate and Future Rewards Differentially Recruits Cortico-Basal Ganglia Loops.” *Nature Neuroscience* 7 (8) (August): 887–893.

Tymula, Agnieszka, Lior A Rosenberg Belmaker, Amy K Roy, Lital Ruderman, Kirk Manson, Paul W Glimcher, and Ifat Levy. 2012. “Adolescents’ Risk-Taking Behavior Is Driven by Tolerance to Ambiguity.” *Proceedings of the National Academy of Sciences* 109 (42): 17135–17140.

Wang, Joseph Tao-yi, Michael Spezio, and Colin F Camerer. 2010. “Pinocchio's Pupil: Using Eyetracking and Pupil Dilation to Understand Truth Telling and Deception in Sender-Receiver Games.” *The American Economic Review*: 984–1007.

Young, L, J A Camprodon, M Hauser, A Pascual-Leone, and R Saxe. 2010. “Disruption of the Right Temporoparietal Junction with Transcranial Magnetic Stimulation Reduces the Role of Beliefs in Moral Judgments.” *Proceedings of the National Academy of Sciences* 107 (15) (April 13): 6753–6758.

Yu, Angela, and Peter Dayan. 2003. “Expected and Unexpected Uncertainty: ACh and NE in the Neocortex.” *Advances in Neural Information Processing Systems*: 173–180.

Zhang, Hang, and Laurence T Maloney. 2012. “Ubiquitous Log Odds: a Common Representation of Probability and Frequency Distortion in Perception, Action, and Cognition.” *Frontiers in Neuroscience* 6.

Appendix

A. The Causal Dependence of Human Altruism on the Functional Integrity of the Right Temporoparietal Junction

This chapter is joint work with Ernst Fehr, Christian Ruff, Sunhae Sul, and Nora Heinzelmann

The Causal Dependence of Human Altruism on the Functional Integrity of the Right Temporoparietal Junction

Chaohui Guo, Sunhae Sul, Nora Heinzelmann, Christian Ruff *, Ernst Fehr *

Abstract

Human altruism has been an important evolutionary force and shapes contemporary social and economic interactions. Converging evidence documents associations between the right Temporoparietal Junction (rTPJ) and human altruistic behavior. However, association does not imply causation as it is not known whether rTPJ activity causes people to be altruistic or whether altruistic choice induces rTPJ activity. In this study, we show that disruption of rTPJ by theta-burst repetitive transcranial magnetic stimulation (TMS) substantially reduces subjects' donations to charities. Specifically, we find that the decreased charitable donations are probably driven by a decrease of the willingness to donate but not by changes in the perceived deservingness of charities. Moreover, we find that the effects of disrupting rTPJ activity are more pronounced for charities with concrete and vivid social contexts. These findings suggest a strong causal dependence of human altruism on the functional integrity of the rTPJ that seems to be causally involved in the encoding of willingness to donate rather than the perceptions of deservingness.

Key words: charitable giving, Temporoparietal Junction, TMS, deservingness

Introduction

Charitable donations, as the major source of revenue for nonprofits and charities, play a crucial role in human society (Fang et al., 2013; Harbaugh, Mayr, & Burghart, 2007; Hare, Camerer, Knoepfle, & Rangel, 2010; Moll et al., 2006). Given such an important role, numerous scientific fields attempt to identify and understand the driving forces of charitable giving (Bekkers & Wiepking, 2011; E. Fehr & Camerer, 2007; Hare et al., 2010). Recent neuroimaging studies have started to explore the neurobiological basis of charitable giving (Behrens, Hunt, Woolrich, & Rushworth, 2008; Harbaugh et al., 2007; Hare et al., 2010; Moll et al., 2006; Tymula et al., 2012;). These studies show that charitable giving activates the fronto-mesolimbic network as well as neural regions involved in social cognition, suggesting that donation decisions are not fundamentally different from other costly choices and that the online computation of such decisions draws on multiple processes such as shifting attention to others, reward processing and valuation. In particular, right temporoparietal junction (rTPJ) seems to play a crucial role in charitable giving, as activity in rTPJ predicts subjects' donation amounts (Hare et al., 2010). Moreover, rTPJ has been shown to be functionally connected with the ventromedial prefrontal cortex (VMPFC), a region typically involved in valuation processes, during the online computation of donation decisions (Hare et al., 2010).

The importance of rTPJ in altruism is suggested by other findings as well. The rTPJ is known to be involved in tasks that require attention to others, such as perception of agency, mentalizing, empathy, theory of mind, perspective-taking and moral judgment (Decety & Lamm, 2007; Morishima et al., 2012; Santiesteban, Banissy, Catmur, & Bird, 2012; Young et al., 2010). These findings suggest an important functional role of rTPJ in theory of mind and attention to others, which may be a prerequisite of altruistic decisions. Moreover, the ability to focus on and take the perspective of others may facilitate altruism, as preschoolers with theory of mind abilities are more altruistic (Takagishi et al., 2010). Results from voxel-based morphometry show that gray matter volume in rTPJ predicts the propensity to behave altruistically. In addition, rTPJ shows stronger functional activity when participants face a higher conflict between altruistic and selfish acts (Morishima et al., 2012). These studies provide solid evidence for the correlation between the functional

activity of rTPJ and altruistic behaviors. However, correlation does not imply causation, as it is unknown whether the activity of rTPJ causes people to be altruistic or whether altruistic choice drives the activity of rTPJ. If the former case is true, rTPJ would be necessary for altruistic behaviors, and the modulation of the functional activity of rTPJ would cause a change in the altruistic decisions. By contrast, if the latter case is true, modulating the activity of rTPJ would not induce any change in the altruistic decisions. This leads to the empirical questions addressed in this study: Does charitable giving causally depend on the functional integrity of rTPJ? What is the specific functional role of rTPJ in the process of making donation decisions? To address these questions, we applied TMS, a technique that induces a temporary disruption of the activity in a brain region and allows researchers to investigate the causal relationship between brain regions and behavioral outcomes.

Donation decisions are influenced by the perceived deservingness of targets. It has been shown that people's donation amounts increase monotonically with respect to the perceived deservingness of charities (e.g. Hare et al., 2010). On the other hand, donation decisions are also greatly influenced by individual's willingness to donate when the perceived deservingness is controlled for (Frydman, Barberis, Camerer, Bossaerts, & Rangel, 2011; Hare et al., 2010). For example, a generous individual might donate more than a selfish one to a charity that they both consider as highly deserving. This leads to two plausible hypotheses concerning the role of rTPJ in charitable giving. One hypothesis is that rTPJ is involved in the encoding of the individual willingness to donate but not in the perception of deservingness per se. Under this hypothesis, disruption of rTPJ will lead to a decrease of the willingness to donate and consequently declined donations while the perceived deservingness remains unaffected (Figure 1A). This hypothesis is consistent with the finding that individuals with stronger rTPJ activation have higher willingness to donate (Hare et al., 2010). An alternative but equally plausible hypothesis is that rTPJ is necessary for the perceptions of the deservingness but not in the encoding of the willingness to donate. According to this hypothesis, disrupting the activity of rTPJ will cause a decrease in the perceived deservingness while the willingness to donate remains unaffected, which also leads to a decline in donations (Figure 1B).

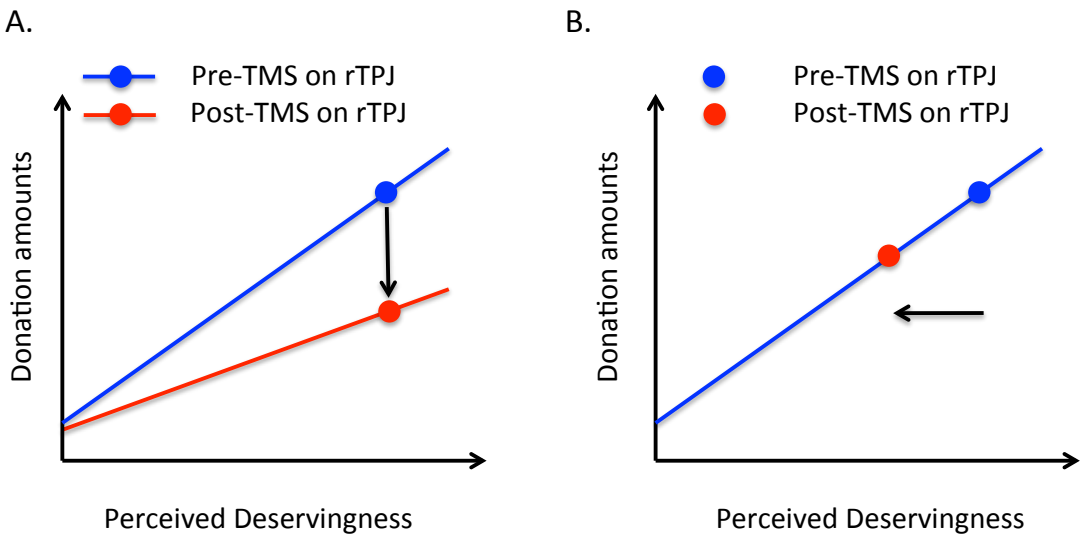

Figure 1. Schematic illustrations of our hypotheses. ***A***. Hypothesis one: rTPJ is involved in the encoding of the willingness to donate but not in the perception of deservingness per se. Under this hypothesis, the disruption of rTPJ will lead to a decrease of the willingness to donate and consequently a decline in donations while the perceived deservingness remains unaffected, i.e. a shift from the pre-TMS (blue line) to the post-TMS (red line). ***B***. Hypothesis two: rTPJ is involved in the forming or getting access to the deservingness of charities but not in the encoding of willingness to donate. According to this hypothesis, disruption of rTPJ will cause a decrease in the perceived deservingness and consequently decreased donations (i.e. a shift from the blue dot to the red dot), while the relationship slope between donations and perceived deservingness remains unaffected.

Methods

To test our hypotheses, we employed continuous theta burst stimulation (cTBS) to disrupt the activity of the target region (rTPJ for the treatment and vertex for control group). cTBS is an effective repetitive TMS protocol that produces powerful and long-lasting (up to 60 min) effects after an application period of 40s. A total of 61 healthy subjects participated in our experiment and were randomly assigned to either the treatment (rTPJ) or control group (vertex). They were asked to complete a set of tasks, and the timeline of tasks and TMS is described in Figure 2a. We first measured subjects' judgments towards 70 charities by asking them to rate the charities on

deservingness, closeness, familiarity and charity age on a 5-point-scale before TMS was applied. Closeness is defined here as the possibility that the subject or someone she knows can directly benefit from this charity). Closeness, familiarity and charity age were included as control dimensions. Immediately after the application of TMS, subjects performed a donation task. In the task, subjects were endowed with 100 points (50 CHF) and asked to decide how much they would like to donate to the charity presented on screen during the trial (Figure 2c). One trial was randomly chosen at the end of the experiment for payment. The donation on the chosen trial was transferred to the charity anonymously and the rest was kept by the subject as payment. After completing the donation task, subjects re-evaluated half of the 70 charities, selected at random, on the same four dimensions while still under the effects of TMS. We included this step to test whether the perceived deservingness of the charities was changed by TMS. Additional details are provided in the *Supplementary materials*.

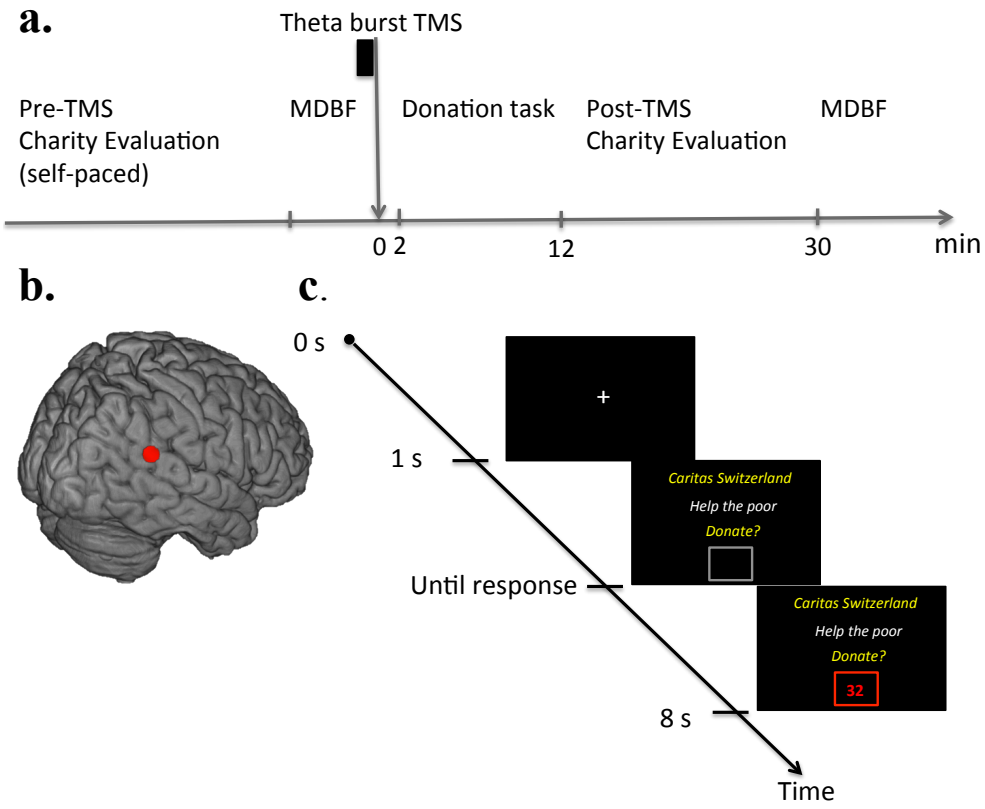

Figure 2. Experimental design. a. Experimental timeline. First, subjects completed a pre-TMS charity evaluation task. In this task subjects were presented with the name, mission, and a one-paragraph description of a charity on each trial and asked to rate the deservingness, closeness, familiarity and age of the charity on a 5-point-scale in a self-paced manner. Upon completion of the first part, subjects were asked to report their mood on a multidimensional mood questionnaire (MDBF, Steyer et.al, 1997). Afterwards, we evaluated the active motor threshold (AMT) for each subject and delivered the theta-burst TMS. Two minutes after the stimulation, subjects performed the donation task. Subjects were endowed 100 points (1 point = 0.5 CHF) for every trial and asked to decide how many points to donate to a given charity. Only one trial was randomly chosen and implemented for real at the end of the experiment. As soon as the donation task was completed, subjects started the post-TMS evaluation task, in which they evaluated a random half of the 70 charities on the four dimensions for the second time. At the end, subjects reported their mood on MDBF again. ***b.*** Stimulation site for TMS was defined as a 5-mm sphere around [51, -45, 21] on the MNI template, based on findings in a previous study (Hare et al, 2010), and then reverse normalized to each subject's anatomical brain (*Supplementary materials*). ***c.*** An example trial of the donation task. On each trial, subjects had 8s to input the donation amount.

Analysis and Results

To investigate whether charitable giving causally depends on the functional integrity of rTPJ, we performed multiple linear regression analysis with the donation amounts as the dependent variable, the site of TMS as the independent variable, and scores from questionnaires as control variables (details see *Supplementary materials, Material and methods*). The results of the multiple linear regression analysis are shown in Table S1. Our results demonstrate that there is a significant main effect of TMS treatment (treatment effect, β = -11.33, $p < .01$), i.e. donation amounts are significantly lower in the rTPJ group compared to the vertex group, suggesting that charitable giving causally depends on the functional integrity of rTPJ.

In a second step, we focused on understanding the specific functional role of rTPJ in the process of donation decisions. Our first hypothesis is that the disruption of rTPJ will decrease the willingness to donate and consequently cause a reduction of overall donations. To test this hypothesis, we performed multiple linear regression analysis with the donation amounts as the dependent variable, the site of TMS, the linear term of deservingness and the interaction term between deservingness and TMS as independent variables and other scores as control variables (*Supplementary materials, Material and methods*). The results of the multiple linear regression analysis are shown in Figure 3 and Table S2. First, our results replicate previous findings (Hare et al., 2010) and showed that donation amounts increased monotonically with deservingness (β = 12.77, $p < .001$). Second, our results demonstrate that, in addition to the main effect of treatment, there was a significant interaction effect of treatment (TMS site) and deservingness (β = -5.16, $p < .05$), i.e. the willingness to donate for each unit increase of deservingness was significantly decreased in the rTPJ compared to the vertex group. As shown in Figure 3, both groups had similarly low donations for the charities that were considered as not deserving at all (6 points for both groups), whereas the increasing donation amounts for each unit increase of the deservingness is significantly smaller in rTPJ group than the vertex group. Thus, our results demonstrate that disruption of rTPJ activity causes a decrease of willingness to donate, which are consistent with the predictions of our first hypothesis.

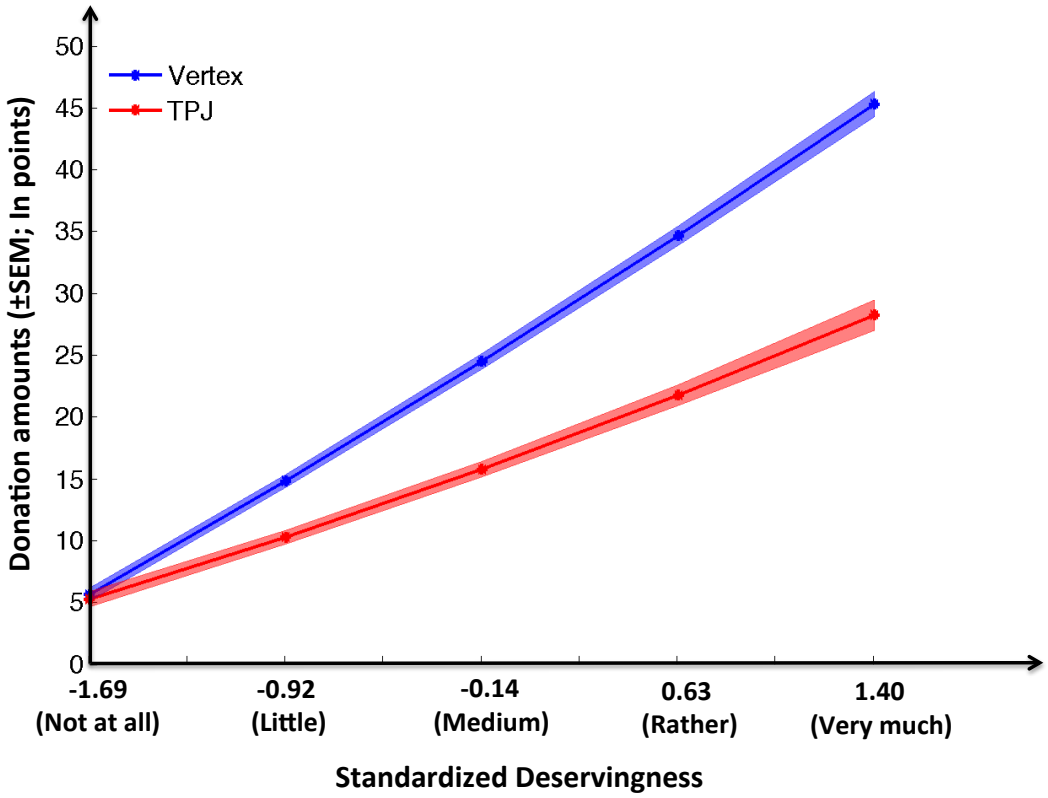

Figure 3. Treatment effects on willingness to donate. Predicted donations as a function of perceived deservingness (converted into z-scores) for vertex (blue) and rTPJ (red) groups based on estimations from multiple linear regression. Shaded areas represent bootstrapped standard errors (*Supplementary, Analyses and Table S2*). This figure is produced only for the purpose of illustration.

Next, we tested whether disrupting the activity of rTPJ influences the perceived deservingness of charities. We found that the deservingness ratings of pre-TMS are strongly correlated with those of post-TMS in both treatment groups (Pearson correlation, mean $r_{\_deservingness}$ = .80 for rTPJ and .79 for vertex), and the correlation coefficients do not differ between two groups (tested after Fisher's r-to-z transformation; Figure 4). These results suggest that disrupting the activity of rTPJ does not influence the perception of deservingness. Similarly, we found that disrupting rTPJ activity does not influence the judgments towards charities in any of the other dimensions (Pearson's correlation, $r_{\_closeness}$ = .64 for rTPJ and .68 for vertex; $r_{\_familiarity}$ = .80 for rTPJ and .83 for vertex; $r_{\_age}$ = .65 for rTPJ and .63 for vertex; tested after Fisher's r-to-z transformation; Figure S1). Our results demonstrate that

disruption of rTPJ activity decreased the willingness to donate while having no influence on the perceived deservingness of charities. Thus, these results support our hypothesis that rTPJ is involved in encoding the willingness to donate but not in evaluating the deservingness of charities.

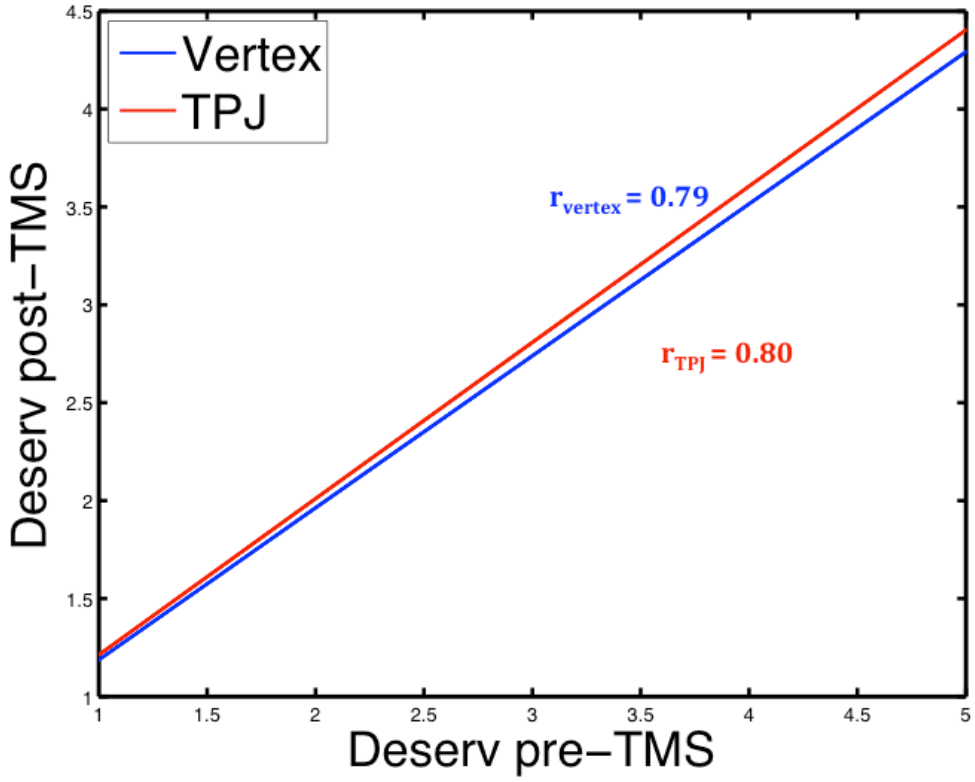

Figure 4. Perceived deservingness was not affected by TMS treatment. Deservingness ratings of pre-TMS were strongly correlated with those of post-TMS in both rTPJ and vertex group (Pearson correlation, mean $r_{\_deservingness}$ = .80 for rTPJ and .79 for vertex), and the correlation coefficients do not differ between two groups (tested after Fisher's r-to-z transformation). We illustrate the linear regression line with the deservingness of post-TMS as the dependent variable and the deservingness of pre-TMS as the independent variable for the Vertex (blue) and TPJ (red) group.

Moreover, based on recent findings that rTPJ has special importance for human behavior in social contexts (Andreoni & Rao, 2011; Batson et al., 1988; Carter et al., 2012; Carter & Huettel, 2013), we predicted that disrupting the rTPJ activity would

have a larger influence on charitable giving for charities with more concrete and vivid social context. To test this prediction, we first classified our charities into two types according to the direct targets of charities. Charities are classified as Human-charity if the recipients of charitable aid are human (e.g. disabled) and Non-human-charity if the recipients are not human (e.g. rainforest, animal shelter), resulting in 51 Human-charity and 19 Non-human-charity. Next, we performed separate linear regressions, as in the second step, for the Human-charity and Non-human-charity classes (Table S3 and S4). Our results showed that there were significant main effect of treatment (β = -8.63, $p < .05$) and interaction effect of treatment and deservingness (β = -6.36, $p < .05$) for the Human-charity, but not for the Non-human-charity. These findings are consistent with our predictions and suggest that rTPJ plays a more important role in donations to charities with humans as recipients of aid than to those with non-humans as direct targets.

Furthermore, to examine whether the application of TMS on different sites induced different levels of discomforts and mood changes for the two treatment groups, we performed linear regressions for the change of mood in three subscales (good-bad, awake-tired, calm-nervous) as a function of treatment group. The results showed that the change of mood did not differ between the two groups in any of the subscales (*Supplementary Table S6*).

Discussion

Taken together, we find that disruption of neural activity in rTPJ reduces charitable donations. Specifically, we find that lower charitable donations are probably caused by the decreased willingness to donate but not by the changes in the perceived deservingness of charities. Moreover, we find that the effect of disrupting rTPJ activity is more pronounced for charities with concrete social contexts. These findings enable us to claim a causal dependency of charitable giving on the functional integrity of rTPJ that seems to be causally involved in the encoding of willingness to donate rather than the perceptions of deservingness.

Our TMS study provides empirical evidence of and new insights into the neurobiology of human altruism. A model motivated by neuroimaging data is that altruistic decisions are constructed via the online computations in VMPFC, the general valuation region, by weighting information from multiple sources, such as the deservingness of the recipients and self-interest (Hare et.al, 2010). Our findings suggest that rTPJ is involved in conveying social perceptions of deservingness to the valuation region (VMPFC) to make donation decisions. Notably, social knowledge and perceptions of charities remained unaffected by the change of the neural activity in rTPJ, additionally supporting the notion that rTPJ is not involved in the encoding of social perception per se, but rather in linking social knowledge to the construction of value signals. Further elucidation of the generalization of this causal role of rTPJ in other forms of altruism will be an important aspect of future research.

In addition, our findings may shed light on the neural basis of inconsistent donation behavior in different contexts. For example, contexts directing one's attention to others can increase altruistic behaviors, such as having an imagined conversation or receiving a direct eye gaze before making decisions (Andreoni & Rao, 2011; Batson et al., 1988). We speculate that these approaches successfully up-regulate the activity in rTPJ, which induces an increased willingness to perform altruistic behaviors, just as a smell of freshly baked bread increases the purchase of bread. This may provide some insight into ways to pre-test the effectiveness of fundraising strategies, e.g. testing whether one strategy can induce higher activity in rTPJ, which might be of great interest to non-profit organizations and charities as donations are their major sources of funding. Moreover, our results may expand economic models of charitable giving by incorporating the neural activity of rTPJ as a component in the models.

Finally, our results well relate to recent work on neuro-developmental disorders. Individuals diagnosed with autism spectrum disorders (ASDs) typically have impairments in social abilities and are found to have deficiencies in the development of TPJ such as decreased grey matter volume (Greimel et al., 2012). Based on our results, we speculate that, compared to healthy controls, ASDs would have reduced donations and a decreased dependency of donations on judgments of a charity's deservingness. These are exactly the findings reported in a recent study on ASDs (Lin et al., 2012).

This study expands previous neuroimaging findings and lends empirical evidence for the causal role of rTPJ in charitable giving. Still, we cannot conclude the degree to which the observed effects are specific to the targeted region or reflect the combined result of the target and other regions to which it is connected, due to the limitation of TMS that the effects might spread over time to regions connected to the target rTPJ.

References

Andreoni, J., & Rao, J. M. (2011). The power of asking: How communication affects selfishness, empathy, and altruism. *Journal of Public Economics*, *95*(7-8), 513–520.

Batson, C. D., Dyck, J. L., Brandt, J. R., Batson, J. G., Powell, A. L., McMaster, M. R., & Griffitt, C. (1988). Five studies testing two new egoistic alternatives to the empathy-altruism hypothesis. *Journal of Personality and Social Psychology*, *55*(1), 52.

Behrens, T. E. J., Hunt, L. T., Woolrich, M. W., & Rushworth, M. F. S. (2008). Associative learning of social value. *Nature*, *456*(7219), 245–249.

Bekkers, R., & Wiepking, P. (2011). Who gives? A literature review of predictors of charitable giving part one: religion, education, age and socialisation. *Voluntary Sector Review*, *2*(3), 337–365.

Camus, M., Halelamien, N., Plassmann, H., Shimojo, S., O Doherty, J., Camerer, C., & Rangel, A. (2009). Repetitive transcranial magnetic stimulation over the right dorsolateral prefrontal cortex decreases valuations during food choices. *European Journal of Neuroscience*, *30*(10), 1980–1988.

Carter, R. M., & Huettel, S. A. (2013). A nexus model of the temporal– parietal Junction. *Trends in Cognitive Sciences*, *17*(7), 328–336.

Carter, R. M., Bowling, D. L., Reeck, C., & Huettel, S. A. (2012). A Distinct Role of the Temporal-Parietal Junction in Predicting Socially Guided Decisions. *Science*, *337*(6090), 109–111.

de Quervain, D. J. F. (2004). The Neural Basis of Altruistic Punishment. *Science*, *305*(5688), 1254–1258.

Decety, J., & Lamm, C. (2007). The Role of the Right Temporoparietal Junction in Social Interaction: How Low-Level Computational Processes Contribute to Meta-Cognition. *The Neuroscientist*, *13*(6), 580–593.

Fehr, E., & Camerer, C. F. (2007). Social neuroeconomics: the neural circuitry of social preferences. *Trends in Cognitive Sciences*, *11*(10), 419–427.

Fehr, E., & Fischbacher, U. (2003). The nature of human altruism. *Nature*, *425*(6960), 785–791.

Morishima, Y., Schunk, D., Bruhin, A., Ruff, C. C., & Fehr, E. (2012). Linking brain structure and activation in temporoparietal junction to explain the neurobiology of human altruism. *Neuron*, *75*(1), 73–79.

Greimel, E., Nehrkorn, B., Schulte-Rüther, M., Fink, G. R., Nickl-Jockschat, T., Herpertz-Dahlmann, B., et al. (2012). Changes in grey matter development in autism spectrum disorder. *Brain Structure and Function*, *218*(4), 929–942.

Harbaugh, W. T., Mayr, U., & Burghart, D. R. (2007). Neural Responses to Taxation and Voluntary Giving Reveal Motives for Charitable Donations. *Science*, *316*(5831), 1622–1625.

Hare, T. A., Camerer, C. F., Knoepfle, D. T., & Rangel, A. (2010). Value computations in ventral medial prefrontal cortex during charitable decision making incorporate input from regions involved in social cognition. *The Journal of Neuroscience*, *30*(2), 583–590.

Lin, A., Tsai, K., Rangel, A., & Adolphs, R. (2012). Reduced social preferences in autism: evidence from charitable donations. *Journal of Neurodevelopmental Disorders*, *4*(1), 8.

Moll, J., Krueger, F., Zahn, R., Pardini, M., de Oliveira-Souza, R., & Grafman, J. (2006). Human fronto–mesolimbic networks guide decisions about charitable donation. *Proceedings of the National Academy of Sciences*, *103*(42), 15623–15628.

Newman, G. E., & Jeremy Shen, Y. (2012). The counterintuitive effects of thank-you gifts on charitable giving. *Journal of Economic Psychology*, *33*(5), 973–983.

Santiesteban, I., Banissy, M. J., Catmur, C., & Bird, G. (2012). Enhancing social ability by stimulating right temporoparietal junction. *Current Biology : CB*, *22*(23), 2274–2277.

Steyer, R., Schwenkmezger, P., Notz, P., & Eid, M. (1997). Der Mehrdimensionale Befindlichkeitsfragebogen (MDBF) Hogrefe. Göttingen, Germany.

Takagishi, H., Kameshima, S., Schug, J., Koizumi, M., & Yamagishi, T. (2010). Theory of mind enhances preference for fairness. *Journal of Experimental Child Psychology*, *105*(1-2), 130–137.

Young, L., Camprodon, J. A., Hauser, M., Pascual-Leone, A., & Saxe, R. (2010). Disruption of the right temporoparietal junction with transcranial magnetic stimulation reduces the role of beliefs in moral judgments. *Proceedings of the National Academy of Sciences*, *107*(15), 6753–6758.

Supplementary materials

Materials and Methods

Subjects

65 healthy subjects (39 female; 18-40 years old, mean age: 23±4 years) with no history of neurological or psychiatric illness participated in our task and were randomly assigned to either the treatment (rTPJ, N = 31) or control (vertex, N = 30) group. Four subjects were excluded due to the excessive missing trials or atypical responses to the TMS. The study was approved by the ethics committee of Canton Zurich. Written informed consent was obtained from each participant.

Experiment procedure

Subjects filled out a set of online questionnaires several days before they came to the lab, including empathy questionnaire (Davis, 1983), personality (NEO FFI, Costa & McCrae, 1992), and social value orientation (SVO, van Lange et al., 1997). Notably, subjects were paid for the completion of the online questionnaires based on their choices in the social value orientation questionnaire. One out of the nine questions was randomly chosen at the end and subjects' choices in this question decided payments for themselves and the anonymous partners that they were randomly matched to.

Each of the subjects who had completed the online questionnaires was invited to the laboratory and asked to perform a behavioral session which consisted of three parts: a pre-TMS charity evaluation, a donation task, and a post-TMS charity evaluation. In the pre-TMS charity evaluation task, subjects were asked to rate the deservingness, closeness, familiarity and age of 70 charities on a 5-point scale in a self-paced manner. We defined deservingness as how much the charity deserves supports, closeness as how much the subject herself or someone she knows can directly benefit from the charity, familiarity as how much she hears of or knows about the charity, and age as how old she assesses the charity. Importantly, deservingness measures subjects' judgments towards the social importance of each charity and thus is included as a factor of our main interest. Nevertheless, donations might also be

influenced by other features of the charity, such as the likelihood of a direct benefit from and the familiarity and perceived history of the charity. Therefore we include the closeness, familiarity and charity age as control variables. On each trial, we presented the name of a charity, a brief description of its mission, and a rating scale. The brief description of each charity consisted of two sentences. The first sentence described the charity's general mission and targets, and the second one provided a concrete example of the charity's projects. Subjects rated the same 70 charities on one of the four dimensions and then moved to another dimension. The order in which the rating dimensions were presented was randomized across subjects. For each rating dimension, 70 charities were presented in a random order. Upon completion of the first part, subjects were asked to report their mood on a multidimensional mood questionnaire (MDBF, (*17*)).

Afterwards, we evaluated the active motor threshold (AMT) for each subject and delivered the theta-burst TMS as described below in the TMS procedure section. Two minutes after the stimulation, subjects performed the donation task. In donation task, the name and main mission of one of the 70 charities were presented for each trial. Charities were presented in random order. Subjects were endowed with 100 points (1 point = 0.5 CHF) for every trial and asked to decide how many points to donate to a given charity (Figure 2c). One out of 70 trials was randomly chosen and implemented at the end of the experiment. That is, if one donated X points to the chosen charity, X*0.5 CHF were transferred to the charity anonymously and (100-X)*0.5CHF were paid to the subject in addition to a base payment. This procedure ensures subjects consider each charity independently and do not need to distribute the money across charities.

As soon as the donation task was completed, subjects started the post-TMS evaluation task, in which they evaluated a random half of the 70 charities on the four dimensions for the second time. Only half of the charities were included due to the limited time range of TMS effects. We included this step to address whether the judgments of the charities were changed by TMS. Afterwards, we asked subjects to report their mood on the MDBF questionnaire again. Notably, to keep the effect of TMS consistent across subjects, we made subjects perform the donation and post-TMS evaluation task within the same time window by fixing the trial length to 8 seconds. If no response

was detected within 8s, this trial was considered as missed and deleted from the following analysis.

TMS procedure

We used Brainsight (Rogue Research, Montreal, Canada), a MR-guided neuronavigational device, to guide the magnetic coil position relative to the cortical surface. Magnetic stimulation was performed using a high-power Magstim SuperRapid2 (Magstim Co., Whitland, Dyfed, UK). A figure-of-eight coil with external loop diameters of 7 cm was held over the targeted region. One continuous train of theta burst rTMS was applied over the targeted region. The theta bursts contained 3 pulses of 50Hz and were repeated at 200 ms intervals for 40s resulting in 600 pulses in total (Huang et al., 2005). To determine the intensity of stimulation, we measured the active motor threshold (AMT) of each subject. Motor evoked potential (MEP) was measured by recording the electromyographic (EMG) activity from the right FDI muscles. AMT was determined at the minimum intensity of a single pulse over the hand area of the left motor cortex that produced a MEP greater than 200 μV on five out of ten stimulations while the subject was maintaining a voluntary contraction of about 20% of maximum force. Theta burst rTMS was delivered at 80% of each individual's AMT.

Anatomical sites for TMS were localized on the basis of individual neuroanatomy. A T1-weighted 3D anatomical brain scan (1 x 1 x 1 mm resolution) was obtained for each subject (TR = 8.1 ms, TE = 3.7 ms, flip angle = 8°) with a 3T Philips Achieva scanner. To localize our target area TPJ, we performed reverse normalization, using the segmentation and normalization procedures implemented in SPM8 (http://www.fil.ion.ucl.ac.uk/spm/software/spm8/). The region of interest (ROI) of a 5-mm sphere was created on the MNI template using the coordinates (51, -45, 21) from a previous study (Hare et. al, 2010) and then reverse normalized to each subject's anatomical brain based on the anatomical parameters from the segmentation.

Analyses

In the second step of our analysis, we performed multiple linear regression analyses to test our hypotheses. We included the donation amounts (DA) as the dependent variable, and the treatment (the site of TMS), the linear term of deservingness ratings, and the interaction between treatment and deservingness as independent variables. In addition, we included the following control variables: the quadratic term of

deservingness, gender, the ratings on closeness, familiarity, and charity age, and the scores of SVO, empathy, and personality (including neuroticism, extroversion, agreeableness, conscientiousness, openness). The multiple linear regression formula is as follows:

$$DA_{ij} = \beta_0 + \beta_1 \times tms_i + \beta_2 \times Deserv_{ij} + \beta_3 \times tms_i \times Deserv_{ij} + \beta_4 \times Deserv_{ij}^{\ 2} + control\ variables + e_{ij} \quad (1)$$

where i and j denotes subject index and charity index respectively, and DA_{ij} stands for donation amount for subject i and charity j, tms_i for the dummy variable of treatment (effect coding,1 for TPJ and 0 for vertex). $Deserv_{ij}$ denotes rating scores for deservingness from subject i for charity j. In control variables, gender and SVO are dummy variables (1 for female and 0 for male; 1 for prosocial and 0 for individualistic and competitive). All the other variables were standardized (i.e. converted into z-scores) before entering the regression analyses. As we have multiple observations from each individual, we applied the linear regression with clustered standard errors using STATA 11.2 (http://www.stata.com, StataCorp, Texas, USA) to control for the within-subject correlations (Rogers, 1993).

We illustrated predicted donations as a function of perceived deservingness for vertex and rTPJ groups based on the results from multiple linear regression (Figure 3). According to our multiple linear regression formula (1), the relationship between DA and deservingness for the TPJ group (tms_i equals 1) is:

$$DA_{ij} = \beta_0 + \beta_1 + (\beta_2 + \beta_3) \times Deserv_{ij} + \beta_4 \times Deserv_{ij}^{\ 2} + e_{ij} \quad (2)$$

And for the vertex group (tms_i equals 0) is:

$$DA_{ij} = \beta_0 + \beta_2 \times Deserv_{ij} + \beta_4 \times Deserv_{ij}^{\ 2} + e_{ij} \quad (3)$$

Based on these two formulas, we calculated the predicted average donation amounts of each deservingness level for the TPJ and vertex group, respectively. In addition, we calculated the standard errors of the predicted average donation amounts through bootstrapping. Bootstrapping is a method for assigning measures of accuracy to sample estimates, which can be implemented by constructing a number of resamples of the observed dataset by random sampling with replacement from the original dataset (*2*, *18*). Bootstrapping was implemented in STATA 11.2. Standard errors were

calculated based on the distributions of the estimated regression coefficients from Bootstrapping (repeated for 1000 times). Notably, Figure 3 is produced only for illustration purpose. The standard error was calculated based on the multiple linear regression formula, which therefore is not directly informative for the significance of each regression coefficient (see Table S1 for the statistical details of the regression coefficients).

It is important to point out that as we standardized deservingness into z-scores, the constant (β_0) represents the average donation amounts of the Vertex group, β_1 tested whether the average donations of the TPJ group is significantly different from the Vertex group, β_2 tested the linear dependence of donation amounts on the deservingness of the Vertex group, and β_3 tested whether the linear dependence in the TPJ group is significantly different from the Vertex group.

Figures

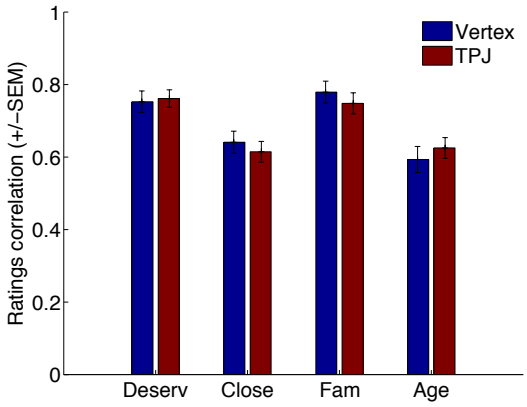

Figure S1. Our TMS treatment had no influence on judgments towards charities. Disrupting rTPJ activity does not influence the judgments towards charities in any of the four dimensions (Pearson's correlation, $r_{\_closeness}$ = .64 for rTPJ and .68 for vertex; $r_{\_familiarity}$ = .80 for rTPJ and .83 for vertex; $r_{\_age}$ = .65 for rTPJ and .63 for vertex; tested after Fisher's r-to-z transformation).

Tables and Legend

Table S1. Main effect for our TMS treatment. Below we illustrated results from multiple linear regression analysis with the donation amounts as the dependent variable, the site of TMS as independent variables and scores from questionnaires as control variables. Robust standard errors (clustered at individual level) were reported in parentheses.

	Donation Amount	**Coefficient (β)**
Effect of Treatment	TMS (TPJ)	-11.33 (3.85)* *
Control variables	SVO	9.63 (4.17)*
	Female	7.04 (3.79)
	Neuroticism	-2.87 (2.55)
	Extroversion	-3.29 (1.85)
	Agreeableness	0.42 (2.55)
	Conscientiousness	-3.50 (2.36)
	Openness	6.60 (2.33) * *
	Empathy	-0.16 (2.58)
Constant		19.57 (3.42)***

* p < .05, ** p < .01, *** p< .001

R-squared = 0.18

Table S2. Treatment effects on the willingness to donate. Below we illustrated results from multiple linear regression analysis with the donation amounts as the dependent variable, the site of TMS, the linear term of deservingness and the interaction term between deservingness and TMS as independent variables and other scores as control variables. Robust standard errors (clustered at individual level) were reported in parentheses.

	Donation Amount	**Coefficient (β)**
Effect of Treatment	TMS (TPJ)	-8.02 (3.93)*
Effect of Deservingness	Deservingness	12.77 (1.77)***
Interaction between TMS and Deservingness	TMS * Deservingness	-5.16 (2.48)*
Control variables	Quadratic Deservingness	0.58 (0.74)
	Closeness	2.54 (1.03)*
	Familarity	0.23 (0.91)
	Age	0.00 (0.74)
	SVO	9.36 (4.17)*
	Female	4.71 (3.80)
	Neuroticism	-2.90 (2.50)
	Extroversion	-3.34 (1.77)
	Agreeableness	1.31 (2.65)
	Conscientiousness	-1.96 (2.23)
	Openness	5.37 (2.45)*
	Empathy	-1.66 (2.70)
Constant		18.91 (3.35)***

* p < .05, ** p < .01, *** p< .001

R-squared = 0.40

Table S3. Treatment effects on willingness to donate for the Human-charity. Below we illustrated results from multiple linear regression analysis for the Human-charity with the donation amounts as the dependent variable, the site of TMS, the linear term of deservingness and the interaction term between deservingness and TMS as independent variables and other scores as control variables. Robust standard errors (clustered at individual level) were reported in parentheses.

	Donation Amount	**Coefficient (β)**
Effect of Treatment	TMS (TPJ)	-8.63 (4.17)*
Effect of Deservingness	Deservingness	12.76 (1.83)***
Interaction between TMS and Deservingness	TMS * Deservingness	-6.36 (2.70)*
Control variables	Quadratic Deservingness	0.27 (0.91)
	Closeness	2.37 (1.07)*
	Familarity	-0.16 (0.82)
	Age	0.46 (0.88)
	SVO	10.00 (4.58)*
	Female	5.77 (4.25)
	Neuroticism	-3.45 (2.69)
	Extroversion	-3.95 (1.94)
	Agreeableness	1.25 (2.79)
	Conscientiousness	-2.51 (2.43)
	Openness	6.19 (2.67)*
	Empathy	-1.74 (2.81)
Constant		18.04 (3.89)***

* p < .05, ** p < .01, *** p< .001

R-squared = 0.39

Table S4. Treatment effects on willingness to donate for the Non-human-charity. Below we illustrated results from multiple linear regression analysis for the Human-charity with the donation amounts as the dependent variable, the site of TMS, the linear term of deservingness and the interaction term between deservingness and TMS as independent variables and other scores as control variables. Robust standard errors (clustered at individual level) were reported in parentheses.

	Donation Amount	**Coefficient (β)**
Effect of Treatment	TMS (TPJ)	-5.28 (4.03)
Effect of Deservingness	Deservingness	11.44 (1.91)***
Interaction between TMS and Deservingness	TMS * Deservingness	-1.76 (2.68)
Control variables	Quadratic Deservingness	1.76 (0.81)
	Closeness	2.91 (1.17)*
	Familarity	1.02 (0.86)
	Age	-0.36 (0.69)
	SVO	7.08 (3.38)*
	Female	2.14 (3.04)
	Neuroticism	-1.49 (2.22)
	Extroversion	-1.71 (1.50)
	Agreeableness	1.42 (2.31)
	Conscientiousness	-0.67 (1.89)
	Openness	3.30 (2.16)
	Empathy	-1.25 (2.52)
Constant		11.60 (4.74)***

* p < .05, ** p < .01, *** p< .001

R-squared = 0.45

Table S5: Coefficients from the linear regression analyses for testing the change of ratings (post- vs. pre- TMS) in four dimensions (deservingness, closeness, familiarity and age) as a function of treatment group (the site of TMS). Robust standard errors were reported in parentheses. The results showed that the change of ratings didn't differ between the TPJ and vertex groups in any of the four dimensions.

	Change of deservingness	**Change of closeness**	**Change of familiarity**	**Change of age**
Treatment	0.09	-0.05	-0.01	-0.004
(TPJ vs. vertex)	(0.05)	(0.05)	(0.04)	(0.04)

Table S6: Coefficients from the linear regression analyses for testing the change of mood (post- vs. pre- TMS) in three subscales (good-bad, awake-tired, calm-nervous) as a function of treatment group. Robust standard errors were reported in parentheses. The results showed that the change of mood didn't differ between the TPJ and vertex groups in any of the three subscales.

	Good-bad	**Awake-tired**	**Calm-nervous**
Treatment	-0.09	-0.09	0.02
(TPJ vs. vertex)	(0.05)	(0.10)	(0.09)

Experiment Instruction

Anleitung

Bitte beachten Sie: Sollte etwas unklar sein, melden Sie sich bitte bei uns. Wir werden es Ihnen dann gerne erklären.

Vielen Dank, dass Sie unsere Forschung unterstützen. In dieser Studie würden wir gerne Ihre Meinung über 70 verschiedene Wohltätigkeitsorganisationen wissen. Diese sind als gemeinnützig anerkannt und national oder international tätig.

Das Experiment besteht aus drei Teilen. Im ersten Teil wird Ihnen eine Liste der Wohltätigkeitsorganisationen mit einer kurzen Beschreibung jeder Organisation gezeigt. Ihre Aufgabe ist es, die Wohltätigkeitsorganisationen in Bezug auf mehrere Kriterien zu bewerten.

Im zweiten Teil werden wir Ihnen einige der Wohltätigkeitsorganisationen aus dem ersten Teil erneut darbieten und Sie bitten, Entscheidungen im Zusammenhang mit diesen Organisationen zu treffen.

Beginnen Sie mit Teil 1. Wenn Sie mit Teil 1 fertig sind, können Sie mit dem zweiten Teil fortfahren. Im Anschluss wird Ihnen ein kurzer dritter Teil präsentiert werden.

Teil 1

Im ersten Teil werden Sie Bilder wie das folgende auf Ihrem Monitor sehen:

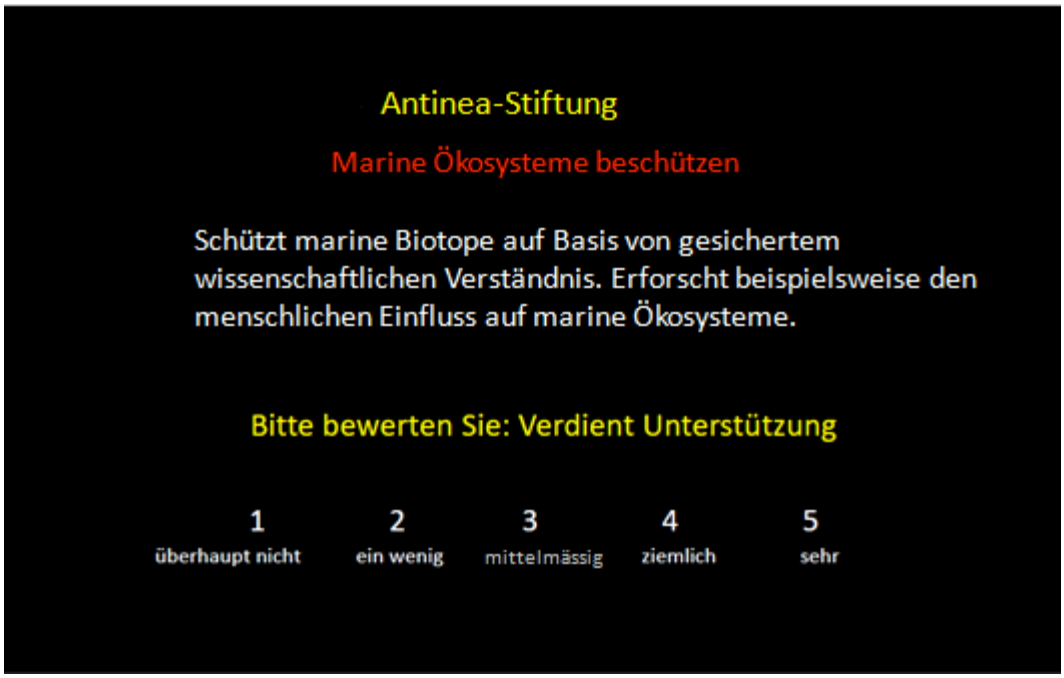

Name, Hauptaufgabe und eine kurze Beschreibung der Wohltätigkeitsorganisation werden in drei verschiedenen Farben angezeigt: Der **Name** in GELB, die **Hauptaufgabe** in ROT und die **Beschreibung** in WEISS. Unter der Beschreibung der Organisation sehen Sie Ihre Aufgabe.

Ihre Aufgabe ist es, die Organisationen in Hinblick auf die folgenden vier Aspekte zu bewerten. Die Aspekte werden in zufälliger Reihenfolge präsentiert.

- **Verdient Unterstützung**

  Wie sehr verdient es die Organisation, unterstützt zu werden?

- **Nähe**

  Wie gross ist die Wahrscheinlichkeit, dass Sie selbst - oder jemand, den Sie kennen - von der Organisation direkt profitieren könnten?

- **Bekanntheit**

  Wie bekannt ist diese Organisation? Haben Sie beispielsweise jemals von dieser Organisation gehört oder etwas über sie erfahren?

- **Alter der Organisation**

  Für wie alt schätzen Sie die Organisation ein?

Sie können diese Informationen über die Bewertungsaspekte auf dem Beiblatt finden. Greifen Sie bitte während dem Lösen der Aufgabe auf das Beiblatt zurück, wann immer Sie die Definition für einen der fünf Bewertungsaspekte brauchen.

Die Bewertungsaspekte erscheinen jeweils in GELB unter der Beschreibung der Organisation, zusammen mit einer Fünf-Punkte-Skala. Ihre Aufgabe ist es, die Organisation auf einen Aspekt hin zu bewerten.

Wenn Sie zum Beispiel dieses Bild sehen…

…dann müssen Sie bewerten, wie sehr die Wohltätigkeitsorganisation Unterstützung verdient.

Falls Sie der Meinung sind, dass die Organisation überhaupt nicht unterstützt werden sollte, wählen Sie „1“ auf Ihrer Tastatur. Falls Sie finden, die Organisation verdient sehr grosse Unterstützung, drücken Sie „5“ auf Ihrer Tastatur.

Wenn Sie eine Zahl gewählt haben, wird diese auf dem Bildschirm rot erscheinen. Daraufhin wird die nächste Organisation zur Bewertung dargeboten. Nachdem Sie

alle Organisationen in Hinblick auf einen Aspekt bewertet haben, werden Sie die Organisationen erneut bezüglich des nächsten Aspekts bewerten.

Wenn Sie im folgenden Durchgang also zum Beispiel dieses Bild sehen…

… müssen Sie bewerten, wie nahe Sie dieser Organisation stehen, also wie gross die Wahrscheinlichkeit ist, dass Sie selbst – oder jemand den Sie kennen – von der Organisation profitieren könnten.

Die Skala ist für jeden Aspekt gleich (**1** für ÜBERHAUPT NICHT, **5** für SEHR), ausser für den Aspekt Alter.

Um das Alter zu schätzen, werden Sie die folgende Skala sehen:

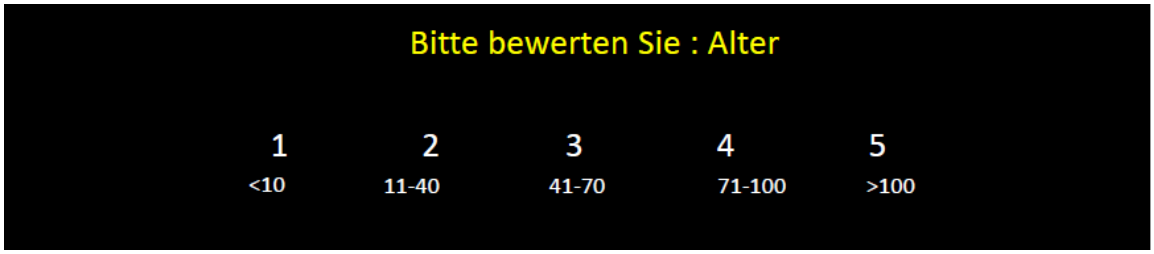

Die Angaben unter der Fünf-Punkte-Skala geben den Altersbereich an: „<10“ heisst „jünger als 10 Jahre“, „11-40“ bedeutet, das Alter der Organisation liegt zwischen 11 und 40 Jahren, und so weiter.

Wenn Sie also beispielsweise glauben, dass das Alter einer bestimmten Wohltätigkeitsorganisation UNTER 10 JAHREN liegt, dann drücken Sie „**1**“.Wenn Sie glauben, das Alter der Organisation ist grösser als 100 JAHRE, dann drücken Sie „**5**“. Wenn Sie glauben, das Alter einer Organisation liegt im Bereich ZWISCHEN 41 UND 70 JAHREN, drücken Sie „**3**“.

Bitte beachten Sie:

1. Bitte lesen Sie die Hauptaufgabe und die kurze Beschreibung aller Wohltätigkeitsorganisationen *äusserst sorgfältig* und versuchen Sie, sich die Hauptaufgabe jeder Organisation zu merken. Sie werden diese Informationen in Teil 2 benötigen. Bitte sehen Sie jedoch davon ab, sich Notizen zu machen, eine sorgfältige Lektüre ist völlig ausreichend.
2. Wenn Sie die jeweilige Zahl eingegeben haben, können Sie diese nicht mehr ändern. Achten Sie deshalb darauf, dass Ihre Finger richtig auf der Tastatur platziert sind und Sie keine falschen Zahlen eingeben.

Wenn Sie irgendwelche Fragen haben, wenden Sie sich bitte an die Versuchsleiterin. Wenn Sie keine Fragen haben, drücken Sie bitte Taste „s“, um zu beginnen. Sie werden am Anfang einige Organisationen nur zur Übung bewerten, damit Ihnen der Ablauf der Aufgabe und die Eingabemöglichkeiten klar werden. Wenn Sie nach der Übung Fragen haben, wenden Sie sich bitte an die Versuchsleiterin. Wenn Sie keine Fragen haben, können Sie den Hauptteil starten, indem Sie die Taste „s“ drücken.

Teil 2

Wir kommen nun zum zweiten Teil des Experiments. In diesem Teil werden Ihnen verschiedene Wohltätigkeitsorganisationen gezeigt, die Sie im ersten Teil bewertet haben.

Ihre Aufgabe ist es nun, zu entscheiden, **welchen Betrag Sie der Wohltätigkeitsorganisation spenden wollen**.

Zu diesem Zweck erhalten Sie 100 Punkte, von denen jeder Punkt 0,5 CHF wert ist. Sie müssen entscheiden, wie viele der 100 Punkte Sie der Organisation geben wollen.

Um ihre Entscheidung treffen zu können, werden wir Ihnen den Namen und die Hauptaufgabe der Organisationen mitteilen. Unten sehen Sie ein Beispiel. Sie werden den **Namen** der Organisation in GELB und die **Hauptaufgabe** in ROT sehen.

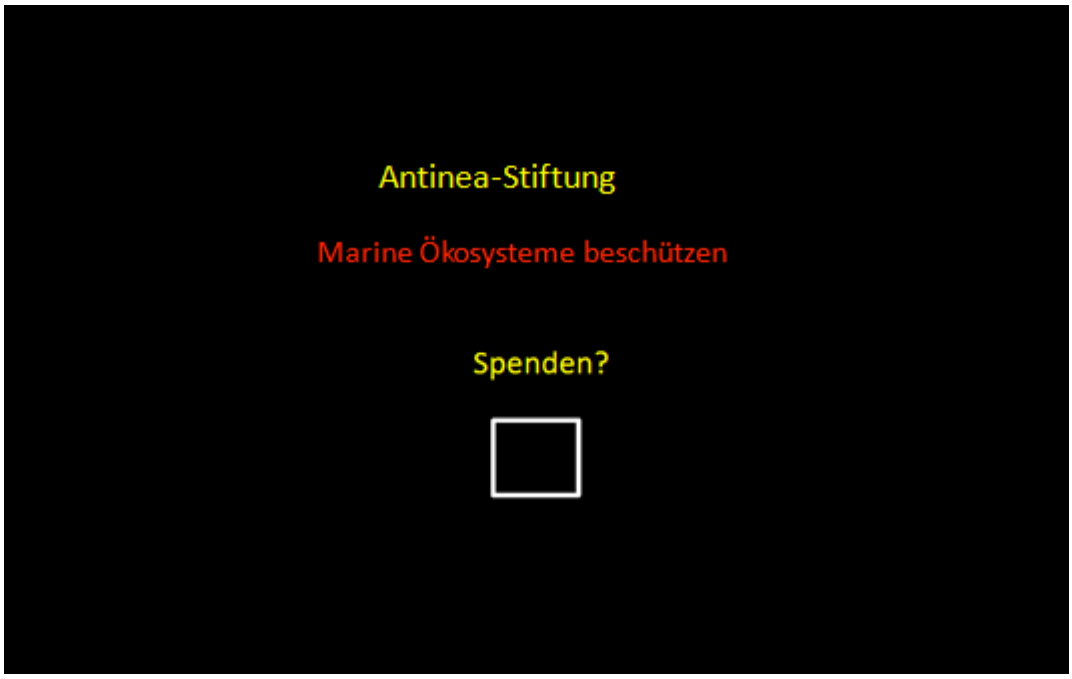

Am Ende des Experiments *wird eine Wohltätigkeitsorganisation zufällig ausgewählt und Ihre Entscheidung bezüglich dieser Organisation wird umgesetzt. Dies heisst, dass Ihre Spende anonym an die Organisation gespendet wird. Sie werden eine schriftliche Bestätigung über die Spende erhalten, sobald diese bei der Organisation eingegangen ist.* Deshalb ist es wichtig, dass Sie eine unabhängige Entscheidung für jede einzelne Wohltätigkeitsorganisation treffen, da am Schluss nur *eine* Ihrer Entscheidungen zählen wird. Gleichzeitig müssen Sie sich *jede Entscheidung ernsthaft überlegen*, da jede Organisation am Ende zufällig gewählt werden kann.

Wenn Sie sich zum Beispiel entscheiden, 35 Punkte an die Organisation X zu spenden, und Organisation X am Schluss des Experiments zufällig gewählt wird, dann bezahlen Sie 35 Punkte an die Organisation X und können die restlichen 65 Punkte

für sich behalten. Da jeder Punkt 0.5 CHF wert ist, spenden Sie 17.5 CHF an Organisation X und erhalten selbst 32.5 CHF (zusätzlich zur Erscheinungsvergütung von 15 CHF).

Sie können die Anzahl Punkte, die Sie der jeweiligen Organisation spenden wollen, in die Box unter dem Wort „Spenden?“ eintragen.

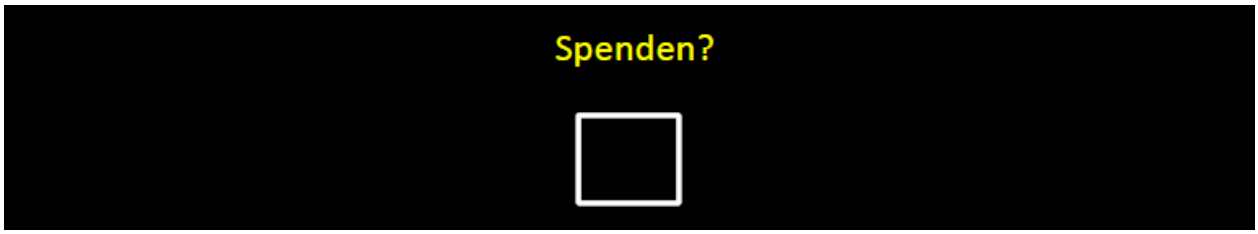

Bitte benutzen Sie die Zahltasten auf Ihrer Tastatur, um die Anzahl der Punkte einzutragen.

Falls Sie versehentlich eine falsche Zahl eingeben haben oder Ihre Entscheidung ändern wollen, können Sie die eingegebene Zahl durch eine neue Zahl ersetzen. In diesem Fall müssen Sie eine dreistellige Zahl eingeben. Wenn Sie zum Beispiel 60 Punkte spenden wollen, aber „80“ eingegeben haben, können Sie dies korrigieren, indem sie „060“ eingeben.

Nach genau 8 Sekunden wird Ihnen die nächste Organisation vorgelegt werden, unabhängig davon, ob Sie eine Eingabe gemacht haben, oder nicht.

Wenn Ihre Entscheidung bestätigt ist, werden als Rückmeldung sowohl die Zahl als auch die Box in Rot erscheinen.

Bitte beachten Sie:

1. Die Spenden sollten innerhalb des Bereichs von 0 bis 100 Punkten eingegeben werden.
2. Sollte die eingegebene Zahl dieses Limit überschreiten, können Sie nicht fortfahren, bevor die Zahl nicht im Rahmen der Anweisungen geändert wurde.
3. Nach 8 Sekunden wird Ihnen die nächste Wohltätigkeitsorganisation vorgelegt werden.
4. Bitte beachten Sie, dass jede Ihrer Entscheidungen Konsequenzen haben kann, da Ihre gewählte Spende Ihre Auszahlung beinflusst und an die betreffende Organisation überwiesen werden wird, wenn diese Organisation am Ende gewählt wird.

Um sicherzustellen, dass Sie die Aufgabe verstanden haben, beantworten Sie bitte die folgenden Fragen:

Wenn Sie 40 Punkte an die Wohltätigkeitsorganisation gespendet haben und diese Entscheidung am Schluss zufällig aus gewählt wird,

1) Wie viele Franken erhalten Sie dann selber (inklusive der Vergütung für die Teilnahme am Experiment)?

2) Wie viele Franken erhält dann die Wohltätigkeitsorganisation?

Teil 3

Wir kommen nun zum dritten und letzten Teil des Experiments. In diesem Teil werden Sie dieselbe Aufgabe wie in Teil 1 bearbeiten; allerdings werden Ihnen nun nur noch 35 Organisationen präsentiert werden und Sie werden wie in Teil 2 jeweils 8 Sekunden Zeit haben, um Ihre Antwort einzugeben. Für die Bearbeitung dieses Teils des Experiments werden Ihnen pauschal 10 CHF ausgezahlt.

Experiment protocol

Procedure:

- Ask subjects to complete the online questionnaires before they come by the lab.
- Ask subjects to read instructions and sign the consent form before the experiment.
- Check the control questions and make sure subjects understand the task.
- Subjects are asked to complete part1, the charity-evaluation task.
- Subjects are asked to complete MDBF.
- The experimenters measure the motor threshold of subjects and determine the stimulation intensity.
- Theta burst TMS stimulation is implemented.
- Subjects complete the donation task and the re-evaluation of charity task.
- Subjects are asked to fill out the MDBF for a second time.

More details:

Preparation before subjects arrive

TMS devices

1) Goggle
2) Subject tracker/ Coil tracker
3) Screw driver (attach subject tracker to the goggle & coil tracker to the coil)
4) Coil calibration block (set the heights of three piles evenly)
5) Remote control
6) TMS device power on/ change the cable attached to the monitor
7) MEP, check the cable connection, prepare tapes, electrodes, and alcohol pads.
8) earplugs
9) chin-rest
10) make sure the right coil is attached

BrainSight

1) Turn on the Mac
2) Turn on the camera
3) Check the cables of MEP devices
4) Start BrainSight
5) Things to prepare in advance
    a. Skin/ Curvilinear brain
    b. References (nosetip, nasion, left/right ear)
    c. Targets (M1 & right TPJ)
    d. Coil calibration

Program:

Turn on the presenting computer. Start the pre-rating program.

Instructions:

1) TMS ethics (two files);
2) Descriptions for TMS (general) and the overview of our study;
3) Instruction for our study;
4) Questionnaires.
5) SubjectsLog

After subject arrive

1) Welcome subjects; introduce ourselves
2) Subject will be seated in the kitchen.
3) The experimenter delivers the description of TMS (one file) and ethics (3 miles) to subjects, ask them to read and sign.
4) The experimenter delivers the instruction of Part 1, answer subjects' questions and then start the practice session for Part 1.
5) The experimenter starts the session of Part 1.
6) After Part I, The experimenter delivers the instruction for Part 2&3. Ask whether subjects have questions. Then start the practice session for part 2.
7) The experimenter asks subjects to fill out the MDBF questionnaire.
8) Determine motor threshold:

3. Goggle – fix it on the subject's head with tapes.
4. Adjust the chin rest. Give earplugs to everyone.
5. Skin preparation for MEP

   - Swap the skin with Alcohol pad
   - Attach electrodes (ground, positive, negative)
   - Connect wire

6. Identify the threshold intensity

Theta Burst protocol

1. Change the coil
2. Use Manfrotto to fix coil
3. Go to Magstim GUI
   1) Select repetitive mode
   2) Select burst mode
   3) N.of Pulses: 3
   4) Frequency: 50 Hz
   5) Burst frequency: 5Hz (repeating every 200ms)
   6) N. of bursts: 200 (600 in total)
   7) Total time: 40 sec

7. Apply theta-burst TMS.

Appendix

B. Neural Correlates of Learning Rate in a Changing Environment

This chapter is joint work with Ernst Fehr, Kerstin Preuschoff and Yosuke Morishima

Neural Correlates of the Learning Rate in a Changing Environment

Chaohui Guo, Yosuke Morishima, Kerstin Preuschoff *, Ernst Fehr *

Abstract

Our interactions with the environment always involve imperfect observations. Updating beliefs correctly based on new observations is central to learning behavior. The learning rate (LR) is a fundamental parameter in reinforcement learning models that represents the weight given to new information. However, the neural substrates that encode the LR still remain unclear. Locus coeruleus (LC) has been proposed as the core component of the neural network of learning under uncertainty, and it has been proposed to have sophisticated regulation function in learning under uncertainty. There has also been indirect evidence that associates the functional activity of LC with the LR, while the direct empirical evidence is still missing. Here we find that participants' LRs vary according to local statistical features: (i) The LR is lower in contexts with a higher noise level, and (ii) The LR is higher in contexts with a changing mean and a stable noise level (a relevant change) compared to contexts with a stable mean and a changing noise level (an irrelevant change). Furthermore, we find that the adaptive LR is positively correlated with the functional activity of a region in pons, consistent with the position of locus coeruleus (LC), at the individual level, providing the first direct empirical evidence for the link between functional activity of LC and the computationally complex function of adaptively weighting new information based on the local contexts.

Key words: Locus coeruleus, learning rate, volatility, noise level, ACC

Introduction

Our interactions with the environment, from naturalist navigation to human social interactions, always involve various changes. The ability to infer the altered state of the world based on imperfect observations is crucial for optimal responses. For example, foraging animals need to evaluate the quality of a dynamic food patch according to the amount of food acquired in the past, and investors have to estimate the value of a stock based on its daily prices and other available information. Reinforcement learning (RL) theory has been proven to be effective in describing important forms of learning behavior and the corresponding neuronal activity (Schultz & Dickinson 2000; Schultz et al. 1997; Tobler et al. 2005; M. X. Cohen 2008; Niv et al. 2012; Glascher et al. 2010; O'Doherty et al. 2003). In such models, an agent updates beliefs in proportion to the prediction error (PE), defined as the difference between the actual and the expected outcome. A fundamental parameter, the learning rate (LR) reflects the weight given to new observations and regulates the relative contribution of outcome history and new observations on beliefs, e.g. a higher LR leads to a stronger influence of new observations on beliefs (Rescorla & Wagner 1972; Sutton & Barto 1998).

Classical reinforcement learning studies have been focused on learning behavior in stationary environments and often assumed that the LR is a constant for the whole period. It is unclear how LRs are adapted in environments where the underlying distribution can change abruptly, and which neural substrates encode the LR. In this study, we aim to address these questions through a mean-guessing task, in which participants are asked to make trial-by-trial inferences of the mean of the underlying distribution based on previous observations. In our paradigm, the change of the environment can either be a change of the mean or a change of the noise level. Based on previous theoretical and empirical studies (Preuschoff & Bossaerts 2007; Behrens et al. 2007; Nassar et al. 2010; Payzan-LeNestour et al. 2013; Chumbley et.al, 2011), we hypothesize that the LR will be higher (i) when the mean changes compared to situations where the mean does not change and (ii) in an environment characterized by a lower noise level.

Previous research provides us with insights into the neural substrates that are involved in the LR encoding. Yu & Dayan (2005) propose that the neurotransmitter noradrenaline signals unexpected uncertainty and facilitates adaptation to changes. Locus coeruleus (LC) is the sole source of noradrenaline, which is hypothetically the core component of the neural network of learning under uncertainty. A recent fMRI study demonstrates that the functional activity of LC represents the unexpected uncertainty (Payzan-LeNestour et al. 2013). Similarly, Aston-Jones et al. (2007) provides solid evidence that links LC to a computationally sophisticated "regulation function" in learning under uncertainty. Pupil diameters have been shown to positively correlate with computational variables representing LR (Nassar et al. 2012). Combined with the findings that pupil dilation is a reliable measure of LC activity (Phillips et al. 2000), this study provides indirect empirical evidence linking LC with the encoding of LR, while the direct empirical evidence is still missing.

In addition to LC, the anterior cingulate cortex (ACC) is considered important in adaptive behavior. It has been implicated in many cognitive functions including arousal, attention, motivation, working memory, response inhibition, and behavioral flexibility (Carter & van Veen 2007; van Veen et al. 2001; Carter et al. 1998; Botvinick et al. 2004; Paus 2001; Carter et al. 1999). Moreover, the activity of ACC has been found to correlate with certain statistical features of environments, such as the average reward rate (Amiez et al. 2006), and the volatility (Behrens et al. 2007). Particularly, the functional activity of ACC have been associated with the heterogeneity of average LRs across subjects (Behrens et al. 2007). However, so far there is no direct evidence that associates the functional activity of ACC with trial-by-trial LR at the individual level. In this study, we examine whether the functional activity of LC and ACC are associated with the LR in changing environments.

Materials and Methods

Subjects

Twenty healthy subjects (10 female; 19-27 years old) with no history of neurological or psychiatric illness participated in our task. One subject was excluded from the final analysis because this subject had difficulty in understanding the task (details in supplementary). The study was approved by the ethical committee of Canton Zurich. Written informed consents were obtained from all participants.

Behavioral paradigm

Our mean-guessing task investigates adaptive learning in changing environments. In this task, random numbers were generated from a hidden Gaussian distribution ($N(\hat{u}, \sigma)$) whose mean ($\hat{u}$) and standard deviation (σ) abruptly changed. Subjects were presented with one realization (observation) on each trial and were asked to report their trial-by-trial estimations of the underlying mean ($\hat{u}$) based on the previous observations. All observations and the underlying means were ranged within 0 to 100.

Each trial consisted of three stages: guess, confirmation and new observation, see Figure 1A. Subjects reported their estimations by placing a square on a slider ranged from 0 to 100, then pressing a button to confirm their guess. There was a maximum of 10s response time. If no confirmation was detected, the last position of the square was accepted as the guess for this trial. Afterwards, a new observation was provided and displayed for 1.5s. Based on this new observation subjects could update their beliefs and be in preparation for the next trial. Inter-trial-interval (ITI) was displayed as a blank screen with a fixation at the centre for 2-6 s (uniform distribution), followed by the next trial. Stimuli were presented using psychotoolbox-3 running in MATLAB.

Each subject completed four sessions of 60 trials in each session in the scanner. In all sessions, the noise level changed multiple times, i.e., the noise level was always volatile. The four sessions differed in either the volatility of the mean or the initial noise level, resulting in four session types: Type I, with stable mean and high initial noise level (an example in Figure S1); Type II, with stable mean and low initial noise level; Type III, with changing mean and high initial noise level (Figure 1B); Type IV, with changing mean and low initial noise level. Presenting orders of the four sessions

were randomized across subjects. Subjects were informed that the underlying mean and observations were within 0 to 100, and the mean and noise level could both change unexpectedly, but independently of each other, for multiple times over each session. Notably, subjects were not informed of the type of sessions or the changes of the underlying distributions, and they could only infer these from the observations they received. More details are described in the supplementary material.

The absolute error for each trial was calculated as the distance between the guessed number and the true underlying mean. At the end of each session, we calculated a performance score by averaging over the absolute error of every trial from the second to last trial and then presented this to subjects. At the end of the experiment, only one session was randomly chosen and the score of this session determined subjects' payment, i.e. payment was scaled inversely with average error (AE) of this randomly chosen session (maximum CHF 120 when AE is 0 and minimum CHF 55 when AE is over 10; Details were illustrated in Table S1).

A.

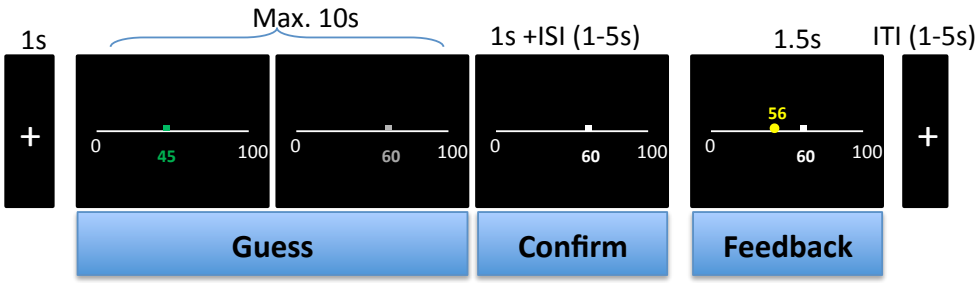

B.

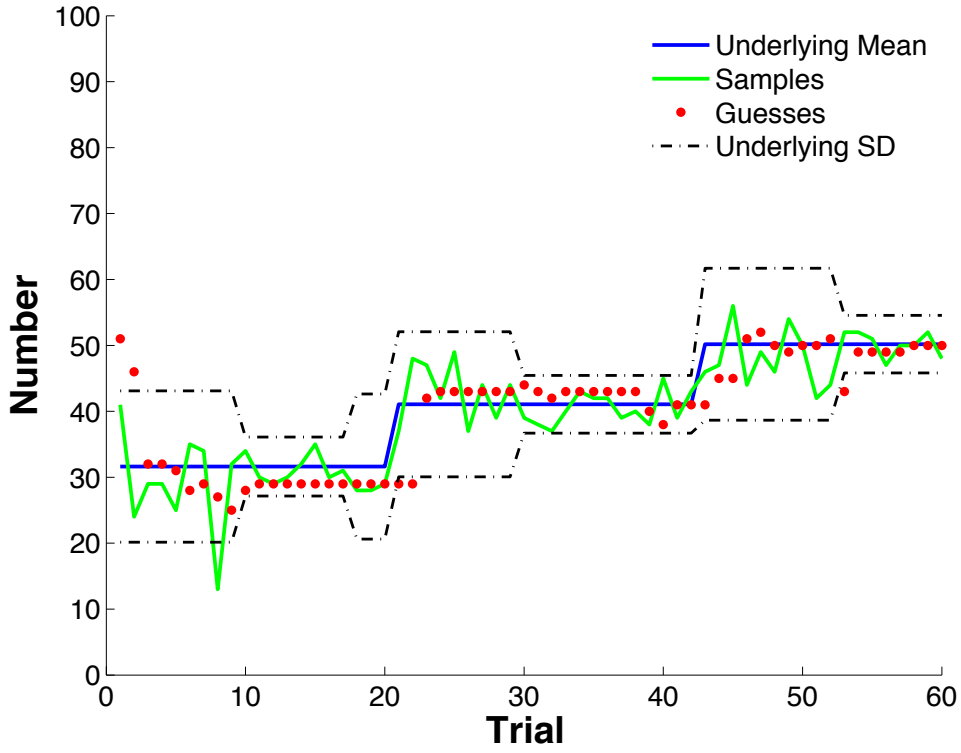

Figure 1. ***A.*** Schematized trial of the mean-guessing task. On each trial, subjects were asked to report their trial-by-trial estimations of the underlying mean of a Gaussian distribution (blue line in B) based on an observation drawn from the underlying distribution by adjusting the position of a square on a slider. The initial position of the square was randomized on each trial (green square in A). ***B.*** An example session with a changing mean. The solid blue line represents the underlying mean, which remained unknown to subjects and had to be guessed. Black dashed lines illustrate the standard deviation (SD) of the underlying distribution, which changed independently of the mean. The green line represents the samples drawn from the underlying distributions. Red dots were the guesses of a subject. Notably, the mean and SD could suddenly change but subjects could only infer that from the observations they received.

Behavioral Data Analysis

The LR is traditionally assumed to be a constant and is estimated through linear least squares regression in classical reinforcement learning studies where the environment is stable over time. However, such an assumption becomes inappropriate in our setting because here the environment changes periodically, which should lead to changes in the LR (Preuschoff & Bossaerts 2007; Behrens et al. 2007; Nassar et al. 2010; Payzan-LeNestour et al. 2013). As we aim to investigate whether and how humans adjust their LR based on the local statistical features (i.e. volatility of the mean and the magnitude of the noise level), we estimated the average LR for each short period with stable statistical features. We define an epoch as all trials between one change and the next change. Each session consists of multiple epochs.

We define:

Term	***Meaning***	***Value Range***
t	*trial index*	[1, 60]
n	*total number of epochs in a session*	[5, 9]
i	*epoch index*	[1, n]
$\hat{u}_t$	*guessed number at trial t*	[0, 100]
s_t	*observation at trial t*	[0, 100]
b_{it}	*dummy variable to identify whether trial t belongs to epoch i*	*= 1, if trial t belongs to epoch i,* *= 0, otherwise*
δ_t	*prediction error at trial t*	
α_i	*average LR for epoch i (we label it as the tonic component of the LR)*	
β_t	*trial-wise adjustment component of the LR on the basis of α_i (we label it as the transient component of the LR)*	
e_t	*residual term of the linear regression*	

We estimated the LR based on the Rescorla-Wagner (RW) rule of reinforcement learning (Rescorla & Wagner, 1972). First, we estimated the average LR for epoch i (α_i) through linear least squares regression based on formula (1).

$$\hat{u}_{t+1} - \hat{u}_t = \sum_{i=1}^{n} \alpha_i \times b_{it} \times \delta_t + e_t \quad (1)$$

We calculated the prediction error (δ_t) as the deviation of the new observation from the guessed number, namely:

$$\delta_t = s_t - \hat{u}_t \quad (2)$$

The residual term e_t in formula (1) contains the trial-wise variance of a subject's belief updates that cannot be explained by the epoch-wise average LR (α_i). We defined a second parameter, β_t, to represent the trial-based adjustment component of

the LR on the basis of α. Based on the RW rule, we explained the trial-wise variance of belief updates through formula (3).

$$e_t = \beta_t \times \delta_t \quad (3)$$

Based on formula (3), we estimated β_t through linear least squares regression (see supplementary material for details).

Next, we classified the epochs into different types based on the volatility of the mean and magnitude of the noise level. The first two types are: FirstL, the starting epoch of a session and with a low noise level; FirstH, the starting epoch of a session and with a high noise level. These two types of epochs both have stable mean, and they only differ in the magnitude of noise level, allowing us to test whether the LR is adjusted to the noise level. Additionally, two other types of epochs enable us to test whether subjects can distinguish between situations with a change of the mean and constant noise level (where a high LR is required to respond to the change) and those with a change of the noise level and constant mean (a low LR is required as the mean still remains the same): Mean-Stable, the epoch during which the mean remains the same as the previous epoch while the noise level changes; Mean-Volatile, the epoch with a changed mean compared to the previous epoch while the noise level remains constant (Details are illustrated in supplementary material).

FMRI Data Acquisition

Data were acquired with a 3T Philips Achieva scanner. High-resolution structural T1-weighted 3D-TFE anatomical scans of the whole brain were also acquired for each participant, with voxel size 1.1×1.1×0.6 mm, TR = 7.5 ms, TE = 3.5 ms, flip angle = 8°. Functional images were taken with a T2-weighted gradient Echo-Planar Imaging sequence (TR = 2500 ms, TE = 36 ms, flip angle = 90 degrees). Whole brain coverage was achieved by 37 slices in ascending order (3 mm thickness, 0.5 mm gap, in-plane voxel size 2 x 2 mm). Subjects' head was restrained with foam pads to decrease head movement. Functional imaging data were acquired in four separate sessions, each lasting about 10 minutes.

FMRI Data Analysis

We performed our image analysis using SPM8 in Matlab (http://www.fil.ion.ucl.ac.uk/spm/software/spm8/). EPI images were realigned to the first volume and co-registered with the anatomical scan. Subjects' T1 images were segmented into gray matter, white matter, and cerebrospinal fluid and the segmentation parameters were used to warp the T1 images to the Montreal Neurological Institute (MNI) template. Functional data were then normalized to the MNI template based on the output parameters from segmentation. Afterwards, the normalized images were spatially smoothed using an isotropic 6mm full-width-half-maximum (FWHM) Gaussian kernel. Sessions with extensive head movements (larger than 3 degrees and 4mm) were excluded from the following analysis (i.e. one session was excluded for two subjects).

A general linear model (GLM) was constructed for each subject to estimate experimental effects. The model included three events time-locked to each of the three stages in each trial: guess, confirmation and new observation. Subjects received new information at the observation stage, which should be a crucial time for the LR and belief updating. To identify the neural correlates for the LR, we included the epoch-wise LR (α_i) and the trial-by-trial adjustment component of the LR (β_t) as two parametric modulators of the observation regressor. To test whether the LR was still represented in BOLD responses at the guess stage, we also included α_i and β_t as parametric modulators of the guess regressor. Notably, for each trial, the LR in the guess stage was different from the LR in the observation stage. Instead, they reflected the LR from the previous observation stage. We included the guessed number as a parametric modulator in the confirmation stage. All regressors of interest were convolved with the canonical hemodynamic response function. We included the six estimated head movement parameters as regressors of no interest. All images were high-pass filtered in the temporal domain (width 128s) and autocorrelation of the hemodynamic response was modelled as an AR(1) process.

Main effects for the regressors of our interest were estimated at the individual-level. Contrast images were taken further to group level analysis. Significant effects were tested with one-sample t tests across the group. To identify significant clusters, we used a threshold of $p<0.001$. Correction for multiple comparisons [familywise error

(FWE), $p < 0.05$] was performed at the cluster level. For our a priori region, the locus coeruleus (LC), we used small-volume correction (FWE, $p<0.05$) for 6 mm spheres surrounding the average anatomical localization of the human LC [(-4, -37, -26) from (Keren et al. 2009).

Results

Learning rates were adapted to the volatility and noise level

To address our question whether and how humans adjust their LRs based on the volatility of the mean and magnitude of the noise level of the local context, we focused on α_i, the average LR of epoch i and compared between α_i of different types of epochs. First, we found that α_i in the FirstH epoch was significantly lower than in the FirstL epoch (paired $t(18) = 3.75$, $p< 0.01$; Figure 2A), supporting our hypothesis that subjects' LRs are lower in periods with a higher noise level, namely that subjects assign a lower weight to the new observations in updating their beliefs when the noise level is higher. Second, we found that α_i in the Mean-Volatile epochs (where mean changed compared to the previous epoch while the noise level remained constant) was significantly higher than in the Mean-Stable epochs (where mean remains the same as the previous epoch while the noise level changes) (paired $t(18) = 3.36$, $p< 0.01$; Figure 2B), suggesting that subjects distinguish the relevant change from irrelevant change of the environment and their LRs are higher in the situation with relevant changes.

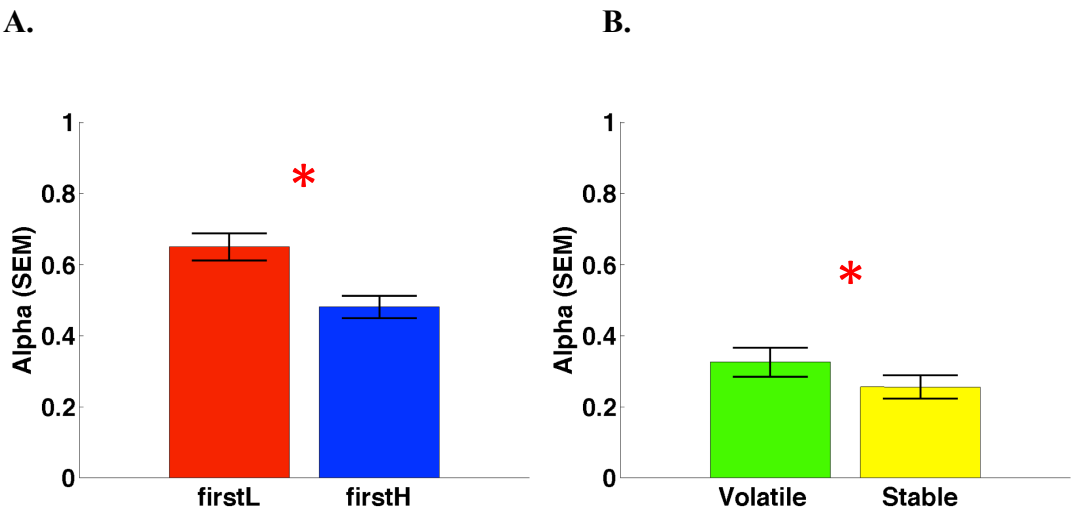

Figure 2. Behavioral effects of the learning rate. A. The epoch-wise LR, *alpha* is significantly higher in epochs with a lower noise level (paired t-test on *alpha* of FirstL and FirstH epochs, t-value = 3.75; $p<0.01$), supporting our hypothesis that subjects' LRs are lower in periods with a higher noise level, namely that subjects assign a lower weight to the new observations in updating their beliefs when the noise level is higher. FirstL, the starting epoch of a session and with a lower noise level; FirstH, the starting epoch of a session and with a higher noise level. ***B.*** *Alpha* of the Mean-Volatile epoch (labelled as Volatile in the figure) is higher than alpha of the Mean-Stable (labelled as Stable) epochs (paired t-test on *alpha* of these two types of epochs, t-value = 3.36; $p<0.01$), suggesting that subjects distinguish the relevant change from irrelevant change of the environment and the LR is higher in situations with relevant changes. Mean-Stable, the epoch during which the mean remains the same as the previous epoch while the noise level changes; Mean-Volatile, the epoch with a changed mean compared to the previous epoch while the noise level remains constant (Details are illustrated in supplementary material).

Neural Correlates for the learning rate

In order to identify the neural substrates that are involved in the encoding of LR, we focused on the observation stage, the crucial period for the LR and belief updating because of the arrival of a new observation. We searched for brain areas in which activity correlated with the tonic and transient component of the LR: α_i and $\beta_{t,}$ respectively.

First, consistent with our hypothesis, we found significant correlations between α_i and the functional activity in the pons, a position consistent with locus coeruleus (LC) [peak at (-6, -30, -24), t = 4.59, $p< 0.05$, FWE small-volume corrected; Figure. 3A].

Moreover, significant correlations ($p < 0.05$, FWE cluster corrected) were also found in the left insula (INS) [left BA48, peak at (-44, 16, 0), $t = 5.68$; Figure 3A], and the left pre-supplementary motor area (preSMA) [left BA 6, peak at (-6, 10, 52), $t = 5.19$; Figure 3A].

Second, we found significant correlations between β_t and the functional activity in anterior cingulate cortex (ACC) [right BA32, peak at (4, 44, 22), $t = 4.48$, $p < 0.05$ at the cluster level; Figure 3B], and in right inferior frontal cortex (IFC)[right BA45, peak at (56, 24, 6), $t = 4.59$, $p < 0.05$, FWE cluster corrected; Figure 3B].

A.

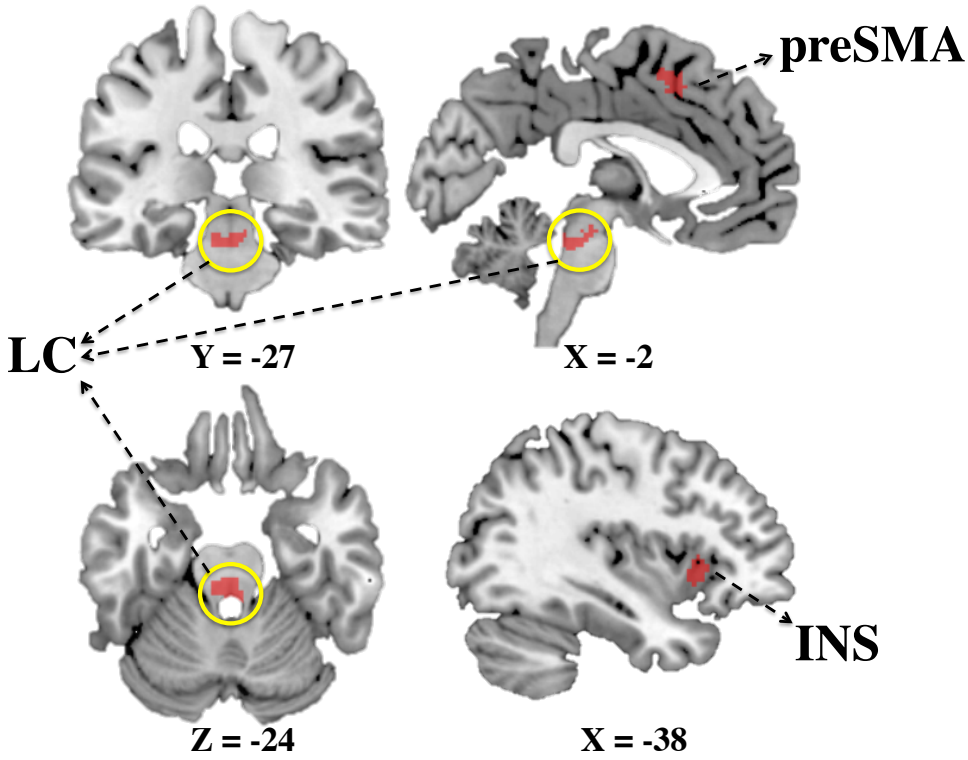

B.

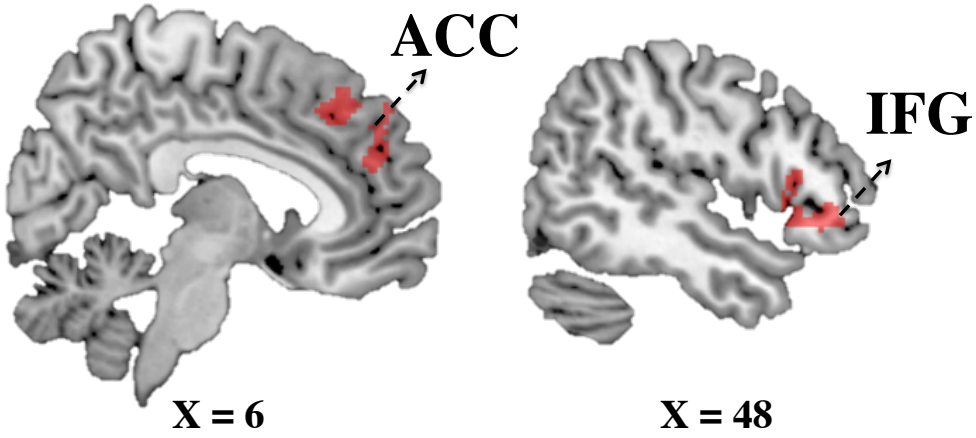

Figure 3. Neural correlates of the learning rate. A. The average LR of epoch i, α_i, is positively correlated with the activity in the pons, a position consistent with LC, and the activity in preSMA and left insula (INS). ***B.*** The trial-by-trial adjustment component of the LR, β_t, is positively correlated with the activity in ACC and right IFG, extending to right insula (clusters in A, B are sig. at $p<0.001$, but shown at $p<0.005$).

In the supplementary material, we report the activations for the guess, confirmation, and new observation stage, and neural correlates for the parametric modulators of the guess and confirmation stage.

Discussion

In this fMRI study we investigate whether and how the LR is adjusted based on the local statistical features in a changing environment and the neural mechanisms involved in the encoding of the LR. We find that the average LR of each epoch (α_i) differs between various contexts: First, α_i is lower in contexts with a higher noise level, supporting our hypothesis that a lower weight is assigned to the new information when subjects update their beliefs in contexts characterized by a higher noise level; second, α_i is higher in contexts with a changing mean and a stable noise level (a relevant change) compared to contexts with a stable mean and a changing noise level (an irrelevant change), suggesting that subjects distinguish the relevant change from irrelevant change of the environment and their LRs are higher in the contexts with relevant changes. Moreover, we find that the average LR of each epoch (α_i) is positively correlated with the functional activity in the pons, a position consistent with the location of LC, and in the left INS and preSMA. Furthermore, we find that the functional activity of a different set of regions, including ACC and RIFG, are positively correlated with β_t, the trial-by-trial adjustment component of the LR on the basis of α_i.

Our finding that the functional activity of LC is associated with the average LR of each epoch (α_i) and that α_i is adapted to the local volatility of the mean and noise level provides the first direct empirical evidence for a link between the functional involvement of LC and the adaptive LR. Such findings provide solid support for the crucial role of LC in the regulation of optimal learning under uncertainty (Yu & Dayan 2003; Aston-Jones & J. D. Cohen 2005). LC has been considered as part of the ascending reticular activating system and acknowledged for the role in regulating the overall alertness and nonspecific arousal (Moruzzi & Magoun 1949; Steriade 1996). Animal studies show that LC neurons fire robustly to novel stimuli during free exploration and conditioning experiments (e.g. Vankov et al. 1995). Such responses of LC disappear when there is no prediction value of the stimuli and reappear as soon

as the stimulus reinforcement contingencies change (Sara et al, 1994; Sara & Segal, 1991). Importantly, LC responses to the changes in stimulus-reinforcement contingencies precede the changes in behavioral responses in both rats and monkeys (Sara et al. 1994; Sara & Segal 1991; Aston-Jones et al. 1997). These existing findings suggest the strong association between the functional activity of LC and learning behavior, whereas few studies have demonstrated such associations in humans. Our findings fill this gap and further link the functional activity of LC with the computationally complex function of adaptively weighting new information based on the local contexts.

In addition to LC, the functional activity of the left INS and preSMA are also positively associated with the average LR of each epoch (α_t). As the Insula has been reported to have an important role in risk processing (Preuschoff et al. 2008), the involvement of the insula in our task may be related to the tracking of noise levels and the adjustment of the LR accordingly. The activation of the preSMA has been associated with voluntary movements, action-based sequential learning, error processing and facilitation of decision-making under time pressure (van Gaal et al. 2011; Kim et al. 2010; Zentgraf et al. 2005; Kennerley et al. 2004; Inase et al. 1996; Forstmann et al. 2008). The activation in preSMA in our task may be related to transforming the LR signals into action.

We find that the transient component of LR (β_t) is associated with a different set of regions: the ACC and RIFG, two core regions in the monitoring system that have been documented to engage in swift cognitive control and working memory (e.g. Aron et al. 2004; Chikazoe et al. 2007; Krawczyk 2002; Botvinick et al. 2004; Holroyd et al. 2004; Achtziger et al. 2012). Additionally, the co-activation of the ACC and RIFG has been shown to be associated with the performance accuracy after a change of the reward contingency in reversal learning (Ghahremani et al. 2010).

The LR encoding may reflect a diverse range of processes involved in linking multiple sources of information and selective retrieval of information from memory, which may be supported by anatomically distributed brain networks that share information in a dynamic manner. Our findings here suggest that there may be two parallel systems supporting the adaptive adjustment of the LR. The first system, including LC, INS and preSMA, is mainly involved in tracking the average features

of a recent history and adapt the LR accordingly; whereas the second system, including ACC and RIFG, complement the first system by providing more precise and swift adjustment based on local information at each time point. Some existing evidence supports this speculation. For example, it has been found that ACC and LC closely interact with each other in learning under uncertainty (e.g. Yu & Dayan, 2005).

In summary, we find that participants' LRs vary according to local statistical features: (i) The LR is lower in contexts with a higher noise level, and (ii) The LR is higher in contexts with a changing mean and a stable noise level (a relevant change) compared to contexts with a stable mean and a changing noise level (an irrelevant change). Furthermore, we find that the adaptive LR is positively correlated with the functional activity of a region in the pons, consistent with the position of locus coeruleus (LC), at the individual level, providing the first direct empirical evidence for the link between functional activity of LC and the computationally complex function of adaptively weighting new information based on the local contexts. Moreover, our finding also suggest there might be another parallel system, consists of of the ACC and RIFG, which is involved in providing a more swift and precise trial-based adjustment for the LR encoding.

Reference

Achtziger, Anja, Carlos Alos-Ferrer, Sabine Hugelschafer, and Marco Steinhauser. 2012. “The Neural Basis of Belief Updating and Rational Decision Making.” *Social Cognitive and Affective Neuroscience* (September).

Amiez, C, J P Joseph, and E Procyk. 2006. “Reward Encoding in the Monkey Anterior Cingulate Cortex.” *Cerebral Cortex (New York, N.Y.: 1991)* 16 (7) (July): 1040–1055.

Aron, Adam R., Trevor W. Robbins, and Russell A. Poldrack. 2004. "Inhibition and the right inferior frontal cortex." *Trends in cognitive sciences* 8, no. 4: 170-177.

Aston-Jones, G, J Rajkowski, and P Kubiak. 1997. “Conditioned Responses of Monkey Locus Coeruleus Neurons Anticipate Acquisition of Discriminative Behavior in a Vigilance Task.” *Neuroscience* 80 (3) (October): 697–715.

Aston-Jones, G, M Iba, E Clayton, J Rajkowski, and J Cohen. 2007. “The Locus Coeruleus and Regulation of Behavioral Flexibility and Attention: Clinical Implications.” *Brain Norepinephrine: Neurobiology and Therapeutics (Ordway GA, Schwartz MA, Frazer a, Eds)*: 196–235.

Aston-Jones, Gary, and Jonathan D Cohen. 2005. “An Integrative Theory of Locus Coeruleus-Norepinephrine Function: Adaptive Gain and Optimal Performance..” *Annual Review of Neuroscience* 28: 403–450.

Behrens, Timothy EJ, Mark W Woolrich, Mark E Walton, and Matthew FS Rushworth. 2007. “Learning the Value of Information in an Uncertain World.” *Nature Neuroscience* 10 (9): 1214–1221.

Botvinick, Matthew M., Jonathan D. Cohen, and Cameron S. Carter. 2004. "Conflict monitoring and anterior cingulate cortex: an update." *Trends in cognitive sciences* 8, no. 12: 539-546.

Carter, C S, and V van VEEN. 2007. “Anterior Cingulate Cortex and Conflict Detection: an Update of Theory and Data.” *Cognitive, Affective, & Behavioral Neuroscience* 7 (4) (December 1): 367–379.

Carter, Cameron S., Matthew M. Botvinick, and Jonathan D. Cohen. 1999. "The contribution of the anterior cingulate cortex to executive processes in cognition." *Reviews in the Neurosciences* 10, no. 1: 49-58.

Carter, Cameron S., Todd S. Braver, Deanna M. Barch, Matthew M. Botvinick, Douglas Noll, and Jonathan D. Cohen. 1998. "Anterior cingulate cortex, error detection, and the online monitoring of performance." *Science* 280, no. 5364: 747-749.

Chikazoe, Junichi, Seiki Konishi, Tomoki Asari, Koji Jimura, and Yasushi Miyashita. 2007. "Activation of right inferior frontal gyrus during response inhibition across response modalities." *Journal of Cognitive Neuroscience* 19, no. 1: 69-80.

Cohen, Michael X. 2008. “Neurocomputational Mechanisms of Reinforcement-Guided Learning in Humans: a Review.” *Cognitive, Affective, & Behavioral Neuroscience* 8 (2) (June): 113–125.

Forstmann, Birte U, Gilles Dutilh, Scott Brown, Jane Neumann, D Yves von Cramon, K Richard Ridderinkhof, and Eric-Jan Wagenmakers. 2008. “Striatum and Pre-SMA Facilitate Decision-Making Under Time Pressure.” *Proceedings of the National Academy of Sciences* 105 (45) (November): 17538–17542.

Ghahremani, D G, J Monterosso, J D Jentsch, R M Bilder, and R A Poldrack. 2010. “Neural Components Underlying Behavioral Flexibility in Human Reversal Learning.” *Cerebral Cortex* 20 (8) (July 9): 1843–1852.

Glascher, Jan, Nathaniel Daw, Peter Dayan, and John P O'Doherty. 2010. “States Versus Rewards: Dissociable Neural Prediction Error Signals Underlying Model-Based and Model-Free Reinforcement Learning.” *Neuron* 66 (4) (May): 585–595.

Holroyd, Clay B, Sander Nieuwenhuis, Nick Yeung, Leigh Nystrom, Rogier B Mars, Michael G H Coles, and Jonathan D Cohen. 2004. “Dorsal Anterior Cingulate Cortex Shows fMRI Response to Internal and External Error Signals.” *Nature Neuroscience* 7 (5) (May): 497–498.

Inase, Masahiko, Hironobu Tokuno, Atsushi Nambu, Toshikazu Akazawa, and Masahiko Takada. 1996. "Origin of thalamocortical projections to the presupplementary motor area (pre-SMA) in the macaque monkey." *Neuroscience research* 25, no. 3: 217-227.

Kennerley, Steve W., Katsuyuki Sakai, and M. F. S. Rushworth. 2004. "Organization of action sequences and the role of the pre-SMA." *Journal of neurophysiology* 91, no. 2: 978-993.

Keren, Noam I, Carl T Lozar, Kelly C Harris, Paul S Morgan, and Mark A Eckert. 2009. “In Vivo Mapping of the Human Locus Coeruleus.” *Neuroimage* 47 (4) (October): 1261–1267.

Kim, Jae-Hun, Jong-Min Lee, Hang Joon Jo, Sook Hui Kim, Jung Hee Lee, Sung Tae Kim, Sang Won Seo et al. 2010. "Defining functional SMA and pre-SMA subregions in human MFC using resting state fMRI: functional connectivity-based parcellation method." *Neuroimage* 49, no. 3: 2375-2386.

Krawczyk, Daniel C. 2002. “Contributions of the Prefrontal Cortex to the Neural Basis of Human Decision Making.” *Neuroscience & Biobehavioral Reviews* 26 (6) (October): 631–664.

Moruzzi, Giuseppi, and Horace W. Magoun. 1949. "Brain stem reticular formation and activation of the EEG." *Electroencephalography and clinical neurophysiology* 1, no. 1: 455-473.

Nassar, Matthew R, Katherine M Rumsey, Robert C Wilson, Kinjan Parikh, Benjamin

Heasly, and Joshua I Gold. 2012. “Rational Regulation of Learning Dynamics by Pupil-Linked Arousal Systems.” *Nature Neuroscience* 15 (7) (June 3): 1040–1046.

Nassar, Matthew R, Robert C Wilson, Benjamin Heasly, and Joshua I Gold. 2010. “An Approximately Bayesian Delta-Rule Model Explains the Dynamics of Belief Updating in a Changing Environment.” *The Journal of Neuroscience* 30 (37) (September): 12366–12378.

Niv, Yael, Jeffrey A Edlund, Peter Dayan, and John P O'Doherty. 2012. “Neural Prediction Errors Reveal a Risk-Sensitive Reinforcement-Learning Process in the Human Brain.” *The Journal of Neuroscience* 32 (2) (January): 551–562.

O'Doherty, J P, P Dayan, K Friston, H Critchley, and R J Dolan. 2003. “Temporal Difference Models and Reward-Related Learning in the Human Brain.” *Neuron* 38 (2): 329.

Paus, T. 2001. “Primate Anterior Cingulate Cortex: Where Motor Control, Drive and Cognition Interface.” *Nature Reviews Neuroscience* 2 (6) (June): 417–424.

Payzan-LeNestour, Elise, Simon Dunne, Peter Bossaerts, and John P O'Doherty. 2013. “The Neural Representation of Unexpected Uncertainty During Value-Based Decision Making.” *Neuron* 79 (1) (July): 191–201.

Phillips, M A, E Szabadi, and C M Bradshaw. 2000. “Comparison of the Effects of Clonidine and Yohimbine on Spontaneous Pupillary Fluctuations in Healthy Human Volunteers.” *Psychopharmacology* 150 (1) (May): 85–89.

Preuschoff, Kerstin, and Peter Bossaerts. 2007. “Adding Prediction Risk to the Theory of Reward Learning.” *Annals of the New York Academy of Sciences* 1104 (May): 135–146.

Preuschoff, Kerstin, Steven R Quartz, and Peter Bossaerts. 2008. “Human Insula Activation Reflects Risk Prediction Errors as Well as Risk.” *The Journal of Neuroscience* 28 (11) (March): 2745–2752.

Rescorla, Robert A, and Allan R Wagner. 1972. “A Theory of Pavlovian Conditioning: Variations in the Effectiveness of Reinforcement and Nonreinforcement.” *Classical Conditioning II: Current Research and Theory*: 64–99.

Sara, Susan J., Andrey Vankov, and Anne Hervé. 1994. "Locus coeruleus-evoked responses in behaving rats: a clue to the role of noradrenaline in memory." *Brain research bulletin* 35, no. 5: 457-465.

Sara, S. J., and M. Segal. 1991. "Plasticity of sensory responses of locus coeruleus neurons in the behaving rat: implications for cognition." *Progress in brain research* 88: 571-585.

Schultz, W, and A Dickinson. 2000. “Neuronal Coding of Prediction Errors.” *Annual Review of Neuroscience* 23: 473–500.

Schultz, W, P Dayan, and P R Montague. 1997. “A Neural Substrate of Prediction and Reward.” *Science* 275 (5306) (March 14): 1593–1599.

Steriade, M. 1996. “Arousal: Revisiting the Reticular Activating System.” *Science* 272 (5259) (April 12): 225–226.

Sutton, Richard S., and Andrew G. Barto. 1998. *Reinforcement learning: An introduction*. Vol. 1, no. 1. Cambridge: MIT press.

Tobler, Philippe N, Christopher D Fiorillo, and Wolfram Schultz. 2005. “Adaptive Coding of Reward Value by Dopamine Neurons.” *Science* 307 (5715) (March): 1642–1645.

van Gaal, Simon, H. Steven Scholte, Victor AF Lamme, Johannes J. Fahrenfort, and K. Richard Ridderinkhof. 2011. "Pre-SMA gray-matter density predicts individual differences in action selection in the face of conscious and unconscious response conflict." *Journal of cognitive neuroscience* 23, no. 2: 382-390.

van Veen, Vincent, Jonathan D. Cohen, Matthew M. Botvinick, V. Andrew Stenger, and Cameron S. Carter. 2001. "Anterior cingulate cortex, conflict monitoring, and levels of processing." *Neuroimage* 14, no. 6: 1302-1308.

Vankov, A, A Hervé-Minvielle, and S J Sara. 1995. “Response to Novelty and Its Rapid Habituation in Locus Coeruleus Neurons of the Freely Exploring Rat.” *The European Journal of Neuroscience* 7 (6) (June 1): 1180–1187.

Yu, Angela, and Peter Dayan. 2003. “Expected and Unexpected Uncertainty: ACh and NE in the Neocortex.” *Advances in Neural Information Processing Systems*: 173–180.

Zentgraf, K., R. Stark, M. Reiser, S. Künzell, A. Schienle, P. Kirsch, B. Walter, D. Vaitl, and J. Munzert. 2005. "Differential activation of pre-SMA and SMA proper during action observation: effects of instructions." *Neuroimage* 26, no. 3: 662-672.

Supplementary materials

Method for generating the task sequence

A sequence of observations was generated from the underlying Gaussian distributions *N (û, σ)* before the experiment. All observations were restricted to be within 0 to 100. The underlying mean (*û*) and standard deviation (*σ*) were generated as following. In the stable session, *û* was randomly initialized and remained constant over the session. In the volatile session, *û* was randomly generated (0 to 100) and remained constant for a short period (block length was drawn from *N (19, 3)*) before a change occurred. The change amplitude was drawn from a Uniform distribution (*U (15, 20)*) and could be either positive or negative with equal probabilities. In both the stable and volatile sessions, *σ* changed multiple times. The block length for each *σ* was drawn from a Gaussian distribution (*N (10, 2)*). The initial *σ* of a session could either be low ($\sigma = 4$) or high ($\sigma = 10$). The change amplitude of *σ* was drawn from a Uniform distribution (*U (6, 7.8)*). In order to prevent subjects noticing obvious change points of the distribution, we imposed restrictions on the new distribution by calculating the likelihood of a new observation coming from either distribution. We used these to make sure that the likelihood of coming from the new distribution was higher but not twice as high as that of the old distribution.

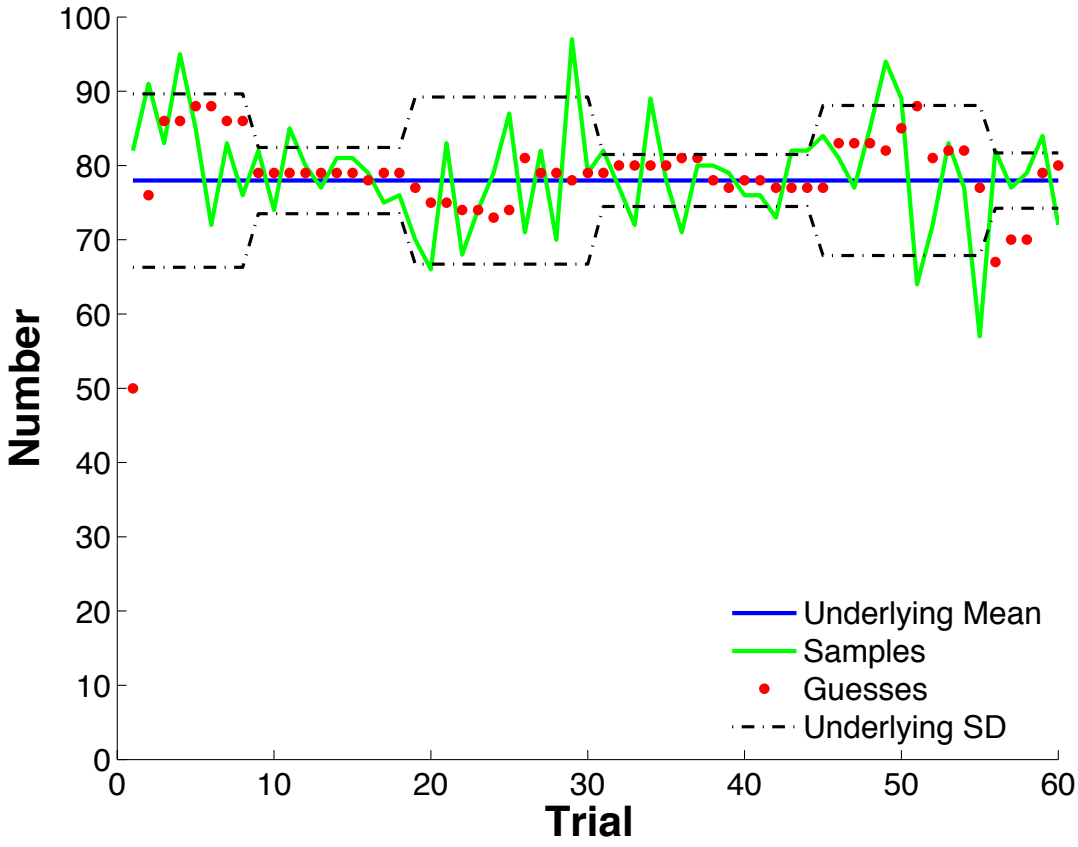

Figure S1. An example of the session with stable mean. The solid blue line represents the underlying mean, which remained unknown to subjects and had to be inferred. Black dashed lines illustrate the standard deviation (SD), which changed independently of the mean. Green line represents the samples drawn from the underlying distributions. Red dots were the guesses of a subject. Notably, the mean and SD could suddenly change but subjects could only infer that from the received observations.

Instruction procedure

We explained the task to our subjects in the following steps. First, we provided some real-life examples where one has to estimate the true value based on noisy observations. Subjects were instructed about the current task and explicitly told that over a session the true value could either keep stable or change multiple times, while the noise level could also change multiple times, but independent of the change of the true value. Subjects were also aware that the observations and the mean are determined at the beginning of each block and do not depend on their previous guesses. Second, subjects watched two demo sessions (one with stable true mean and

the other with volatile mean), with the true value and corresponding observations shown. The demo sessions had identical structures as the main sessions but with only 20 trials. Third, subjects had two sessions (one with stable true mean and the other with volatile mean) of practice outside the scanner and immediately followed by a replay of these sessions where they could observe their own responses together with the underlying mean. Subjects practiced how to make responses in the scanner before the scanning session started.

Payment mechanism

At the end of the experiment, only one session was randomly chosen and the performance score of this session decided the payment, i.e. payment was monotonically decreasing with the average error of this randomly chosen session. Detailed information was provided to subjects in Table S1.

Table S1: Payment table of our task.

Average Error	Total Payment (CHF)	Average Error	Total Payment (CHF)
0	120	**6**	75
1	100	**7**	70
2	95	**8**	65
3	90	**9**	60
4	85	**≥ 10**	55
5	80		

Our payment mechanism provided incentives for subjects to report their best guesses for each trial. In order to maximize the payment, subjects needed to minimize the average distance between their estimations of the mean at trial t ($\hat{u}_t$) and μ_t across the session, i.e. $E(|\hat{u}_t - \mu_t|)$. The underlying sequence was determined before the experiment and did not depend on subjects' responses. Consequently, subjects should minimize $|\hat{u}_t - \mu_t|$ in each trial, i.e. report their best estimation for μ_t.

Subjects

One subject was excluded from the final analysis because of difficulty in understanding the task reported in the post-experiment interview. Also this subject reported falling asleep during the experiment in the scanner.

Behavioral data analysis procedure

Below we provide the detailed procedure of our analysis through an example subject. First, we divided each session into epochs based on changes in the underlying distribution (either the mean or the noise level). Trials between changes were considered as belonging to an epoch. The length of epochs (mean ± s. d.) is 8.14 ± 3.69 (trials). An example is provided in Figure S1.

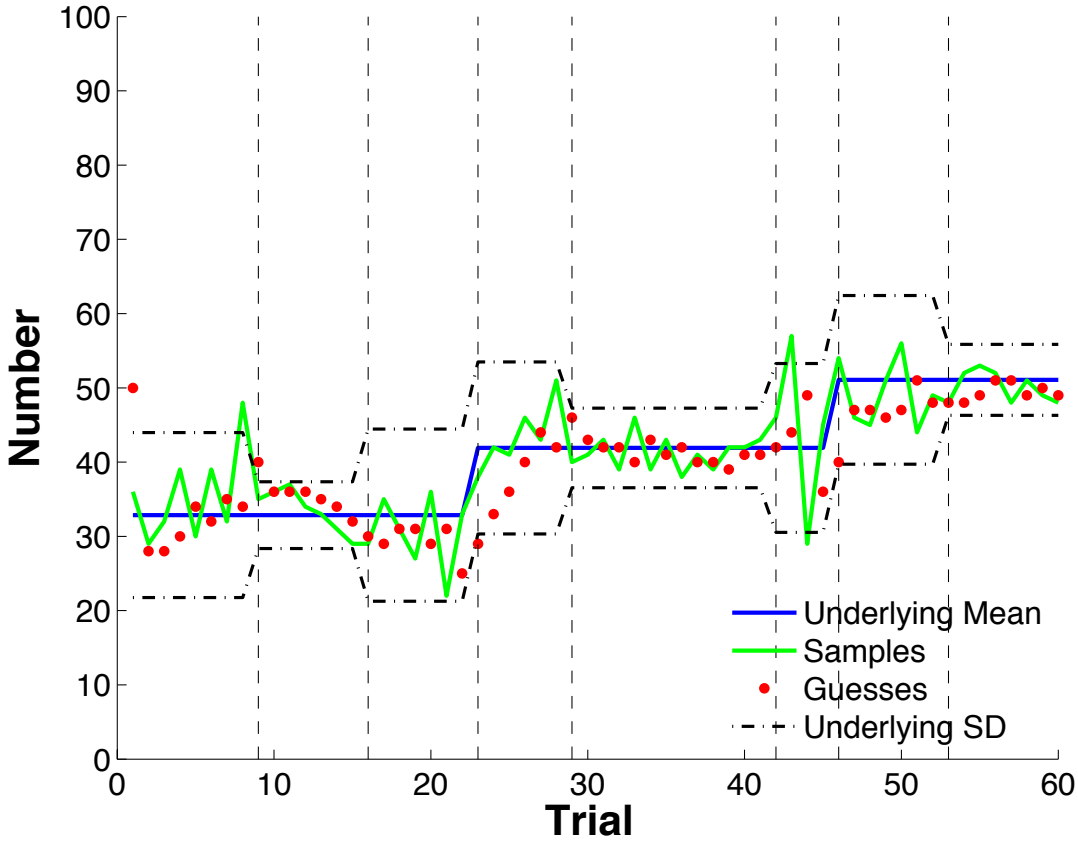

Figure S2. Data of an example session. Here we divided the whole session into different epochs based on changes in the underlying distribution. The time points where the change occurred are illustrated as black dashed vertical lines, and trials between two dashed lines constituted an epoch.

Second, we estimated the average LR for epoch *i* (α_i) based on Rescorla-Wagner rule through linear least squares regression. For example, in the example session we illustrated in Figure S1, there were eight epochs (n = 8). Therefore formula (1) became:

$$\hat{u}_{t+1} - \hat{u}_t = \sum_{i=1}^{8} \alpha_i \times b_{it} \times \delta_t + e_t \quad (4)$$

and,

$$e_t = \beta_t \times \delta_t \quad (5)$$

We illustrate the estimated α_i, β_t, e_t in Figure S3 a, b, c, respectively. In addition, in order to evaluate how well subjects' guesses can be explained by our assumption of the constant LR for each epoch, we calculated the predicted guesses based on α_i, namely:

$$Predicted\text{-}guesses_{t+1} = \sum_{i=1}^{n} \alpha_i \times b_{it} \times \delta_t + \hat{u}_t \quad (6)$$

We illustrate the predicted guesses together with the original subject's guesses of an example session in Figure S3d. In addition, we provide a scatter plot of the predicted guesses against subjects' guesses from all sessions across subjects in Figure S4. From both figures we can see that the constant LR for epoch *i* (α_i) can give a good explanation of subjects' actual guesses.

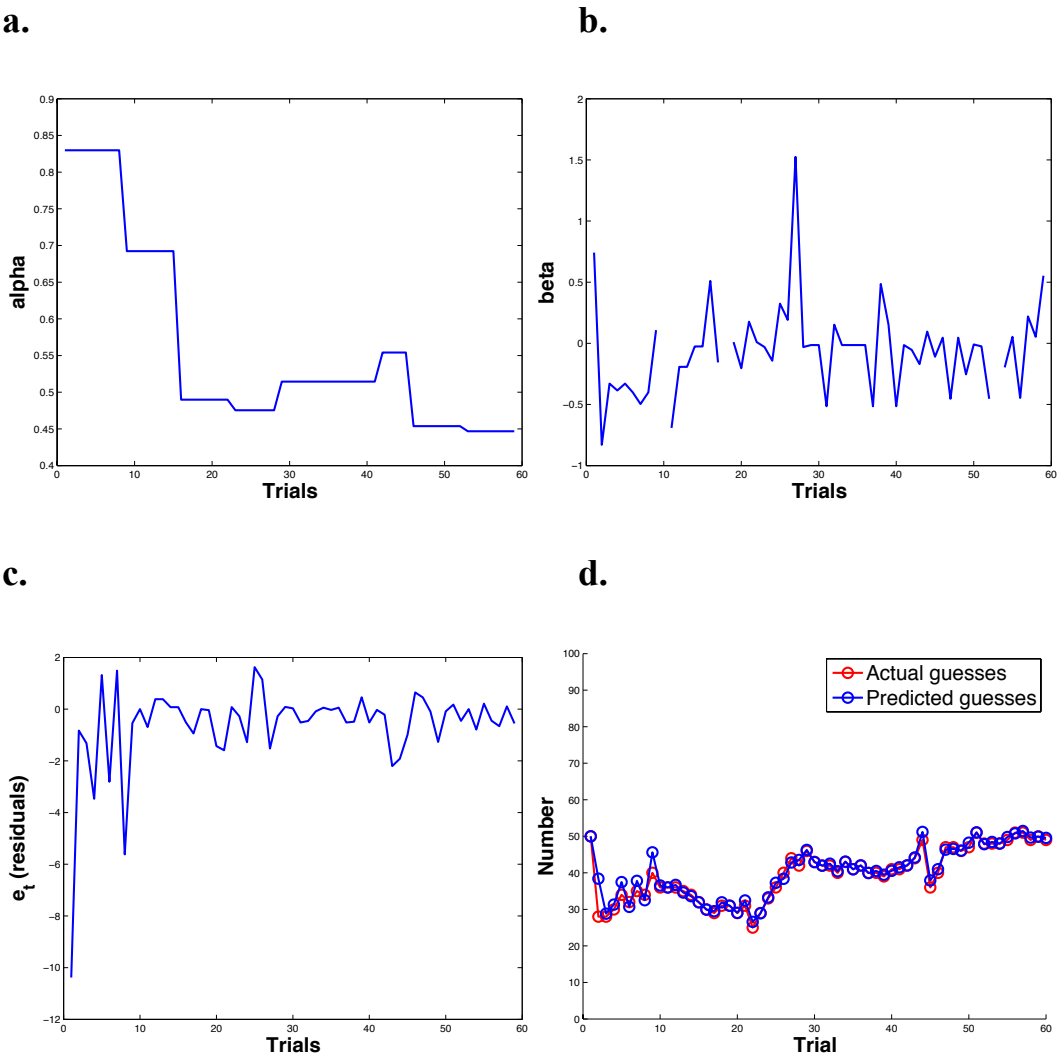

***Figure S3*. a.** Estimated alpha of an example session. **b.** Estimated beta of an example session. **c.** e_t (residuals from regression) of an example session. **d.** Predicted guesses based on our estimated alpha following formula (6) of an example session. Here we can see that the constant LR for each epoch can give a good explanation of subjects' actual guesses.

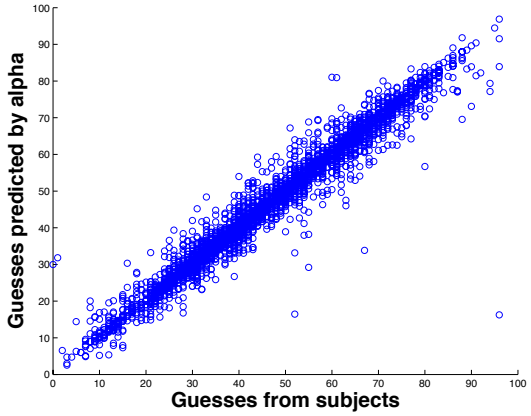

Figure S4. Scatter plot between subjects' guesses and the predicted guesses based on alpha. The result suggests that the assumption of a constant LR for each epoch gives a good explanation of subjects' guesses.

Third, we classified epochs into different types based on the volatility of the mean and noise level, as described in the Methods section.

Behavior results

The average distance over subjects (mean ± s.d.) was 3.62 ± 0.97. The average reaction time across subjects (mean ± s.d.) was 5.06 ± 0.89 s.

fMRI results

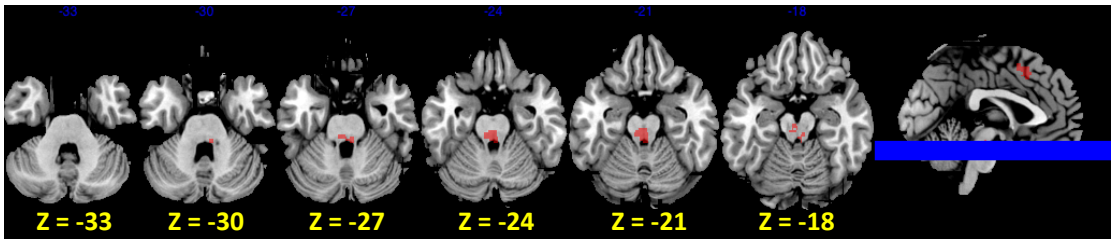

Figure S5. The position of our activation in LC. Similar to Keren et.al (2009), we display the activation in LC in multiple slices. The activation here in the pons matches the reported position of LC in Keren et.al (2009).

Table S2: Significant whole-brain clusters that were positively correlated with α (a) and β (b) at the observation stage. Data were first reported at a threshold of $p < 0.001$, cluster level FWE corrected and small volume FWE corrected for our hypothesized region LC (shown in bold). We also reported clusters significant at a sub-threshold of $p < 0.001$ and cluster level uncorrected $p < 0.05$. Local maxima within these clusters are reported together with the number of voxels (cluster size); Hemisphere (HEM); Left (L); Right (R); Brodmann area (BA); x, y, z are MNI coordinates of the local maximum.

a. Neural correlates of α at the observation stage

HEM	Region name	BA	X (mm)	Y (mm)	Z (mm)	t value	Cluster pFWE	Cluster uncorr	Cluster Size
L	**Insula**	**48**	**-44**	**16**	**0**	**5.68**	**0.048**	**0.002**	**68**
L	**Supplementary motor**	**6**	**-6**	**10**	**52**	**5.19**	**0.025**	**0.001**	**79**
L	**Locus Coeruleus**		**-6**	**-30**	**-24**	**4.33**	**0.659**	**0.038**	**25**
R	Thalamus		2	-20	6	5.07	0.723	0.046	23

b. Neural correlates of β at the observation stage

HEM	Region name	BA	X (mm)	Y (mm)	Z (mm)	t value	Cluster pFWE	Cluster uncorr	Cluster size
R	**Inferior Frontal cortex**	**45**	**56**	**24**	**6**	**4.59**	**0.042**	**0.002**	**81**
R	Anterior Cingulate	32	4	44	22	4.48	0.14	0.006	58
R	Superior Medial Frontal cortex	32	6	32	40	4.62	0.313	0.016	43
R	Insula	48	34	14	-10	5	0.678	0.048	27

Table S3. Significant whole-brain clusters that were positively correlated with α (a) and β (b) at the guess stage. Data were first reported at a threshold of $p < 0.001$, cluster level FWE corrected (shown in bold). We also reported clusters significant at a sub-threshold of $p < 0.001$ and cluster level uncorrected $p < 0.05$. Local maxima within these clusters are reported together with the number of voxels (cluster size).

a. Neural correlates of α at the guess stage

Region name	**MNI coordinates (x y z)**	**t value**	**Cluster pFWE**	**Cluster uncorr**	**Cluster size**
Inferior Parietal	-42 -48 48	5.16	0.18	0.008	50
SupraMarginal	-58 -30 38	5.08	0.13	0.006	55

b. Neural correlates of β at the guess stage

Region name	**MNI coordinates (x y z)**	**t value**	**Cluster pFWE**	**Cluster uncorr**	**Cluster size**
Precuneus	**10 -66 50**	**5.23**	**0.007**	**0.000**	**109**
SupraMarginal	-58 -30 38	4.73	0.64	0.04	27

c. Neural correlates of guessed number at the confirmation stage

Region name	**MNI coordinates (x y z)**	**t value**	**Cluster pFWE**	**Cluster uncorr**	**Cluster size**
Lingual	22 -72 4	3.87	0.463	0.026	35

Table S4. Functional activations at the guessing, confirmation and new observation stage of a trial. Significant results were shown at an uncorrected threshold of p<0.001, FWE corrected at the cluster level.

a. Functional activations at the observation stage

Region name	MNI coordinates (x y z)	t value	Cluster pFWE	Cluster uncorr	Cluster size	Peak p(FWE -cor)
Calcarine_R	16 -86 4	11.82	< 0.001	< 0.001	15530	< 0.001
Frontal_Mid_R	28 14 50	8.97	< 0.001	< 0.001	2094	0.003
Frontal_Inf_Tri_L	-52 26 30	8.97	< 0.001	< 0.001	703	0.003
Precentral_L	-30 6 48	8.32	< 0.001	< 0.001	279	0.01
Insula_R	34 14 -14	7.01	< 0.001	< 0.001	353	0.078
Paracentral_L	-6 -30 58	6.79	< 0.001	< 0.001	464	0.107
Insula_L	-32 20 -6	6.33	0.041	0.003	114	0.205
Temporal_Mid_L	-56 -48 14	5.3	0.013	0.001	148	0.685
Frontal_Sup_R	26 54 8	5.22	0.02	0.001	136	0.732

b. Functional activations at the guess stage

Region name	MNI coordinates (x y z)	t value	Cluster pFWE	Cluster uncorr	Cluster size	peak p(FWE -cor)
Parietal_Inf_L	-26 -50 46	13.02	< 0.001	< 0.001	13549	< 0.001
Fusiform_R	32 -50 -14	9.88	< 0.001	< 0.001	732	0.001
Precentral_L	-56 6 24	8.58	< 0.001	< 0.001	386	0.007
Precentral_R	28 -4 58	7.95	< 0.001	< 0.001	649	0.02
Cerebelum_4_5_L	-4 -30 -8	7.12	0.011	0.001	133	0.078
Frontal_Inf_Oper_R	58 8 24	6.56	< 0.001	< 0.001	259	0.174
Cingulum_Mid_L	-12 -22 42	6.33	0.036	0.002	103	0.238

c. Functional activations at the confirmation stage

Region name	MNI coordinates (x y z)	t value	Cluster pFWE	Cluster uncorr	Cluster size	peak p(FWE -cor)
Cerebelum_4_5_R	10 -56 -20	14.97	< 0.001	< 0.001	60835	< 0.001
Frontal_Inf_Tri_L	-46 42 14	5.09	< 0.001	< 0.001	351	0.745

Experiment Instruction

Vielen Dank für Ihre Teilnahme an diesem Experiment!

Wir leben in einer ungenauen Welt, in der wir Zahlenwerte auf Basis einer Reihe unvollkommener Beobachtungen abschätzen müssen. Z.B.

- indem wir jeden Tag die Temperatur beobachten, können wir für verschiedene Jahreszeiten in einer Gegend Durchschnittstemperaturen schätzen;
- indem wir den täglichen Preis einer Aktie beobachten, können wir *mit der Zeit* den wahren Wert dieser Aktie abschätzen;
- indem wir verschiedene Wege von Zürich nach Bern abfahren, können wir den wahren Abstand zwischen den beiden Städten und die mittlere Fahrzeit abschätzen.

In allen drei Beispielen müssen wir den wahren Wert aus fehlerbehafteten Beobachtungen schätzen. Manchmal bleibt der korrekte Wert über die Zeit hin konstant, wie etwa die Distanz zwischen Zürich und Bern, manchmal ändert er sich jedoch, wie etwa der Wert einer Aktie auf dem Finanzmarkt.

Die Beobachtungen können mehr oder weniger genau sein:

- Bitten wir z.B. 10 Personen die heutige Temperatur mit Hilfe eines Thermometers zu bestimmen, so werden die Beobachtungen sehr eng beieinander liegen.
- Bitten wir hingegen die gleichen 10 Personen, die Temperatur ohne Hilfe eines Thermometers zu bestimmen, so werden die Beobachtungen weit auseinander liegen.

Im heutigen Experiment ist es Ihre Aufgabe, den wahren Wert mit Hilfe fehlerhafter Beobachtungen zu bestimmen. Ihre Auszahlung wird durch die Genauigkeit Ihrer Schätzung beeinflusst.

Der heutige Ablauf ist wie folgt:

- Demo (ausserhalb des Scanners)
- Probedurchläufe (ausserhalb des Scanners)
- Experiment (im Scanner)
- Post-scanning session (ausserhalb des Scanners; post-rating, Fragebogen)
- Auszahlung

Demo

In der Demo auf dem Computer vor Ihnen können Sie sehen wie fehlerhafte Beobachtungen und wahrer Wert zusammenhängen können. Sie sehen nacheinander fehlerbehaftete Beobachtungen (gelb) und den wahren Wert (rot). Der wahre Wert und die Beobachtungen werden entlang einer horizontalen Linie von 0 bis 100 dargestellt (siehe Abbildung). Sie können sich die gelben Ziffern z.B. als Schätzungen der Wassertemperatur oder schwankende Aktienpreise vorstellen. Die rote Ziffer wäre dann die wahre Wassertemperatur oder der wahre Aktienwert.

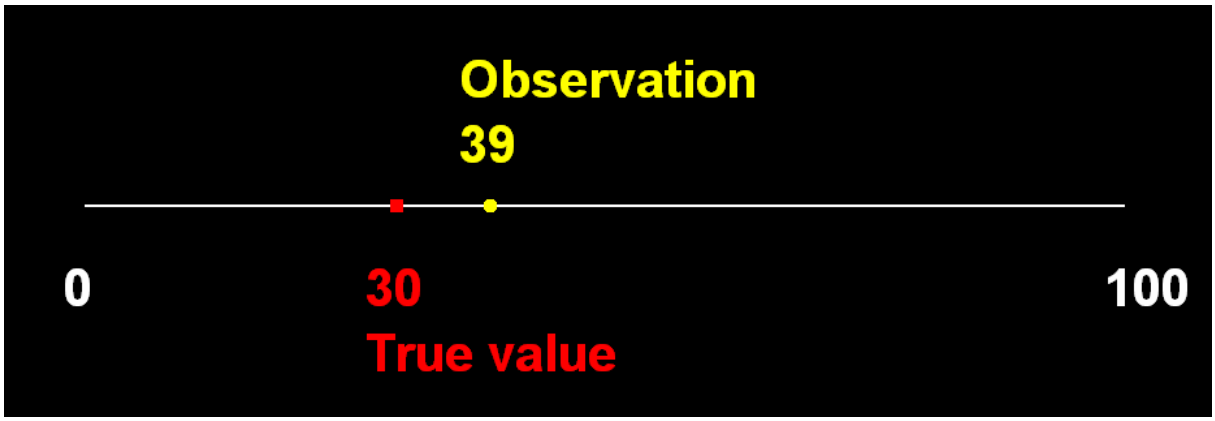

WICHTIG: Während des Experiments werden Sie nur die gelben Beobachtungen sehen. Ihre Aufgabe wird es sein, den roten Wert mit Hilfe dieser Beobachtungen zu schätzen.

Um die Demo zu starten, drücken Sie 's'. Schauen Sie der Demo aufmerksam zu und beantworten Sie dann die folgenden 2 Fragen bevor Sie auf der nächsten Seite fortfahren. Wenn Sie Fragen zur Demo haben oder eine weitere Demo sehen möchten, melden Sie sich bitte beim Versuchsleiter.

Fragen zur Demo:

1) Hat sich der wahre Wert während der Demo geändert?
   A. Ja
   B. Nein
2) Hat sich während der Demo die Genauigkeit des Beobachtungswerts verändert (d. h. der durchschnittliche Abstand zwischen den gelben und roten Zahlen)?
   A. Ja
   B. Nein

Probedurchlauf & Experiment

Während des Probedurchlaufs und Experiments, werden Sie wiederum verschiedene Beobachtungen zwischen 0 und 100 sehen. Nach jeder Beobachtung geben Sie Ihre derzeitige Schätzung des wahren Wertes ein. **Beachten Sie, dass Sie den wahren Wert (rote Zahl in der Demo) nie sehen werden, sondern nur die fehlerbehafteten Beobachtungen (gelbe Zahlen). In jedem Durchlauf kann sich der wahre Wert gelegentlich ändern (aber auf keinen Fall nach jeder Runde). Sie sollten den wahren Wert so akkurat wie möglich schätzen.** Am Ende jedes Durchlaufs errechnet der Computer Ihren durchschnittlichen Fehler für diesen Durchlauf.

Der Ablauf des Experiments ist wie folgt:

1. Zu Beginn der ersten Runde, sehen Sie eine grüne zufällige Zahl, die Ihre nächste Schätzung repräsentiert.
2. Wenn Sie den **blauen Knopf** drücken (Zeigefinger), verringern Sie die Zahl. Wenn Sie den **gelben Knopf** drücken (Mittelfinger), vergrössern Sie die Zahl.
3. Um Ihre Schätzung zu bestätigen, drücken Sie den **grünen Knopf** (Ringfinger). Ihr Schätzwert erscheint jetzt in weiss. **Sie haben zehn Sekunden Zeit, um Ihre Wahl zu treffen.** Danach wird die momentane Position der grünen Zahl automatisch als Ihre Wahl betrachtet
4. Die Runde endet mit einem neuen Beobachtungswert (gelb). Ausgehend von diesem Beobachtungswert können Sie ihre soeben getroffene Entscheidung überdenken und einen neuen Schätzwert abgeben. Im untenstehenden Beispiel war "65" die Schätzung der Versuchsperson und "55" ist der neue Beobachtungswert.

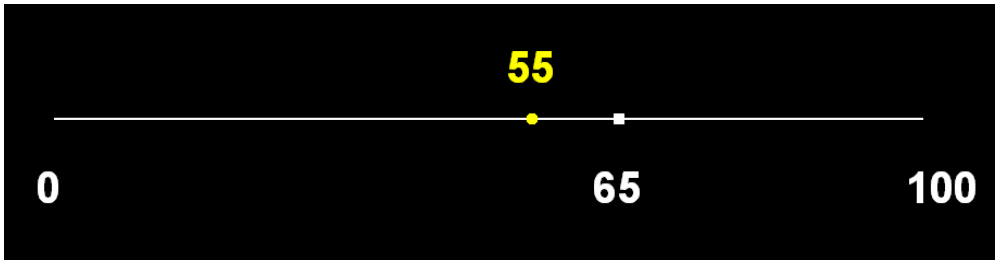

5. Die nächste Runde beginnt. Der Schätzwert aus der vorangegangenen Runde wird grau dargestellt, der neue Beobachtungswert gelb und die neue Zufallszahl grün. Im untenstehenden Beispiel war "65" die Schätzung der Versuchsperson, der letzte Beobachtungswert "55" und die momentane Zufallszahl "22". Danach geht es wie oben (Punkt 2.) weiter.

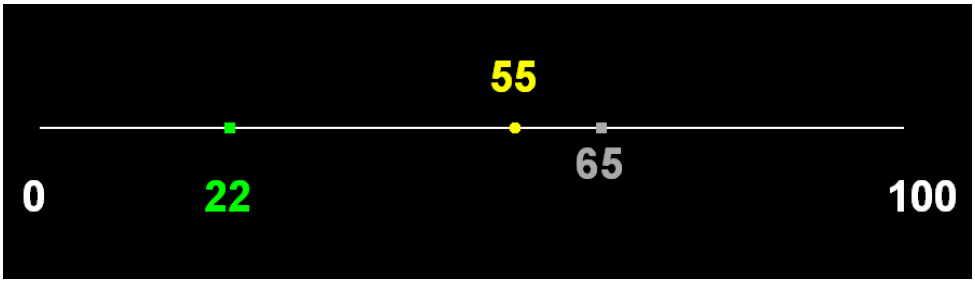

Sie werden das Experiment zunächst ausserhalb des Scanners üben. Ihre Schätzungen während dieses Probedurchlaufes werden Ihre Auszahlung **nicht** beeinflussen.

Im Anschluss spielen Sie 4 Durchläufe mit jeweils 60 Beobachtungen (Runden) im Scanner. Ihre Schätzungen während dieses Durchläufe werden Ihre Auszahlung beeinflussen. .

Auszahlung:

Die Gesamtsumme, die Ihnen ausgezahlt wird, hängt vom Durchschnittsfehler ab, um den Ihre Schätzungen von der korrekten Zahl abweichen (in der Demo rot angegeben und nicht mit den gelben Beobachtungswerten zu verwechseln!).
Nach dem Experiment werden Sie zufällig einen der vier Durchläufe auswählen. Das Ergebnis des Blocks wird wie folgt zur Vergütung Ihres Erscheinens (30 CHF) addiert: Wenn der Durchschnittsfehler des ausgewählten Blocks 1 ist, werden Sie zusätzlich 70 CHF erhalten (gesamt: 70+30=100). Wenn der Durchschnittsfehler bei 2 liegt, werden Sie 65 CHF erhalten, liegt der Fehler bei 3, erhalten Sie CHF 60 usw. (siehe Tabelle für Gesamtauszahlung).

Durchschnittsfehler	Gesamt-Auszahlung (CHF)	Durchschnittsfehler	Gesamt-Auszahlung (CHF)
0	120	**6**	75
1	100	**7**	70
2	95	**8**	65
3	90	**9**	60
4	85	**≥ 10**	55
5	80		

Beachten Sie bitte, dass

- **es nicht die Differenz zwischen Ihrer Schätzung und der nächsten Beobachtung ist die zählt, sondern die Differenz zwischen Ihrer Schätzung und dem wahren Wert.**

- **der wahre Wert und die Beobachtungen zu Beginn des Durchlaufs bestimmt werden und nicht durch Ihre bisherigen Schätzungen beeinflusst werden.**

- **jede Runde zählt und zu Ihrer Endauszahlung beiträgt. Entscheiden Sie daher sorgfältig und so genau und schnell wie möglich.**

Probedurchlauf:

Wir beginnen mit den Probedurchläufen (30 Beobachtungen pro Durchlauf), damit Sie ein Gespür für die Aufgabe und das Schätzen bekommen. Um den Probedurchlauf zu starten, drücken Sie ‘s’. Drücken Sie die **rechte Pfeiltaste**, um die Zahl nach rechts zu bewegen, und die **linke Pfeiltaste**, um die Zahl nach links zu bewegen, sowie die **nach oben Pfeiltaste,** um Ihre Schätzung zu bestätigen.

Nach der Übung werden wir Ihnen den Durchlauf vorspielen. Ihre Schätzungen, die Beobachtungswerte, die sie gesehen haben, und der korrekte Wert werden Ihnen nacheinander für jede Runde des Probedurchlaufes gezeigt.:

1. Der korrekte Wert (rot) und Ihr Schätzwert für die aktuelle Runde (weiß) werden dargestellt:

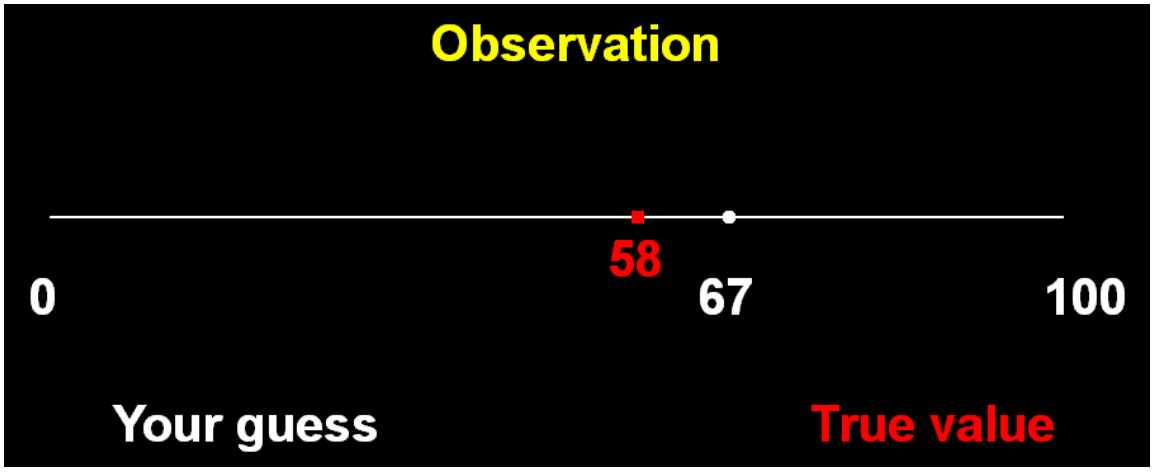

2. Der Beobachtungswert wird gelb dargestellt, Ihr Schätzwert weiß und der korrekte Wert rot:

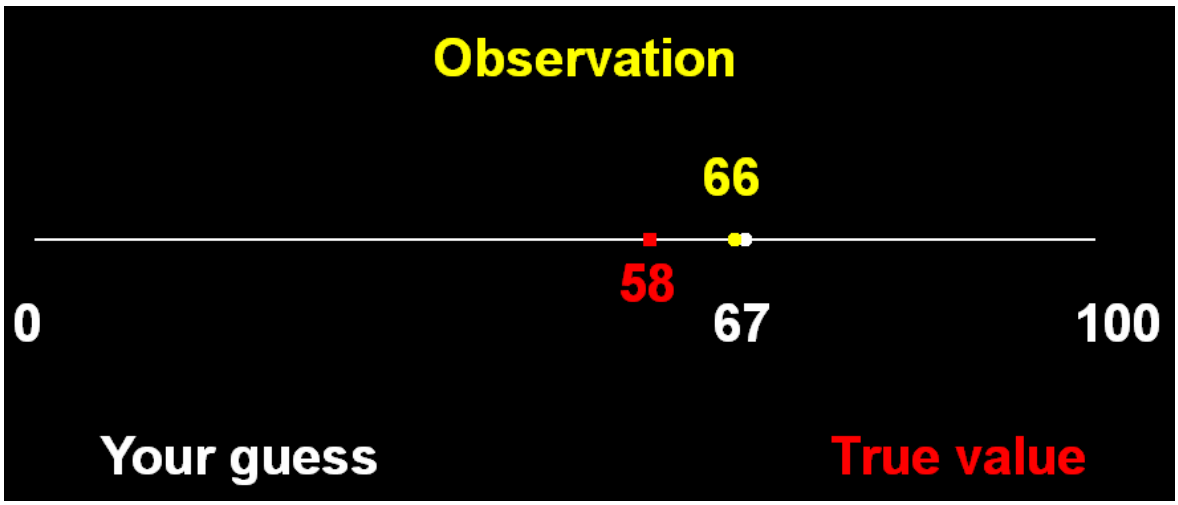

Bitte benachrichtigen Sie den Versuchsleiter, wenn Sie weiter üben möchten.

.

Bevor das Experiment beginnt, bitten wir Sie, folgende Fragen zu beantworten:

1) Verändert sich der korrekte Wert in jeder Runde?
   A. Ja
   B. Nein
2) Verändert sich die Genauigkeit der Beobachtungen in jeder Runde?
   A. Ja
   B. Nein
3) Können Sie den korrekten Wert während des Experiments sehen?
   A. Ja
   B. Nein
4) Was sollen Sie während des Experiments abschätzen?
   A. den fehlerbehafteten Beobachtungswert.
   B. den vorangegangenen Beobachtungswert.
   C. den korrekten Wert.

Sie können nun mit dem eigentlichen Experiment beginnen. Wir wünschen Ihnen dabei viel Spaß und viel Glück bei den Schätzungen!

Experiment protocol

1. Pre-scanning practice.
   1) The experimenter gives the consent form (ask English or German), ethic form, and fMRI potential risk checking-list to the subject.
   2) Subjects read instruction, watch the experiment demo and complete a practice session. We check whether subjects have understood the task and answered the control questions correctly. Note: we display the same demo for a second time if the subject doesn't fully understand the task and would like to watch the demo again. To keep the consistency between subjects, we used the same learning sequence in the demo for every subject.

2. The subject enters the scanner room and is instructed about the response buttons.

3. The subject has a practice session in the scanner to get familiarized with the response buttons.

4. The subject completes all four functional scanning sessions.

5. The experimenter gives the payment to the subject according to his/her performance in the randomly chosen session.

Appendix

C. Structural and Functional Neural Correlates of Individual Learning Ability

This chapter is joint work with Ernst Fehr, Kerstin Preuschoff and Yosuke Morishima

Structural and Functional Neural Correlates of Individual Learning Ability

Chaohui Guo, Yosuke Morishima, Kerstin Preuschoff *, Ernst Fehr *

Abstract

Individuals differ in the ability of learning the state of the world and hidden reward contingencies, particularly when the situation involves a high degree of uncertainty. However, it still remains unclear what the neuroanatomical determinants underlying such heterogeneity are. Here we measure individual learning ability by comparing the learning performance of each individual with that of a Bayesian updating model. We find that there is a large variety in the learning performance across subjects and such individual differences are associated with both the grey matter (GM) volume and the functional involvement of the cerebellum and a brain area covering the right postcentral gyrus, Inferior Parietal cortex and Supramarginal gyrus. These results provide congruent structural and functional evidence for the importance of these regions in the information integration process and suggest a link between the lower-order sensorimotor learning and the belief updating in higher-order learning under uncertainty.

Key words: learning; computational modelling; VBM; cerebellum; changing environment;

Introduction

Individuals differ in their abilities to learn the state of the world and hidden reward contingencies based on noisy observations, particularly when the situation involves a high degree of uncertainty. A previous study shows that the degree of the functional representation of reinforcement learning signals in the striatum differs between learner and non-learners in a reward-learning task (Schonberg et al. 2007). However, it still remains unclear what the neuroanatomical determinants underlie these behavioral and functional inter-individual differences are. In this study, we aim to identify the brain regions whose structural properties and functional involvement are associated with inter-individual differences in the learning ability in a changing environment. Based on the existing findings that higher gray matter (GM) volume accompanies better cognitive ability (de Lange et al. 2008; Hogan et al. 2011; Kanai & Rees 2011), we hypothesized that better learning performance would accompany higher GM volume and higher functional involvement during learning of some brain regions, and these brain regions may be the ones involved in higher-order cognition such as the prefrontal cortex or in lower-order sensorimotor learning such as the cerebellum, which we explain in details in the following.

Our first hypothesis that individual learning performance is associated with the structural and functional properties of the prefrontal cortex is based on the massive findings on the functional importance of the prefrontal cortex in cognition, working memory, memory retrieval, executive control and other functions important for higher-order decision-making (e.g. Wagner et al. 2001; Hampton et al. 2006; Coricelli & Nagel 2009; Barraclough et al. 2004; Boes et al. 2009; Morgan 1999; Badre & Wagner 2007; Petrides 2005; Krawczyk 2002; de Lange et al. 2008). Moreover, the GM volume of regions in the prefrontal cortex has been reported to be associated with inter-individual differences in cognitive abilities (e.g. Schonberg et al. 2007; Matsuo et al. 2009; Ceccarelli et al. 2009; Frangou et al. 2004; Narr et al. 2007; de Lange et al. 2008).

Our second hypothesis is that individual differences in the learning performance will be associated with the structural and functional properties of the cerebellum. The cerebellum, one of the oldest brain regions in humans and animals, has been

considered as the efficient neuronal system for fast online state estimation based on noisy sensory inputs (Wagner et al. 2001; Miall et al. 2007; Hampton et al. 2006; Paulin 2005; Coricelli & Nagel 2009; Bastian 2006; Barraclough et al. 2004; Boes et al. 2009; Morgan 1999; Badre & Wagner 2007; Petrides 2005; Krawczyk 2002; de Lange et al. 2008). The cerebellum has been proposed to serve a general function of learning to predict and prepare for imminent information acquisition, analysis, or action (Raymond et al. 1996). Moreover, its functional role has been extended to higher cognitive functions, such as probabilistic reasoning (Passot et al. 2013), working memory (Chen et al. 2012), error processing (Ide & Li 2011), prediction of future events (Bastian 2006) and other crucial functions for successful learning under uncertainty (Blackwood et al. 2004). There has been increasing evidence that links the cerebellum with learning behaviors. For example, patients with lesion in the cerebellum show significant impairments in the reward-based reversal learning and sequence learning (Dirnberger et al. 2013; Thoma et al. 2008).

In order to test our hypotheses, we measure individual learning ability in a changing environment by comparing the learning performance of each individual with that of an Ideal Learner model (ILM), which integrates new observations following Bayesian updating rules, in a mean-guessing task (Guo et al. in preparation). We used Particle filter (PF), one of Bayesian inference methods, to estimate the hidden variables in ILM. PF is a Markov chain-Monte Carlo (MCMC) approach to recursive dynamical state estimation and has been widely applied in neuroscience studies to investigate the neural organizations of the brain, such as the sensorimotor information updating process in the cerebellum (Paulin 2005), the representation of action value in the striatum (Samejima et al. 2005), and the perceptual inference on cortical hierarchies (Lee & Mumford 2003). We choose PF as our Bayesian inference method because the principles of this method are remarkably compatible with those of the neural systems in the brain, and PF requires no assumptions about the form of the posterior distributions of variables.

Methods

Subjects

Twenty healthy subjects (10 female; 19-27 years old) with no history of neurological or psychiatric illness participated in our task. The study was approved by the ethical committee of Canton Zurich. Written informed consents were obtained from all participants.

Task

We employed the dataset from a previous study (Guo et.al, In preparation). In this dataset, we adopted a mean-guessing task to investigate human learning behavior in a changing environment. Below we provide some basic information about the task, and see more details in the Methods part of *Guo et al (in preparation)*.

In this task, we generated random numbers from a hidden Gaussian distribution ($N(\hat{u}, \sigma)$) where its mean ($\hat{u}$) and standard deviation (σ) can change unexpectedly. Subjects were presented with one observation on each trial and were asked to report their trial-by-trial estimations of the underlying mean ($\hat{u}$) based on observations. All observations and the underlying mean were ranged within 0 to 100. Each subject completed four sessions of 60 trials in each session. Presenting orders of the four sessions were randomized across subjects. The four sessions differed in the volatility of the mean: two sessions were with stable mean over the session (Figure S1), and the other two sessions were with volatile mean (Figure 1). Subjects were informed that the mean and the observations were within 0 to 100, and the mean and the noise level could both change, but independently of each other, for multiple times over each session. Notably, subjects were not informed of the type of the block.

Absolute error for each trial was calculated as the absolute distant between the guessed number and the true underlying mean. At the end of each session, a score was calculated by averaging the trial-by-trial absolute error from the second to the last trial and was presented to subjects. At the end of the experiment, only one session was randomly chosen and the score of this session decided the payment, i.e. payment was scaled inversely with the score of this randomly chosen session.

Behavioral analysis

We examined the inter-individual differences in the ability of learning the mean of underlying distributions in the following two steps. First, we provided the trial-by-trial optimal estimates of the underlying mean based on an Ideal Learner model (ILM), which integrates new information through Bayesian updating. Second, we compared each individual's learning performance with that of the ILM under the same learning sequences (including underlying distributions and observations).

For the first step, we adopted the same estimation procedure as in Samejima et al, 2005. In our ILM model, hidden variables are $x\ (i) = \{B_t, \alpha_t\}$ and the observable variable is $y\ (i) = \{S_t\}$, where B_t is the estimation of the underlying mean, α_t is the learning rate, and S_t is the observation at time t. We used 20,000 particles to approximate the distributions of the hidden variables, and set the initial prior particles for B_0 to be beta distributed within 0 to 100 while shape parameters both equal two (i.e. 100 × *beta (2,2)*; the distribution range of 0 to 100 is due to the fact that the mean and observations are within this range) and for α_0 to be beta distributed (*beta (0.5,0.5)*) within 0 to 1 (the standard range assumed by classical reinforcement learning models). Beta distribution was chosen because it allows us to restrict variables within a certain range.

The conditional probability of the hidden variables P (x (i)| y (i), i = 1, … , t-1) is updated recursively following the Rescorla-Wagner rule:

$$B_{t+1} = B_t + \alpha_t \times (S_t - B_t) + \varepsilon_t \qquad (1)$$

where ε_t follows Gaussian distribution $N\ (0, 2)$. As so far there is no conclusion about the update algorithm for α_t in a changing environment, we took α_t as flat distributed within 0 to 1 (*beta (0.5,0.5),* the same as the prior distribution) for every time point. Notably, B_t and α_t were always restricted within the range of [0,100] and [0,1], respectively, over the recursive estimation process.

As the samples were generated from the underlying Gaussian distribution, the measurement equation (the relationship between the observation and hidden variables) is: $S_t \sim N\ (B_t, \sigma_t)$. Here σ_t was calculated as the standard deviation of the distribution of B_t. Importantly, to make sure that the estimates from IML were not dependent on

our settings of priors, we compared the estimated results from ILM with different settings of priors (details in supplementary materials).

In the second step, we first calculated the trial-by-trial absolute distance of subjects' guesses to the estimates of ILM. Next we calculated the learning performance of each session by averaging the trial-by-trial absolute distance from the second to the last trial of the session. Finally, an index (labeled as *guess2est*) for each individual's learning performance was calculated by averaging the performance across sessions. Notably, as *guess2est* measures the distance to the performance of ILM, a smaller number of *guess2est* stands for better learning performance.

Additionally, we calculated the average distance of subjects' guesses to the underlying mean over sessions (labeled as *guess2mu*). The learning sequences for subjects were randomly determined and were different across subjects, which may result in differences in the learning difficulty of sequences. Therefore, *guess2mu* is a coarse measurement of individual's learning performance, as it might be confounded by the difficulty of the learning sequences. We calculate this variable to provide a second dimension for evaluating subjects' learning behaviours, whereas we don't use it to identify the neural correlates for individual learning ability.

Image Acquisition and MRI Data Analysis

Data were acquired with a 3T Philips Achieva scanner. High-resolution structural T1-weighted 3D-TFE anatomical scans of the whole brain (voxel size 1.1×1.1×0.6 mm, TR = 7.5 ms, TE = 3.5 ms, flip angle = 8°) were acquired for each participant right before they started the behavioral sessions. Data were analyzed in SPM8 (http://www.fil.ion.ucl.ac.uk/spm) according to the standard procedure in the Voxel-based Morphology (VBM) tutorial (Ashburner 2010). First, T1 images for each subject was segmented in the native space into six classes of tissue: gray matter (GM), white matter (WM), Cerebrospinal fluid (CSF), skull, soft tissue outside the brain, and other signals outside the head. Second, the deformations that best align the images together were estimated by iteratively registering the imported images (the GM and WM images generated from the first step) with their average in DARTEL (Ashburner 2007). Third, the DARTEL template from the previous step was registered to the

Montreal Neurological Institute (MNI) space through affine transformation. The estimated parameters and DARTEL flow-fields were used to generate spatially normalized GM images. The normalized GM images were then spatially smoothed using a Gaussian kernel of 6mm full width at half-maximum (FWHM).

Individual GM images were taken into multiple regression models to identify the brain structures whose gray matter density were associated with inter-individual differences in learning ability in a changing environment. We included *guess2est* (mean-centered) in the regression model for each subject as a covariate to identify the brain regions that are positively correlated with the inter-individual differences in learning ability. In addition, we included total brain gray matter volume as a covariate to adjust for individual differences in brain size. Age and gender were also included as covariates (without centering) to control for the potential confounding effects. We included an explicit mask (created by applying a 0.2 absolute threshold masking on the averaged GM images of all subjects) to restrict the reasonable searching area. Significant results were reported (unless explicitly specified) at the threshold of $p<0.001$ at the voxel level, FWE corrected at the cluster level $p<0.05$, with the non-stationary cluster correction (details in the supplementary).

Results

Behavior results

We first illustrate subjects' guesses together with the underlying distributions to examine whether subjects are able to track the underlying mean (Figure 1 for a representative example). We observe that, on the whole, subjects are able to track the underlying mean. When the mean changes, subjects detect the change with a delay of several trials and adjust their guesses accordingly (Figure 1). Average distance of guesses to the underlying mean across subjects, *guess2mu,* (mean ± SD) was 3.9 ± 1.2.

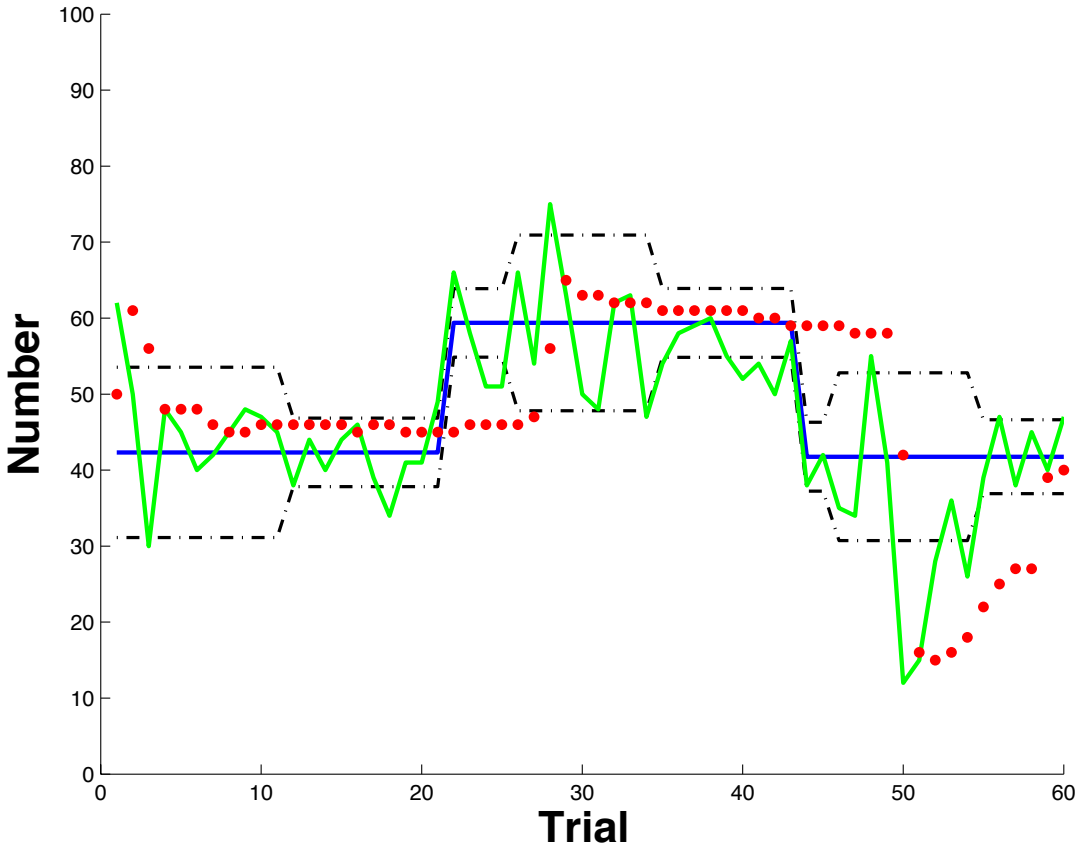

Figure 1. An example session and data. The solid blue line represents the underlying mean, which remains unknown to subjects and has to be guessed. Black dashed lines illustrate the standard deviation (SD), which changes independently of the mean. Green line represents the samples drawn from underlying distributions. Red dots are the guesses from a representative subject. The mean and noise level can suddenly change without informing subjects, which they can only infer based on the received observations.

Estimations from ILM

We illustrate the trial-by-trial estimation of the underlying mean from ILM. See Figure 2 for a representative example. The average departure of the estimations of ILM from the underlying mean across sessions (mean ± SD) is: 3.6 ± 0.6. Further test shows that ILM performed slightly better compared to participants (one-sided, paired t-test, $t\ (19) = 1.9$, $p < 0.05$). The difference of learning performance between subjects and ILM, *guess2est* (mean ± SD) is: 0.4 ± 0.9. Notably, the estimations from the ILM

are not influenced by the prior settings, suggesting that these effects are robust to the use of different model parameters (details in the supplementary materials).

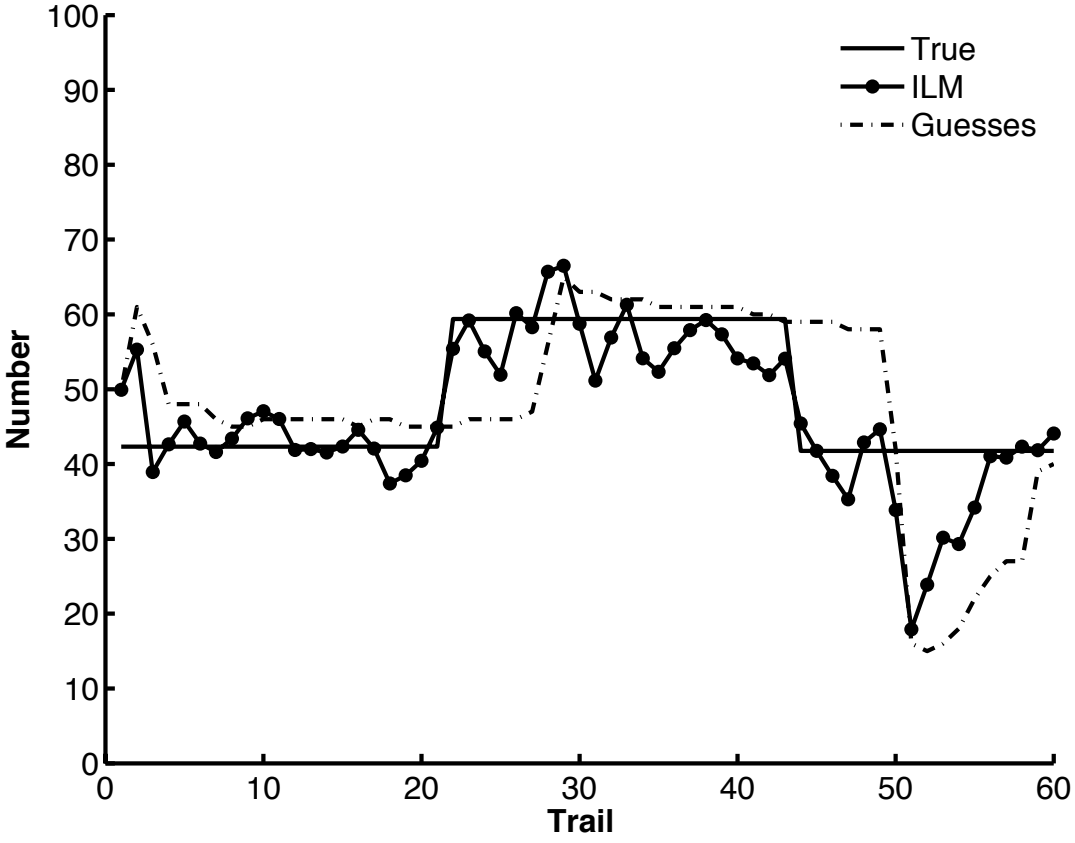

Figure 2. An example of estimated results from the ILM. The solid line represents the mean of the underlying sequence. The line with filled dot illustrates the estimations of the underlying mean from the ILM. Dashed line represents guesses from the subject. From the figure we can observe that on the whole the ILM and subjects are both able to track the underlying mean, while the ILM detects the underlying change and adapts to the change faster.

Structural correlates of the individual differences in learning performance

To identify the structural correlates of the inter-individual differences in the learning performance, we conduct a VBM analysis and search for brain regions whose GM volume are positively correlated with individual's learning ability. As *guess2est*

measures the distance to the performance of the ILM, a smaller number of *guess2est* stands for better learning performance. Therefore, we search for regions whose GM volume are negatively correlated with *guess2est*.

We find that GM volume of regions in the cerebellum (peak: [-2, -58, -17], t = 5.21, z = 3.88; Figure 3a) and a cluster covering right postcentral gyrus, Inferior Parietal cortex and Supramarginal gyrus (with peak: [49, -28, 49], t = 4.97, z = 3.76; We label it as right postcentral parietal cortex; Figure 3b) show strong negative correlations with *guess2est* (Figure 3c, d), i.e. the higher of the GM volume in these regions are associated with lower *guess2est* (i.e. better learning performances). Our results here, by demonstrating a significant association between increased GM volume in the cerebellum and right postcentral parietal cortex with the learning performance, highlight a direct link between individual differences in the structural properties of these regions and the individual learning ability in a changing environment.

Functional correlates of the individual differences in learning performance

The results from our VBM analysis suggest that regions in the cerebellum and right postcentral parietal cortex are important for the learning performance in a changing environment. Based on this finding, we further investigate whether the functional involvement of these two regions during the presentation of new observations in our mean-guessing task also associates with individual differences in learning performance. To address this question, we apply a multiple linear regression analysis and search across the whole-brain for regions whose activities are negatively correlated with *guess2est* at the time when a new observation is presented. Significant results at $p<0.001$, FWE cluster corrected at $p<0.05$ are reported in Table S5. We find that the cerebellum and right postcentral parietal cortex indeed showed greater functional activation at the presentation of a new observation for subjects with better learning performance (significant at the threshold of $p<0.001$ at the voxel level, corrected for multiple comparison using small-volume FWE correction, $p<0.05$, for 12 mm spheres surrounding the coordinates found in our VBM analysis above). These results suggest the congruency between the structural and functional features of the brain regions, and together they suggest that better learning ability in a changing environment is related to both the structural properties and the functional involvement of the cerebellum and right postcentral parietal cortex.

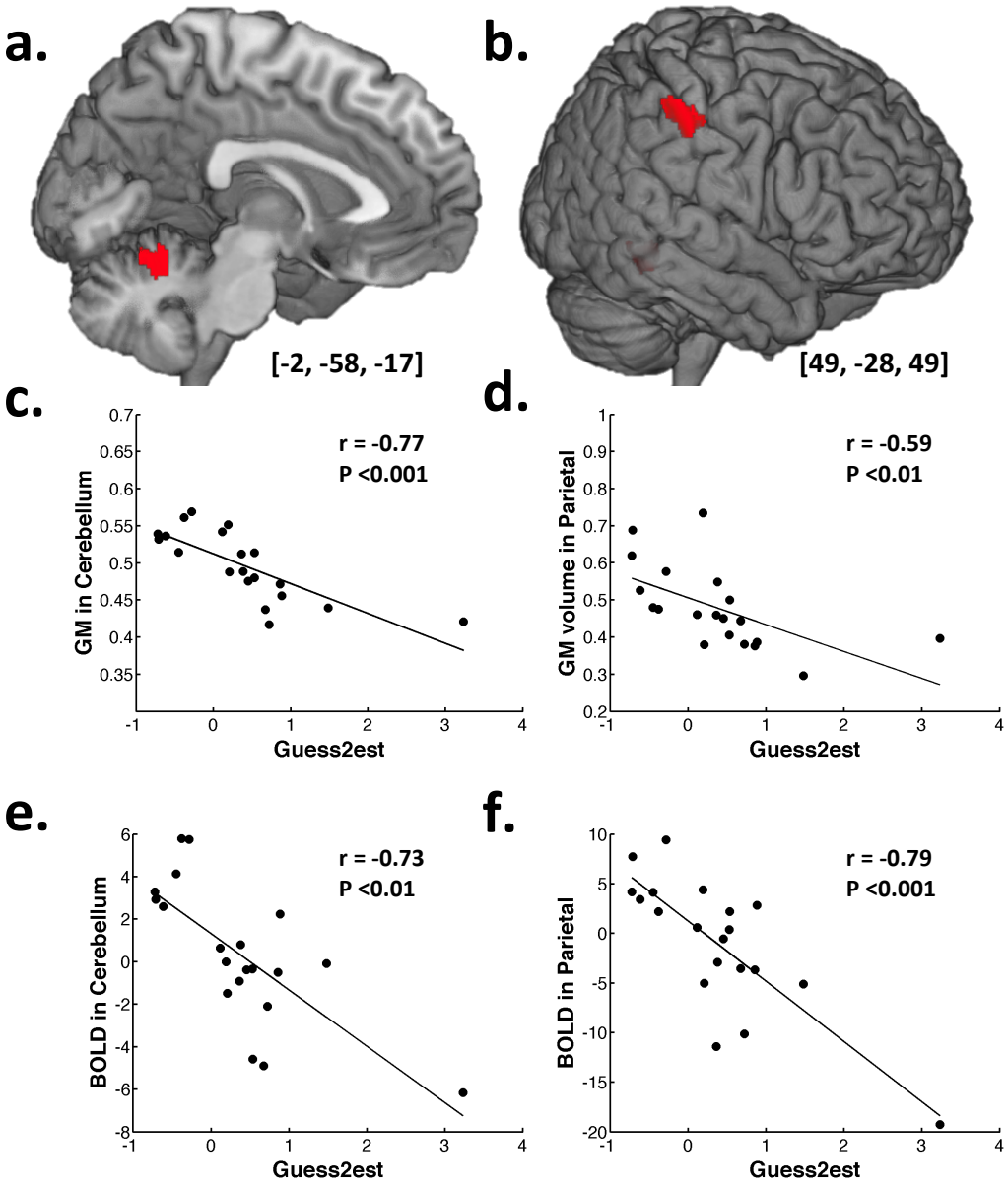

Figure 3. Structural and functional neural correlates of individual learning ability. Individual learning performance is associated with GM volume of regions in the cerebellum (illustrated in ***a***) and a region covering right postcentral gyrus, Inferior Parietal cortex and Supramarginal gyrus (we label it as postcentral parietal cortex; illustrated in ***b***). ***c, d.*** GM volume extracted from the peak in cerebellum and postcentral parietal cortex are negatively correlated with *guess2est,* the reverse index of learning ability. ***e, f.*** The functional activities in the cerebellum and postcentral parietal cortex during the presentation of a new observation are also negatively correlated with *guess2est*. All Pearson correlation reported here remains significant ($p< 0.01$) after excluding the subject who seems to have significantly worse performance than others.

Discussion

In this study we investigate the structural and functional neural correlates of inter-individual differences in learning performances in a changing environment. We find that there is great heterogeneity in individual learning performance in a changing environment and such individual differences are associated with the GM volume of regions in the cerebellum and right postcentral parietal cortex and with the functional involvement of these two regions during learning. These findings provide congruent structural and functional evidence for the importance of the cerebellum and right postcentral parietal cortex in the successful learning and information integration.

Our finding that the GM volume and functional involvement of the cerebellum and postcentral parietal cortex are associated with individual learning performance suggest a link between the lower-order sensory-motor information processing and the belief updating in higher-order learning under uncertainty. Existing research has established that the sensory and motor system can efficiently integrate online new information in a statistically optimal manner (Ernst & Banks 2002). The cerebellum has been shown to be involved in adapting movements to novel situations through trial-by-trial learning mechanisms (Bastian 2006). In addition, the co-activation of postcentral gyrus, Inferior Parietal lobe and the cerebellum have been reported in the perceptual sensorimotor learning (Hadjikhani & Roland 1998; Inoue et al. 2000), enactment effect (Russ et al. 2003), arithmetic fact retrival (Grabner et al. 2009), visuospatial working memory and response-based sequence learning (Bischoff-Grethe et al. 2004). During evolution of human being, higher cognitive functions are evolved from the basic sensory-motor functions. Therefore, it is possible that the information updating mechanism of the sensory-motor system also serves the belief updating process in higher-level decision-making. Consistently, it has been reported that a relationship exists between the cerebellum brain volume and cognitive function (Hogan et al. 2011), between abnormal exploration in autism and the cerebellum abnormality and between the cerebellum brain volume with children with attention deficit hyperactivity (ADHD) (Pierce & Courchesne 2001).

Furthermore, our findings may shed new light on developing treatments for clinical psychological patients. Negative emotions (e.g. frustration, anxiety and helplessness)

and even psychological disorder symptoms (e.g. depression and anxiety disorders) can be induced if individuals are lack of the ability to correctly learn the state of the world. On one hand, individuals could deviate from optimal updating by overweighting the history, which leads to insensitivity to the fundamental changes of environments and failure of adapting to new situations. On the other hand, individuals may overweight new information, which causes over alertness and response to stochastic fluctuations. The cerebellum has been proposed to be a highly plastic and good target for clinical intervention (Mackie et al. 2007), providing new approaches for improving individual's learning ability and consequently alleviating negative emotions induced by the failure of adapting to the changes of environments.

Finally, we would like to point out that the relatively small sample size employed in our study allowed for the detection of moderate-sized effects, while brain structures whose GM volume correlate with learning performance of a less magnitude were not able to detect. Future research is required to test the generalizability of our findings, with larger and more diverse samples of participants.

Reference

Ashburner, John. 2007. “A Fast Diffeomorphic Image Registration Algorithm.” *Neuroimage* 38 (1): 95–113.

Ashburner, John. 2010. “VBM Tutorial.”

Badre, David, and Anthony D Wagner. 2007. “Left Ventrolateral Prefrontal Cortex and the Cognitive Control of Memory.” *Neuropsychologia* 45 (13) (January): 2883–2901.

Barraclough, Dominic J, Michelle L Conroy, and Daeyeol Lee. 2004. “Prefrontal Cortex and Decision Making in a Mixed-Strategy Game.” *Nature Neuroscience* 7 (4) (March 7): 404–410.

Bastian, Amy J. 2006. “Learning to Predict the Future: the Cerebellum Adapts Feedforward Movement Control.” *Current Opinion in Neurobiology* 16 (6) (December): 645–649.

Bischoff-Grethe, Amanda, Kelly M Goedert, Daniel T Willingham, and Scott T Grafton. 2004. “Neural Substrates of Response-Based Sequence Learning Using fMRI.” *Journal of Cognitive Neuroscience* 16 (1) (January): 127–138.

Blackwood, Nigel, Dominic Ffytche, Andrew Simmons, Richard Bentall, Robin Murray, and Robert Howard. 2004. “The Cerebellum and Decision Making Under Uncertainty.” *Brain Research. Cognitive Brain Research* 20 (1) (June): 46–53.

Boes, Aaron D, Antoine Bechara, Daniel Tranel, Steve W Anderson, Lynn Richman, and Peg Nopoulos. 2009. “Right Ventromedial Prefrontal Cortex: a Neuroanatomical Correlate of Impulse Control in Boys.” *Social Cognitive and Affective Neuroscience* 4 (1) (March): 1–9.

Ceccarelli, Antonia, Maria Assunta Rocca, Elisabetta Pagani, Andrea Falini, Giancarlo Comi, and Massimo Filippi. 2009. “Cognitive Learning Is Associated with Gray Matter Changes in Healthy Human Individuals: a Tensor-Based Morphometry Study.” *Neuroimage* 48 (3) (November): 585–589.

Chen, Shen-Hsing Annabel, Moon-Ho Ringo Ho, and John E Desmond. 2012. “A Meta‐Analysis of Cerebellar Contributions to Higher Cognition From PET and fMRI Studies.” *Human Brain Mapping*.

Coricelli, Giorgio, and Rosemarie Nagel. 2009. “Neural Correlates of Depth of Strategic Reasoning in Medial Prefrontal Cortex.” *Proceedings of the National Academy of Sciences* 106 (23) (June): 9163–9168.

de Lange, Floris P, Anda Koers, Joke S Kalkman, Gijs Bleijenberg, Peter Hagoort, Jos W M van der Meer, and Ivan Toni. 2008. “Increase in Prefrontal Cortical Volume Following Cognitive Behavioural Therapy in Patients with Chronic Fatigue Syndrome.” *Brain* 131 (Pt 8) (August): 2172–2180.

Dirnberger, Georg, Judith Novak, and Christian Nasel. 2013. “Perceptual Sequence Learning Is More Severely Impaired Than Motor Sequence Learning in Patients with Chronic Cerebellar Stroke.” *Journal of Cognitive Neuroscience* 25 (12) (December): 2207–2215.

Ernst, Marc O, and Martin S Banks. 2002. “Humans Integrate Visual and Haptic Information in a Statistically Optimal Fashion.” *Nature* 415 (6870) (January): 429–433.

Frangou, Sophia, Xavier Chitins, and Steven C R Williams. 2004. “Mapping IQ and Gray Matter Density in Healthy Young People.” *Neuroimage* 23 (3) (November): 800–805.

Grabner, Roland H, Anja Ischebeck, Gernot Reishofer, Karl Koschutnig, Margarete Delazer, Franz Ebner, and Christa Neuper. 2009. “Fact Learning in Complex Arithmetic and Figural-Spatial Tasks: the Role of the Angular Gyrus and Its Relation to Mathematical Competence.” *Human Brain Mapping* 30 (9) (September 15): 2936–2952.

Guo Chaohui, Sunhae Sul, Nora Heinzelmann, Christian C Ruff, and Ernst Fehr. “Neural Correlates of Learning Rate in Changing Environment.” *In Preparation*.

Hadjikhani, Nouchine, and Per E. Roland. 1998. "Cross-modal transfer of information between the tactile and the visual representations in the human brain: a positron emission tomographic study." *The Journal of Neuroscience* 18, no. 3: 1072-1084.

Hampton, Alan N, Peter Bossaerts, and John P O'Doherty. 2006. “The Role of the Ventromedial Prefrontal Cortex in Abstract State-Based Inference During Decision Making in Humans.” *The Journal of Neuroscience* 26 (32) (August): 8360–8367.

Hogan, Michael J, Roger T Staff, Brendan P Bunting, Alison D Murray, Trevor S Ahearn, Ian J Deary, and Lawrence J Whalley. 2011. “Cerebellar Brain Volume Accounts for Variance in Cognitive Performance in Older Adults.” *Cortex; a Journal Devoted to the Study of the Nervous System and Behavior* 47 (4) (April): 441–450.

Ide, Jaime S, and Chiang-Shan R Li. 2011. “A Cerebellar Thalamic Cortical Circuit for Error-Related Cognitive Control.” *Neuroimage* 54 (1) (January): 455–464.

Inoue, K, R Kawashima, K Satoh, S Kinomura, M Sugiura, R Goto, M Ito, and H Fukuda. 2000. “A PET Study of Visuomotor Learning Under Optical Rotation.” *Neuroimage* 11 (5 Pt 1) (May): 505–516.

Kanai, Ryota, and Geraint Rees. 2011. “The Structural Basis of Inter-Individual Differences in Human Behaviour and Cognition.” *Nature Reviews Neuroscience* 12 (4) (April): 231–242.

Krawczyk, Daniel C. 2002. “Contributions of the Prefrontal Cortex to the Neural Basis of Human Decision Making.” *Neuroscience & Biobehavioral Reviews* 26

(6) (October): 631–664.

Lee, Tai Sing, and David Mumford. 2003. “Hierarchical Bayesian Inference in the Visual Cortex.” *Journal of the Optical Society of America. a, Optics, Image Science, and Vision* 20 (7) (July): 1434–1448.

Mackie, Susan, Philip Shaw, Rhoshel Lenroot, Ron Pierson, Deanna K Greenstein, Tom F 3rd Nugent, Wendy S Sharp, Jay N Giedd, and Judith L Rapoport. 2007. “Cerebellar Development and Clinical Outcome in Attention Deficit Hyperactivity Disorder.” *American Journal of Psychiatry* 164 (4) (April): 647–655.

Matsuo, Koji, Mark Nicoletti, Kiyotaka Nemoto, John P Hatch, Marco A M Peluso, Fabiano G Nery, and Jair C Soares. 2009. “A Voxel-Based Morphometry Study of Frontal Gray Matter Correlates of Impulsivity.” *Human Brain Mapping* 30 (4) (April): 1188–1195.

Miall, R Chris, Lars O D Christensen, Owen Cain, and James Stanley. 2007. “Disruption of State Estimation in the Human Lateral Cerebellum.” *PLoS Biology* 5 (11) (November): e316.

Morgan, M. 1999. “Contribution of Ventrolateral Prefrontal Cortex to the Acquisition and Extinction of Conditioned Fear in Rats.” *Neurobiology of Learning and Memory* 72 (3) (November): 244–251.

Narr, Katherine L, Roger P Woods, Paul M Thompson, Philip Szeszko, Delbert Robinson, Teodora Dimtcheva, Mala Gurbani, Arthur W Toga, and Robert M Bilder. 2007. “Relationships Between IQ and Regional Cortical Gray Matter Thickness in Healthy Adults.” *Cerebral Cortex (New York, N.Y.: 1991)* 17 (9) (September): 2163–2171.

Passot, Jean-Baptiste, Niceto R Luque, and Angelo Arleo. 2013. “Coupling Internal Cerebellar Models Enhances Online Adaptation and Supports Offline Consolidation in Sensorimotor Tasks.” *Frontiers in Computational Neuroscience* 7: 95.

Paulin, M G. 2005. “Evolution of the Cerebellum as a Neuronal Machine for Bayesian State Estimation.” *Journal of Neural Engineering* 2 (3) (September): S219–34.

Petrides, M. 2005. “Lateral Prefrontal Cortex: Architectonic and Functional Organization.” *Philosophical Transactions of the Royal Society B: Biological Sciences* 360 (1456) (April 29): 781–795.

Pierce, K, and E Courchesne. 2001. “Evidence for a Cerebellar Role in Reduced Exploration and Stereotyped Behavior in Autism.” *Biological Psychiatry* 49 (8) (April): 655–664.

Raymond, J L, S G Lisberger, and M D Mauk. 1996. “The Cerebellum: a Neuronal Learning Machine?” *Science* 272 (5265) (May): 1126–1131.

Russ, Michael O., Wolfgang Mack, Carina-Raluca Grama, Heinrich Lanfermann, and Monika Knopf. "Enactment effect in memory: evidence concerning the function of the supramarginal gyrus." *Experimental brain research* 149, no. 4 (2003): 497-504.

Samejima, Kazuyuki, Yasumasa Ueda, Kenji Doya, and Minoru Kimura. 2005. "Representation of action-specific reward values in the striatum." *Science* 310, no. 5752: 1337-1340.

Schonberg, Tom, Nathaniel D Daw, Daphna Joel, and John P O'Doherty. 2007. "Reinforcement Learning Signals in the Human Striatum Distinguish Learners From Nonlearners During Reward-Based Decision Making." *The Journal of Neuroscience* 27 (47) (November): 12860–12867.

Thoma, Patrizia, Christian Bellebaum, Benno Koch, Michael Schwarz, and Irene Daum. 2008. "The Cerebellum Is Involved in Reward-Based Reversal Learning." *Cerebellum (London, England)* 7 (3): 433–443.

Wagner, Anthony D., Anat Maril, Robert A. Bjork, and Daniel L. Schacter. "Prefrontal contributions to executive control: fMRI evidence for functional distinctions within lateral prefrontal cortex." *Neuroimage* 14, no. 6 (2001): 1337-1347.

Supplementary materials

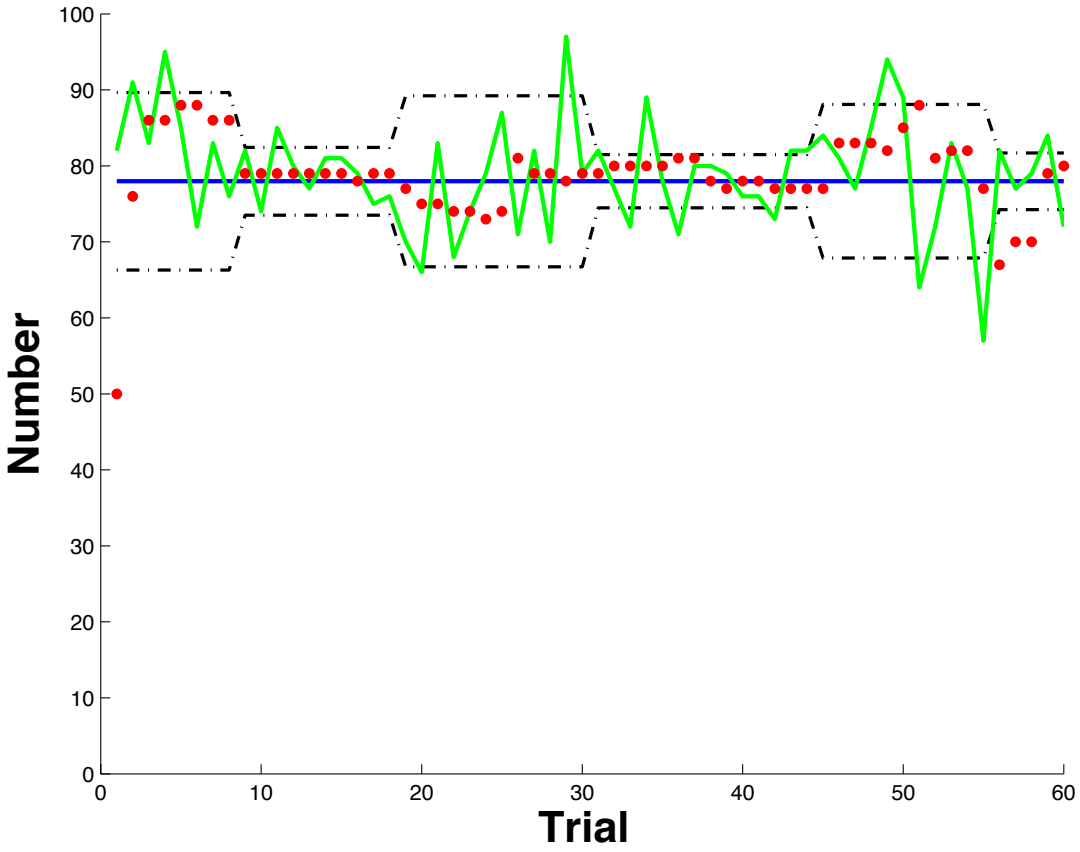

Figure S1. An example sequence and data of a session with stable mean. The solid blue line represented the underlying mean, which remained unknown to subjects and had to be guessed. Black dashed lines illustrated the standard deviation (SD), which changed independently of the mean. Green line represented the samples drawn from underlying distributions. Red dots were the guesses from a representative subject. The mean and noise level could suddenly change without informing subjects.

VBM non-stationary cluster correction

Non-stationary occurs due to non-isotropic (non-uniform) smoothness of VBM data. Because cluster size distribution varies depending on local smoothness, some clusters tend to be large in smooth areas, while in rough regions clusters tend to be small. This leads in particularly in VBM to invalid cluster size statistics and clusters sizes will be over- or underestimated. Therefore, we applied the non-stationary cluster correction when we reported the significant clusters based on the approach suggested by Ged

Ridyway: i.e., setting defaults.stats.rft.nonstat = 1 in spm_defaults.m, and fwhm_vox = 8 in spm_est_smoothness.m in SPM 8.

	B_0 (Belief of underlying mean at time t = 0)	α_0 (Learning rate at time t = 0)
1st set of priors	*Beta distributed with shape parameters = 2* 100 × *beta (2,2)*	*Beta distributed with shape parameters = 0.5* 100 ×*beta (0.5,0.5)*
2nd set of priors	Random integer numbers from uniform distribution within 0 to 100	*Beta distributed with shape parameters = 0.5* 100 × *beta (0.5,0.5)*
3rd set of priors	*Beta distributed with shape parameters = 2* 100 × *beta (2,2)*	*Beta distributed with shape parameters = 2* 100 × *beta (2,2)*
4th set of priors	Random integer numbers from uniform distribution within 0 to 100	Random numbers from uniform distribution within 0 to 1
5th set of priors	Random integer numbers from uniform distribution within 0 to 100	Random numbers from normal distribution, with mean = 0.5, SD = 1 *N (0.5,1)*

Table S4. Different sets of priors for ILM. In order to check whether the estimates of ILM are dependent on our settings of priors, we compare the estimated results from ILM with different sets of priors. Here each row represents one set of priors for B_0 (Belief of underlying mean at time t = 0; second column), and α_0 (Learning rate at time t = 0; third column).

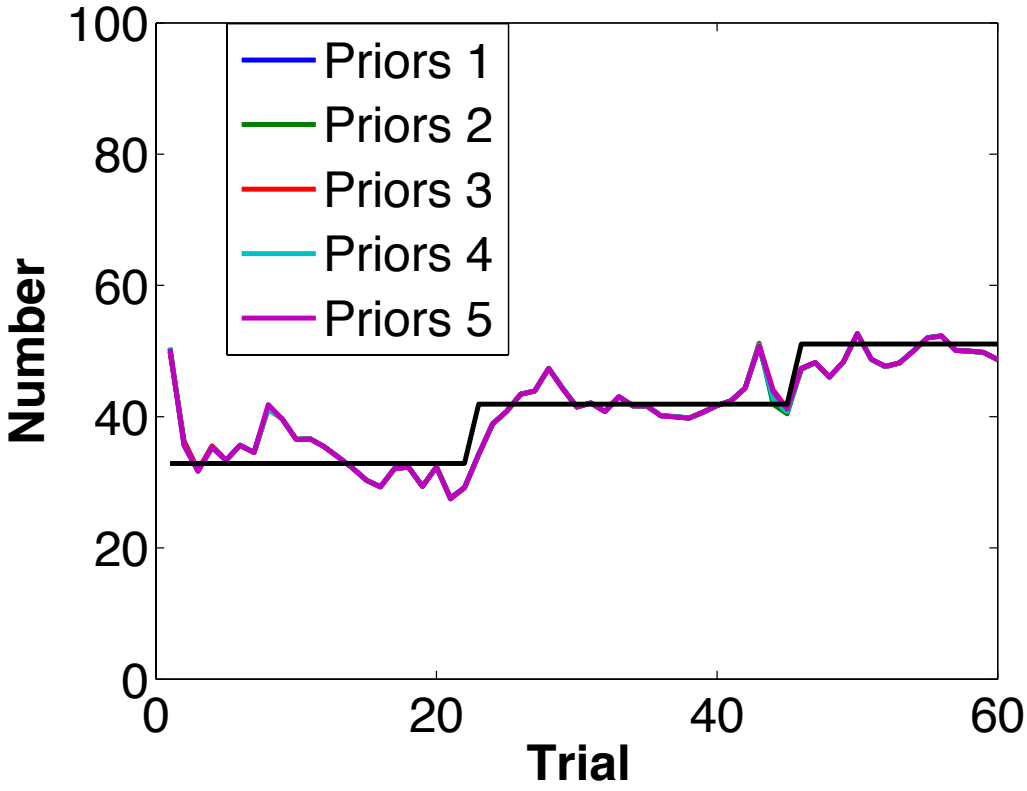

Figure S4. One example session of the estimated results from ILM with five different sets of priors. We can see that it seems that the estimates of ILM are not dependent on our settings of priors. Furthermore, to evaluate the consistency of the estimated results of all subjects, we calculate the average correlation coefficient between the estimates from ILM with each set of priors. The average Pearson correlation coefficient is 0.9996.

Region name	MNI coordinates (x y z)	t value	Cluster size
Parietal_Inf_R	38 -44 40	7.58	3361
Cerebellum_4_5_R	28 -44 -24	6.79	425
Frontal_Mid_L	-32 54 8	6.73	237
Cerebellum_6_L	-30 -54 -20	6.64	100
Parietal_Inf_L	-50 -30 46	6.2	40
Thalamus	22 -30 0	4.87	44
Parietal_Inf_L	-40 -48 56	4.77	37
Frontal_Mid_R	42 34 18	4.6	72

Table S5. Regions whose activities are negatively correlated with guess2est at the time when a new observation is presented. Significant results were shown at the threshold of $p<0.001$ at the voxel level, and cluster level FWE corrected at $p<0.05$.

Chaohui Guo

DATE OF BIRTH: 1985.01.30

EDUCATION

2010-2014: University of Zurich, PhD program in Neuroeconomics

Supervisor: Prof. Ernst Fehr (Department of Economics, Zurich Univ.)

2008-2009: University of Cambridge, Master in Psychology

Supervisor: Prof. Lorraine Tyler (Centre for Speech, Language and the Brain, Cambridge Univ.)

2003- 2007 Xi'an Jiaotong University, B.S., Physics (Graduated with Distinction)

TEACHING EXPERIENCE

2012: Teaching Assistant for Scientific programming for neuroeconomic experiments.
2007- 2008: Research Assistant in the lab of Prof. Xiaolin Zhou (Center for Brain and Cognitive Sciences, Peking Univ.)